Distribution Agreement

In presenting this thesis or dissertation as a partial fulfillment of the requirements for an advanced degree from Emory University, I hereby grant to Emory University and its agents the non-exclusive license to archive, make accessible, and display my thesis or dissertation in whole or in part in all forms of media, now or hereafter known, including display on the world wide web. I understand that I may select some access restrictions as part of the online submission of this thesis or dissertation. I retain all ownership rights to the copyright of the thesis or dissertation. I also retain the right to use in future works (such as articles or books) all or part of this thesis or dissertation.

Signature:

_____ _____

Alev Cagla Ozdemir Date

GNB3 overexpression leads to obesity in a mouse model

By

Alev Cagla Ozdemir
Doctor of Philosophy

Graduate Division of Biological and Biomedical Sciences
Genetics and Molecular Biology

_____
M. Katharine Rudd, Ph.D.
Advisor

_____
Anita Corbett, Ph.D.
Committee Member

_____
Andrew Escayg, Ph.D.
Committee Member

_____
Carlos Moreno, Ph.D.
Committee Member

_____
Shanthi Srinivasan, M.D.
Committee Member

_____
Peter Thule, M.D.
Committee Member

Accepted:

_____
Lisa A. Tedesco, Ph.D.
Dean of the James T. Laney School of Graduate Studies

_____
Date

GNB3 overexpression leads to obesity in a mouse model

By

Alev Cagla Ozdemir

B.S., University of Michigan – Ann Arbor, 2007

Advisor: M. Katharine Rudd, Ph.D.

An abstract of
A dissertation submitted to the Faculty of the
James T. Laney School of Graduate Studies of Emory University
in partial fulfillment of the requirements for a degree of
Doctor of Philosophy
in Graduate Division of Biological and Biomedical Sciences
Genetics and Molecular Biology
2017

Abstract

GNB3 overexpression leads to obesity in a mouse model

By Alev Cagla Ozdemir

Obesity is a highly heritable disorder of excess accumulation of body fat. As a worldwide epidemic, obesity and its associated comorbidities such as type 2 diabetes, cardiovascular disease and cancer, impose major public health challenges. We described a genetic syndrome of obesity and intellectual disability in humans, where an unbalanced chromosomal translocation leads to an 8.5-Megabase (Mb) duplication of chromosome 12p and a 7.0-Mb deletion of chromosome 8p. One of the duplicated genes is *GNB3*, which encodes G protein β3. A cytosine to thymine (C825T) polymorphism in *GNB3* is associated with hypertension, obesity and metabolic syndrome in genome-wide association studies; however, the mechanism of *GNB3*-related obesity is unknown. We created bacterial artificial chromosome (BAC) transgenic mice that carry an extra copy of the T risk allele of *GNB3*. *GNB3*-T/+ mice weighed significantly more than wild-types (WT) starting at age 6-7 week onwards. We show that *GNB3*-T/+ mice have increased adiposity, indicated by greater subcutaneous and visceral white adipose tissue (WAT) and brown adipose tissue (BAT) depots, larger white adipocytes, and larger livers compared to WT. Lean mass is approximately the same in *GNB3*-T/+ and WT mice, suggesting that the difference in weight is strictly due to an increase in fat mass. *GNB3*-T/+ mice have similar food intake, activity levels and heat production compared to WT. Strikingly, *GNB3*-T/+ mice have decreased *Ucp1* expression and increased adipogenic marker expression in subcutaneous WAT, suggesting a conversion of subcutaneous WAT into a less $UCP1^{+}$ and a less beige but whiter tissue. We also created BAC transgenic mice that have an extra copy of the non-risk C allele of *GNB3* or the mouse ortholog of *Gnb3*. *GNB3*-C mice weigh less than WT, have proper glucose tolerance, and elevated blood lipid levels, suggesting that *GNB3*-C overexpression is protective of weight gain, but not of elevated blood lipids. On the other hand, mice with additional copies of *Gnb3* weigh more and have greater adiposity than WT, depending on BAC copy number. Taken together, these data demonstrate that *GNB3* alleles and expression levels impact body weight, and support a role for *GNB3* overexpression in obesity.

GNB3 overexpression leads to obesity in a mouse model

By

Alev Cagla Ozdemir

B.S., University of Michigan – Ann Arbor, 2007

Advisor: M. Katharine Rudd, Ph.D.

A dissertation submitted to the Faculty of the
James T. Laney School of Graduate Studies of Emory University
in partial fulfillment of the requirements for a degree of
Doctor of Philosophy
in Graduate Division of Biological and Biomedical Sciences
Genetics and Molecular Biology
2017

Acknowledgements

My advisor, Katie Rudd. Thank you for being the best advisor I could have ever hoped for. Thank you for letting me take ownership of my project and always being available to guide me when in need. You are a great scientist, teacher, writer, presenter, who has been an remarkable role model to me. Thank you for everything you thought me regarding various aspects of science and the scientific world. I feel lucky to be your student.

My dissertation committee. Andrew Escayg, Carlos Moreno, Shanthi Srinivasan, Peter Thule, Anita Corbett. Thank you for your valuable contribution to this project. You made me a better scientist by sharing your wisdom and scientific intelligence.

Former members of the Rudd Laboratory. Thank you for creating a supportive and warm laboratory environment that I looked forward to spending time in every day. Grace, thank you for your friendship, support and your tremendous help with this project.

My classmates and colleagues from GMB. Good luck to you all. Shannon, who has been with me every step of the Ph.D. journey in the last six years, I am so lucky to have met a wonderful person like you.

Most importantly, my family. Mom, you mean everything to me. You are the kindest, most loving and hardest working person I know. You are truly my role model. I exist, and can write these words, only because of you. Thank you for giving your life to me. Dad, Grandma, Grandpa, Aunt #1 and Aunt #2. We have been apart and missing each other for far too long. Thank you for the endless sacrifices you made all my life, so I have become the person I am today. I love you all with all my heart.

My cats. Thinking of you, your craziness grounds me and warms my heart. I love you. Oglum (Requiescat in pace), this dissertation is for you, my heart. I miss you.

Friends. You know who you are. Thank you for the moments we shared.

To all the artists, athletes and scientists who have touched my heart, given me inspiration and strength, thank you.

Table of Contents

List of Figures and Tables

CHAPTER 3: *GNB3* OVEREXPRESSION CAUSES OBESITY AND METABOLIC SYNDROME

Chapter 1

General Introduction

1. Obesity

1.a Obesity and statistics

Obesity is a disorder defined by an excess accumulation of body fat due to an imbalance between energy intake and energy expenditure. Several methods can be applied for classification of obesity and measurement of adiposity. The most common measure of obesity in clinical practice is the World Health Organization (WHO) body mass index (BMI) classification. BMI is calculated by dividing a person's weight in kilograms by the square of the person's height in meters. Individuals with BMI in the range of 25-30 kg/m^2 are considered overweight, while individuals with a BMI of 30 kg/m^2 or more are obese (World Health Organization, 2016a).

Obesity is a global epidemic and a major public health issue, affecting each continent of the world. Between 1980 and 2014, the global prevalence of obesity more than doubled. Based on recent WHO global estimates, in 2014, over 600 million adults were obese, corresponding to 13% of the world's adult population (World Health Organization, 2016a). In the United States (U.S.), in 2011-2014, 36.5% of adults were obese (Ogden et al., 2015). Worldwide and in the U.S., obesity is more common in women than in men. The respective prevalence of female and male obesity is 15% and 11% globally, and 38.3% and 34.3% in the U.S. (Ogden et al., 2015; World Health Organization, 2016a).

Obesity is associated with significant morbidity and mortality, including type 2 diabetes, hypertension, cardiovascular diseases, osteoarthritis and sleep apnea (Chan et al., 1994). Obesity is also linked with higher risk of developing certain cancers such as

endometrial, breast, colon, prostate, ovarian, liver, kidney and gallbladder tumors (McMillan et al., 2006; World Health Organization, 2016a). Additionally, life expectancy is shortened due to obesity, especially among young adults (Fontaine et al., 2003). Obesity combined with its morbidities and mortalities result in heavy clinical, public health and economical burdens worldwide (Kelly et al., 2008).

1.b Genetics of obesity

1.b.i. Obesity and genetic variation

The worldwide obesity epidemic and its rising prevalence have piqued scientists' interest in obesity pathogenesis. As the fundamental cause of obesity is an energy imbalance between calories consumed and calories expended, any activity that results in a positive energy balance will lead to accumulation of fat, and if in excess, to weight gain and obesity. The plethora of highly processed, calorie dense, readily available foods, as well as a reduction in physical activity and increase in sedentary lifestyle are all factors contributing to the positive energy balance. These obesogenic environmental influences affect some individuals more than others. Studying the genetics of obesity can answer important questions about why some individuals are more vulnerable to obesogenic environmental influences. As genetic susceptibility to obesity is uncovered and explained, we will have a deeper understating of how to help prevent and combat obesity.

1.b.ii Heritability

Whether the observed variation in a particular trait is due to biological factors or environmental factors is an important question in biology. The fraction of variation controlled by genetics relative to the total phenotypic variability is referred to as heritability (Visscher et al., 2008). Twin and adoption studies are two common strategies to generate heritability estimates.

1.b.ii.1 Twin and adoption studies

Genetic identity shared between monozygotic twins is 100% and between dizygotic twins is 50%. For heritable traits, the closer the estimates of concordance between monozygotic twins is to 1, and between dizygotic twins to 0.5, the greater the heritability. In 1986, using a sample of 1974 monozygotic and 2097 dizygotic twin pairs, Stunkard estimated heritability for weight and BMI to be 0.78 and 0.77, respectively (Stunkard et al., 1986a). After a 25 year follow up, the estimated heritability for weight and BMI increased to 0.81 and 0.84, respectively (Stunkard et al., 1986a). A review of twin studies estimates the heritability of BMI to be between 50 and 90% (Maes et al., 1997).

In an adoption study published in 1986, Stunkard demonstrated that adopted children have body weight similar to their biological parents rather than their adopted parents (Stunkard et al., 1986b). Additionally, the strong relationship between the BMI of biological parents and adoptees was present across the range of all weight classes (from very lean to very obese), and was not just confined to the obesity weight class (Stunkard et al., 1986b). In 1990, Stunkard examined monozygotic and dizygotic twins who were raised together and apart. The intra-pair correlation coefficients for BMI of monozygotic twins reared apart were 0.70 for men and 0.66 for women (Stunkard et al., 1990). Shared

childhood environment had no influence on BMI, and unshared individual environment contributed about 30% of the variance in BMI (Stunkard et al., 1990).

The studies discussed above were done before the onset of the obesity epidemic. A study carried out more recently and during the obesity epidemic concluded that heritability for BMI is 77%, and therefore has not changed (Wardle et al., 2008). The studies mentioned above and others suggest that genetics play a significant role in individuals' BMI, and that the state of being fat, adiposity, is considered a highly heritable trait.

1.b.ii.2 Racial and ethnic differences

There are differences in the prevalence of obesity among racial and ethnic groups. For instance, in Pima Indians, obesity risk is over 50% (Knowler et al., 1990). In Nauru, obesity prevalence is high at 45.1% in the general population (World Health Organization, 2016b). Over 15% of women in Nauru are morbidly obese (BMI $\geq$ 40 kg/m^2), which is striking compared to the 1.6% global prevalence of morbid obesity in women in 2014 (NCD Risk Factor Collaboration (NCD-RisC), 2016). In contrast, in Eritrea, the prevalence of obesity in the general population is low at 3.3% (Mufunda et al., 2006; Usman et al., 2006), and even lower among males at 1.2% (World Health Organization, 2016c). Environmental factors and lifestyle alone cannot explain these differences, indicating an important role of genetics in the pathogenesis of obesity.

1.b.iii Monogenic obesity

Studies of obese rodents with single gene disorders uncovered the first genes implicated in obesity. Although monogenic forms of obesity are rare, discovering their genetic basis has contributed tremendously to the understanding of obesity pathogenesis and pathways involved in this disease.

1.b.iii.1 Leptin deficiency and leptin receptor mutations

In 1950, the first obese mouse strain, *ob*/*ob*, was described in the Jackson Laboratories (Ingalls et al., 1950). Adult *ob*/*ob* mice weigh three times more than their normal littermates on the same diet and have impaired reproductive behavior (Ingalls et al., 1950). Another obese mouse strain called *db*/*db*, which has an identical phenotype to the *ob*/*ob* strain, was described in 1966 (Hummel et al., 1966). In 1994, the mutation in the *ob*/*ob* mice was cloned and mapped to the leptin gene (*LEP*) which encodes a 16 kDa protein product, produced predominantly in the adipose tissue (Zhang et al., 1994). The mutation in the *db*/*db* strain was later identified in the leptin receptor gene (*LEPR*), which is expressed in the hypothalamus (Chen et al., 1996; Chua et al., 1996; Lee et al., 1996; Tartaglia et al., 1995). The *ob*/*ob* phenotype was rescued by recombinant administration of leptin, but no effects were seen in the *db*/*db* mice (Campfield et al., 1995; Halaas et al., 1995; Pelleymounter et al., 1995). Autosomal recessive leptin mutations are also seen in humans with severe early-onset obesity with extreme hyperphagia. The first identified individuals with congenital leptin deficiency had homozygous frameshift mutations in the *LEP* gene (Montague et al., 1997). Humans with early-onset obesity and homozygous mutations in *LEPR* have also been identified (Clément et al., 1998).

1.b.iii.2 Melanocortin 4 receptor (*MC4R*) mutations

As scientists investigated energy balance and appetite regulation, components of the leptin-melanocortin pathway were elucidated. *MC4R* has roles in energy homeostasis, and controls the effects of leptin on food intake and body weight (Seeley et al., 1997). Mice with targeted disruptions in the *MC4R* gene develop mature-onset obesity with hyperphagia (Huszar et al., 1997). Several mutations in the *MC4R* gene have been identified in humans with dominantly inherited obesity (Gu et al., 1999; Hinney et al., 1999; Vaisse et al., 1998; Yeo et al., 1998). In a study of 500 children with severe childhood obesity, 5.8% had mutations in the *MC4R* gene (Farooqi et al., 2003). These results support the idea that *MC4R* mutations were the most common genetic cause of obesity identified prior to the genome-wide association study (GWAS) era.

1.b.iii.3 POMC/Prohormone convertase 1

The expression of the proopiomelanocortin (*POMC*) gene is regulated by leptin, and POMC has roles in controlling feeding behavior (Cheung et al., 1997). Homozygous null mutations in the *POMC* gene have been described in early-onset obesity in humans (Krude et al., 1998). The *PCSK1* gene encodes the prohormone convertase 1 (PC1) enzyme, which is responsible for processing POMC. A woman with severe early-onset obesity was identified to be compound heterozygote for mutations in *PC1* (Jackson et al., 1997). Other compound heterozygous and homozygous mutations in the *PCSK1* gene have been identified which lead to early-onset obesity with hyperphagia (Creemers et al., 2012; Farooqi et al., 2007; Jackson et al., 2003).

1.b.iv Genetic obesity syndromes with developmental delay

Obesity is part of the phenotype in several genetic syndromes, and characterization of the genetic obesity syndromes has provided insight into mechanisms regulating body weight and adiposity in humans.

1.b.iv.1 Prader-Willi syndrome

Prader-Willi syndrome (PWS) has an incidence of approximately 1 in 25,000 and is the most common genetic obesity syndrome. Patients with PWS have poor weight gain and hypotonia in infancy, obesity with hyperphagia (with a rapid onset between ages 1-6 years), hypogonadism, short stature and developmental delay (Goldstone). PWS is caused when the genes on the paternally inherited chromosome 15q11-q13 are not expressed. Deletion of the paternal derived copy of 15q11-q13 is seen in 75% of the cases. Maternal uniparental disomy, where the paternal copy of chromosome 15 is lost and two maternal copies of chromosome 15 are present, occurs in 22% of the cases (Goldstone). Deletions of HBII-85 non-coding small nucleolar RNAs (snoRNAs) on chromosome 15q11-q13 also lead to the PWS phenotype, suggesting that HBII-85 snoRNAs have a role in obesity (Sahoo et al., 2008; de Smith et al., 2009).

1.b.iv.2 Bardet-Biedl syndrome

Bardet-Biedl syndrome (BBS) is a rare autosomal recessive obesity syndrome associated with ciliary dysfunction, polydactyly, intellectual disability, hypogonadism and renal failure. BBS is genetically heterogeneous, with at least 14 genes coding for BBS proteins with roles in ciliary action (Sabin et al., 2011). Basal body defect of ciliated cells may

cause BBS (Ansley et al., 2003). Moreover, other disorders of ciliary function, including Alström syndrome and Carpenter syndrome, have clinical features of obesity. In mice, BBS proteins are required for leptin receptor signaling in the hypothalamus, suggesting a link between leptin signaling and ciliary function (Seo et al., 2009).

1.b.iv.3 Albright hereditary osteodystrophy

Albright hereditary osteodystrophy (AHO) is an autosomal dominant disorder with clinical features of obesity, short stature and skeletal defects, caused by mutations in *GNAS1* that decrease the expression or function of the Gsα protein. Paternal transmission of *GNAS1* mutations leads to AHO; on the other hand, maternal transmission leads to AHO and resistance to several hormones, including parathyroid hormone. (Weinstein et al., 2002).

1.b.iv.4 BDNF and TRKB deficiency

Brain-derived neurotropic factor (BDNF) and its receptor, tropomysin-related kinase B (TRKB), are involved in regulation of food intake (Cordeira et al., 2010). Mouse models with disrupted *BDNF* are obese with hyperphagia. A *de novo* mutation disrupting *TRKB* was reported in a child with severe hyperphagic obesity and developmental delay (Yeo et al., 2004). Another patient with the same phenotype has a *de novo* chromosomal inversion involving the *BDNF* locus that leads to *BDNF* haploinsufficiency (Gray et al., 2006). Furthermore, heterozygous deletion of *BDNF* is responsible for the early-onset obesity seen in patients with WAGR syndrome (Han et al., 2008).

1.b.iv.4 SIM1 deficiency

Single-minded homolog 1 (*SIM1*) is a transcription factor involved in the development of the paraventricular and supraoptic nuclei of the hypothalamus. In humans and mice, loss of function mutations in *SIM1* result in severe obesity with hyperphagia (Faivre et al., 2002; Holder et al., 2000; Kublaoui et al., 2006; Michaud et al., 2001).

1.b.v Genome-wide association studies of obesity

Since the completion of the Human Genome Project and the HapMap project, it has become apparent that most of the human genome sequence is the same between all humans, but several forms of variation also exist, where one example is single nucleotide polymorphism (SNP) (International HapMap Consortium, 2005). Variants in the genome have long been associated with disease, and GWAS allowed a hypothesis-free test of a great number of genetic variants for disease associations. Associations of common variants and the trait of interest reaching $P \leq 5 \times 10^{-8}$ are considered genome-wide significant (Panagiotou et al., 2012).

In 2007, the first robust GWAS associating BMI and obesity risk identified a common variant in the *FTO* (fat mass and obesity associated) gene (Frayling et al., 2007). Since then, several other studies have replicated the results and identified *FTO* as an obesity susceptibility locus (Loos et al., 2008; Okada et al., 2012; Speliotes et al., 2010; Thorleifsson et al., 2009; Wen et al., 2012; Willer et al., 2009). The *FTO* variant only accounted for 0.34% of the variance in BMI (Speliotes et al., 2010). Another study identified common variants near *MC4R* that associated with BMI (Loos et al., 2008). In 2009, a study identified six new loci, *TMEM18*, *KCTD15*, *GNPDA2*, *SH2B1*, *MTCH2*

and *NEGR1*, that associated with BMI (Willer et al., 2009). The most current and the largest GWAS meta-analysis for BMI to date from 339,224 individuals identified 97 loci associated with BMI, of which 56 are novel. These 97 loci account for 2.7% of the phenotypic variance in BMI (Locke et al., 2015). Including obesity-related phenotypes other than BMI, a total of 188 loci have been identified that are associated with phenotypes such as fat distribution, waist circumference, waist-hip ratio and waist-hip ratio adjusted for BMI (Sandholt et al., 2015). However, the biological mechanisms, causal genes and pathways behind these associations, and how these loci contribute to obesity risk are unknown.

1.b.vi Copy number variants and obesity

Copy number variation (CNV) is a DNA segment which is 50 base pairs to over a megabase (Mb) in size and has different copy number compared to a reference genome (Zarrei et al., 2015). CNVs can be simple deletions and duplications or more complex tandem arrays of repeats (Redon et al., 2006). CNVs are widely distributed throughout the genome (Conrad et al., 2010; Korbel et al., 2007; Redon et al., 2006; de Smith et al., 2007). 4.8-9.5% of the human genome contains CNVs (Zarrei et al., 2015). Phenotypically healthy individuals carry CNVs (Korbel et al., 2007; de Smith et al., 2007; Zarrei et al., 2015); however, CNVs can also cause disease by deletion and duplication of entire genes or by disrupting genes (Redon et al., 2006). Additionally, CNVs can alter gene expression levels by insertion or disruption of regulatory elements in the genome including enhancers or silencers (Haraksingh and Snyder, 2013). The

effect of CNVs on phenotype, such as body weight and susceptibility to disease, such as obesity is a growing topic of interest.

The association between CNVs and BMI was tested in a Chinese Han population, and elevated copy number of a common CNV on 10q11.22, covering the obesity related *PPYR1* gene, was associated with lower BMI (Sha et al., 2009). Another group reported a common CNV on chromosome 11q11 covering olfactory receptor genes *OR4P4, OR4S2* and *OR4C6* to be associated with early-onset extreme obesity (Jarick et al., 2011).

A 593-kilobase (kb) heterozygous deletion containing 29 genes on chromosome 16p11.2 has also been associated with high risk of obesity (Bochukova et al., 2010; Walters et al., 2010). Interestingly, the reciprocal duplication of the same region on chromosome 16p11.2 was associated with high risk of being underweight (Jacquemont et al., 2011). Hyperphagia was observed among the deletion carriers (Walters et al., 2010), while the duplication carriers had restrictive eating behaviors (Jacquemont et al., 2011). Another 220-kb deletion covering the leptin and insulin signaling related *SH2B1* gene was also associated with severe early-onset obesity (Bochukova et al., 2010).

Global burden of rare CNVs are also of interest in addition to identification of single CNVs. Large, rare deletions were enriched in individuals with moderate to severe early-onset obesity (Bochukova et al., 2010; Wang et al., 2010). Duplications that are 100-200 kb and deletions greater than 100 kb were most significantly enriched among the severely obese cases (Wheeler et al., 2013). Additionally, deletion of genes that encode G protein-couples receptors (GPCRs) due to rare CNVs was associated with severe obesity (Wheeler et al., 2013).

1.b.vii Epigenetics of obesity

Epigenetics is the study of heritable changes affecting gene expression caused by mechanisms other than changes in the DNA sequence. Individuals who were prenatally exposed to famine have reduced methylation of the imprinted *IGF2* gene (Heijmans et al., 2008; Tobi et al., 2012). These individuals exposed to famine during gestation have increased weight, greater adiposity, decreased glucose tolerance, elevated total cholesterol and triglycerides (Lumey et al., 2009; Ravelli et al., 1998; Stein et al., 2007). Through epigenetic changes, the fetus can be programmed to adapt to famine, leading to weight gain and obesity when the child is raised with access to food (Fiese et al., 2013). In another study, higher methylation of the *RXRA* gene was associated with greater neonatal adiposity (Godfrey et al., 2011). Increased methylation of the *HIF3A* locus was associated with increased BMI (Dick et al., 2014). Variably methylated regions in or near genes *PM20D1*, *MMP9*, *PRKG1* and *RFC5*, which are related to body weight regulation or diabetes, have also been associated with BMI (Feinberg et al., 2010). Progress has been made in discovering epigenetic mechanisms related to obesity risk; however, much remains to be fully elucidated.

1.b.viii Missing heritability in obesity

Several loci and genes have been identified for obesity; however, these only explain a small proportion of the phenotypic variance of weight and heritability (Bogardus, 2009). Identifying the missing heritability has been a goal in obesity and other complex diseases (Manolio et al., 2009). Rare variants, CNVs and epigenetic changes have been proposed to explain rest of the missing heritability, not only for obesity, but also for other complex

traits (Walley et al., 2009). On the other hand, it has been suggested that estimates of heritability may be incorrect and highly inflated (Zuk et al., 2012). Regardless, many other genes and mechanisms causing obesity remain to be discovered.

2. Adipose Tissue

Adipocytes are cells that form and store fat in adipose tissue. Adipose tissue plays a major role in energy homeostasis and thermoregulation, while regulating satiety and reproduction (Berry et al., 2013). In addition to being a fat storage depot, adipose tissue is the largest endocrine organ in the body (Gesta et al., 2007). In mammals, two main classes of adipose tissue exist that have different functions and anatomical locations. White adipose tissue (WAT) is responsible for storing energy. Brown adipose tissue (BAT) is responsible for dissipating energy and generating heat.

2.a White adipose tissue (WAT)

WAT has two main types: subcutaneous WAT and visceral WAT. Subcutaneous and visceral depots have different anatomical locations, microscopic appearance and biological function. Histologically, subcutaneous fat is heterogeneous while visceral fat is uniform. Subcutaneous fat consists of mature unilocular adipocytes with small multilocular adipocytes. In contrast, visceral fat contains primarily large unilocular adipocytes (Berry et al., 2013). In humans, fat distribution influences risks associated with obesity. Measurements of the ratio of waist to the hip circumference (WHR) can be used to estimate fat distribution. Obese individuals with a high WHR, otherwise known as apple-shaped or visceral obesity, are at a high risk for type 2 diabetes, hyperlipidemia

and cardiovascular disease (Grauer et al., 1984). However, obese individuals with a low WHR, otherwise known as pear-shaped or subcutaneous obesity, are at a low risk for metabolic complications due to obesity (Snijder et al., 2003a, 2003b).

2.b Brown adipose tissue (BAT)

BAT is a major site of nonshivering thermogenesis. Originally, BAT was defined as a hibernating organ responsible for maintaining body temperature in hibernating animals (Wu et al., 2013). The thermogenic process in BAT that increases energy expenditure happens through the uncoupling of oxidative metabolism from ATP production. Uncoupling protein 1 (UCP1) is a brown adipocyte specific protein that uncouples the respiratory chain in the mitochondria (Giralt and Villarroya, 2013). BAT consists uniformly of multilocular lipid droplets, and is different in morphology compared to WAT (Berry et al., 2013). Brown adipocytes can be found in WAT following cold exposure (Cinti, 2005).

2.c Tools to study adiposity

Characterizing the physiology of obesity mouse models of is an essential and valuable method in elucidating the roles of genes in obesity. The first step is to generate a weight curve by weighing the genetically modified mice and WT littermates from weaning until death. The age at which the weight difference is significant can be determined and the following experiments can be done at that chosen time point. Subcutaneous and visceral WAT, BAT as well as liver should be dissected and weighed. Fat and lean mass and distribution can be measured by Dual-Energy X-Ray Absorptiometry (DXA) (Gesta et

al., 2007). Hematoxylin and eosin (H&E) staining can reveal cell size of adipocytes, while Oil Red O dye can be used for staining of neutral triglycerides and lipids on frozen sections. Cell size will reveal if there is hypertrophy (increase in cell size) or hyperplasia (increase in cell number) of the adipose tissue. To determine whether the increase in adiposity is due to an increase in calorie intake, how much food mice consume ad libitum should be measured. If the mice have greater food intake compared to WT mice, a pair feeding experiment can be done where the mice are fed the amount of food consumed by WT mice, to see if there will be a loss in adiposity. Cages equipped with beams that can measure horizontal ambulatory and vertical movement can be used to compare activity levels of mice. Metabolic cages that measure the amount of oxygen consumed and carbon dioxide produced can be used to calculate heat output by the mice. The first method that is generally used to test if a dysfunction in BAT function exists is an acute cold challenge where the mice are kept at 4°C for a short period of time to measure core body temperature. Mice that cannot maintain their core body temperature as well as WT mice may have a dysfunction in their BAT, and should be tested further. Gene expression of WAT and BAT markers, BAT-specific and mitochondrial genes, especially *Ucp1*, can hint at BAT dysfunction. The gold standard to directly measure BAT function in mice is the assessment of maximal thermogenic capacity, which is the greatest quantity of heat a mouse can produce. Energy expenditure can be measured in metabolic chambers following the administration of a supramaximal dose of a thermogenic drug to mice in order to activate BAT. A BAT dysfunction in mice prior to obesity can indicate that the modified gene in that mouse model may be involved in BAT function.

3. G proteins

One of the ways cells communicate with each other is through transmembrane signaling. Extracellular stimuli can be recognized by receptors on the cell membrane and turned into intracellular signals. Heterotrimeric guanine nucleotide-binding proteins (G proteins) act as signal transducers which communicate signals from receptors to effectors. G protein-mediated signaling controls diverse cellular and organismal functions such as differentiation, sensation, growth, and homeostasis (Wettschureck and Offermanns, 2005).

3.a Principles of G protein signaling

In mammals, over 1000 different GPCRs exist, which are bound to G proteins residing on the cytoplasmic side of the cell membrane. G proteins are heterotrimers consisting of α, β and γ subunits. To date, 21 α subunits encoded by 16 genes, 6 β subunits encoded by 5 genes and 12 γ subunits have been identified in humans (Oldham and Hamm, 2008). Unique combinations of these subunits form heterotrimeric G proteins which can couple with various GPCRs and activate a variety of effectors. The α subunit has intrinsic GTPase activity. When the GPCR is not bound and is in its basal state, the GDP-bound α subunit is tightly associated with the βγ complex (Figure 1.1). Once the GPCR is bound by a ligand and activated, GDP is exchanged for GTP on the α subunit. The GTP-bound α subunit then dissociates from the βγ complex and the GPCR. The free α subunit and the βγ complex can modulate activity of effectors (Lania et al., 2001; Wettschureck and Offermanns, 2005). The α subunit was originally considered to be the only subunit

involved in signal transduction; however, evidence suggests that the βγ subunit also has a role in activating intracellular effectors (Clapham and Neer, 1997; Ford et al., 1998).

3.b G protein β subunits

G protein β (Gβ) subunits are conserved throughout evolution. In humans, Gβ subunits have high amino acid sequence similarity. Gβ1-4 subunits are 79-90% identical in amino acid sequence. Gβ5 subunit shares 52% sequence similarity to G β1-4 subunits (Khan et al., 2013). Even though high sequence conservation exists, evidence suggests that different Gβ subunits do not have redundant roles in mammals. For example, Gβ1 deficient mice have defects in neural tube closure and neural progenitor cell proliferation resulting in neonatal lethality (Okae and Iwakura, 2010). This phenotype implies that Gβ1 is required for and has specific roles in neurogenesis that are not compensated by Gβ2-5 subunits. On the other hand, mice deficient in Gβ5 are viable but exhibit impaired vision, neurobehavioral development, and neuronal development in cerebellum and hippocampus, as well as dysregulation of multiple genes in the brain (Zhang et al., 2011). Mice deficient in Gβ3 do not have a change in body weight, glucose tolerance and insulin sensitivity or blood pressure, but have slower heart rates compared to WT mice (Ye et al., 2014). These data support that Gβ subunits have distinct functions in signaling. All Gβ subunits are expressed in the mouse brain. Gβ1 and Gβ2 subunits are expressed at higher levels compared to Gβ3 and Gβ5, which are expressed at higher levels compared to Gβ4 in the mouse brain (Lein et al., 2007).

3.c G protein β3 (GNB3) and the *GNB3* C825T polymorphism

Gβ3 is encoded by the *GNB3* gene. In humans, *GNB3* is located on chromosome 12p13 and has 11 exons. One of the best characterized polymorphisms in *GNB3* is the C825T polymorphism (rs 5443) which is located in exon 10 (Figure 1.2). The C to T change does not change the amino acid sequence; TCC to TCT remains Serine. However, alternative splicing of part of exon 9 (nucleotides 498-620) results in an exonic 123-basepair (bp) deletion. The presence of the T allele is associated with the shorter splice variant of Gβ3, called Gβ3-s (encoded by *GNB3*-s), which is 41 amino acids shorter than Gβ3 (Siffert et al., 1998). Cells from individuals with the T allele predominantly express Gβ3-s. Gβ3-s is a functional protein and is also associated with increased activation of G proteins by cell culture (Rosskopf et al., 2003). In order to study the functional properties of Gβ3-s, WT Gβ3 and Gβ3-s were expressed in Sf9 insect cells. [^{35}S] GTPγ binding to permeabilized Sf9 cells was evaluated as a measure of activation of G proteins, and the authors concluded that Gβ3-s is associated with enhanced activation of G proteins (Siffert et al., 1998). However, follow-up studies have shown that Gβ3-s is an unstable and functionally inactive protein, that does not form functional dimers with Gγ subunits (Ruiz-Velasco and Ikeda, 2003; Sun et al., 2012). The specific α and γ subunits that bind Gβ3 are unknown. The allele distribution of the C825T polymorphism differs between ethnicities. The T allele frequency is 79% in black Africans, 46% in Mongoloids, and 33% in Caucasians (Rosskopf et al., 2002; Siffert et al., 1999). The C825T polymorphism in *GNB3* has been associated with increased risk for hypertension, obesity, diabetes, metabolic syndrome, atherosclerosis, depression and tumors (López-León et al., 2008; Sheu et al., 2007; Siffert, 2005; Siffert et al., 1998). Instead of the T or C allele in humans, mice have the A allele, and the amino acid remains Serine. In mice, *Gnb3* is

expressed in the brain, especially in the hypothalamus, thalamus and the olfactory bulb (Lein et al., 2007).

3.d G proteins in obesity

Mutations in some G protein subunit genes result in abnormal signal transduction, and are involved in human disease (Lania et al., 2001; Offermanns and Simon, 1998). For example, impaired taste sensation, defects in metabolism, and a variety of endocrine disorders are caused by mutations in different human Gα subunits (Lania et al., 2001; Moxham and Malbon, 1996; Wettschureck and Offermanns, 2005). Not surprisingly, many G proteins are also candidate genes for obesity (Wettschureck and Offermanns, 2005; Wheeler et al., 2013). Mice deficient in Gβ5 are leaner than WT, resistant to high-fat diet, have increased locomotor activity and increased thermogenesis. On the other hand, mice that lack a single copy of *Gnb5* are heavier than WT, have increased adiposity, insulin resistance, obesity, type 2 diabetes and metabolic syndrome (Wang et al., 2011). Based on the association of the C825T polymorphism in *GNB3* with increased risk for hypertension, obesity and metabolic syndrome, Gβ3 likely has a physiological function related to obesity.

3.e *GNB3* duplication in a childhood obesity syndrome

Our group described a new syndrome associated with obesity and intellectual disability in humans, in which an unbalanced chromosomal translocation leads to duplication of an 8.5-Mb region of chromosome 12p and deletion of a 7.0-Mb region of chromosome 8p (Goldlust et al., 2013) (described in Chapter 2). Though *GNB3* lies within the duplication

of chromosome 12, how *GNB3* copy number or expression contributes to obesity is not known. Since Gβ subunits are important mediators of transmembrane signaling (Ford et al., 1998), an extra copy of *GNB3* could enhance signal transduction in a variety of tissues relevant to obesity. How the *GNB3*-T allele, the associated splice variant, and increased G protein signal transduction contribute to obesity risk are not understood.

4. Dissertation goals

Our group created bacterial artificial chromosome (BAC) transgenic mice with extra copies of *GNB3*-T that weigh significantly more than sex- and age-matched littermates, recapitulating obesity found in patients with the unbalanced translocation (Goldlust et al., 2013). To test whether an extra copy of *GNB3*-T, but not the other 13 genes on the *GNB3*-T BAC, causes obesity, we created transgenic mice with the same BAC, where *GNB3*-T is replaced with a neomycin cassette (Δ*GNB3*-T). Δ*GNB3*-T mice have similar weights compared to their sex- and age-matched WT littermates, showing that overexpression of *GNB3*-T, and not other genes on the BAC, causes obesity in *GNB3*-T/+ mice (described in Chapter 2).

Until now, the role of *GNB3* in feeding, activity and adiposity and the physiological changes associated with overexpression of *GNB3* was undefined. Likewise, we did not know if obesity only occurred when the risk allele, *GNB3*-T, was overexpressed, or if other *GNB3* alleles could also cause a phenotype. In this dissertation, I will test my hypothesis that *GNB3* alleles and expression level alter metabolic profiles and dictate severity of obesity. The goals of my dissertation are as follows:

1. Comprehensively characterize the phenotypic consequences of *GNB3* duplication in *GNB3*-T mice. Describe weight gain, adiposity, adipose histology, feeding, activity, energy expenditure, blood metabolites and gene expression profiles of *GNB3*-T mice (described in Chapter 3).
2. Create other transgenic mouse lines with extra copies of the non-risk allele (*GNB3*-C) and mouse *Gnb3*. Evaluate the contributions of *GNB3* alleles and *GNB3* expression level on obesity (described in Chapter 4).

Together, these goals elucidate the roles of risk allele and gene expression in *GNB3*-related obesity.

Figure 1.1

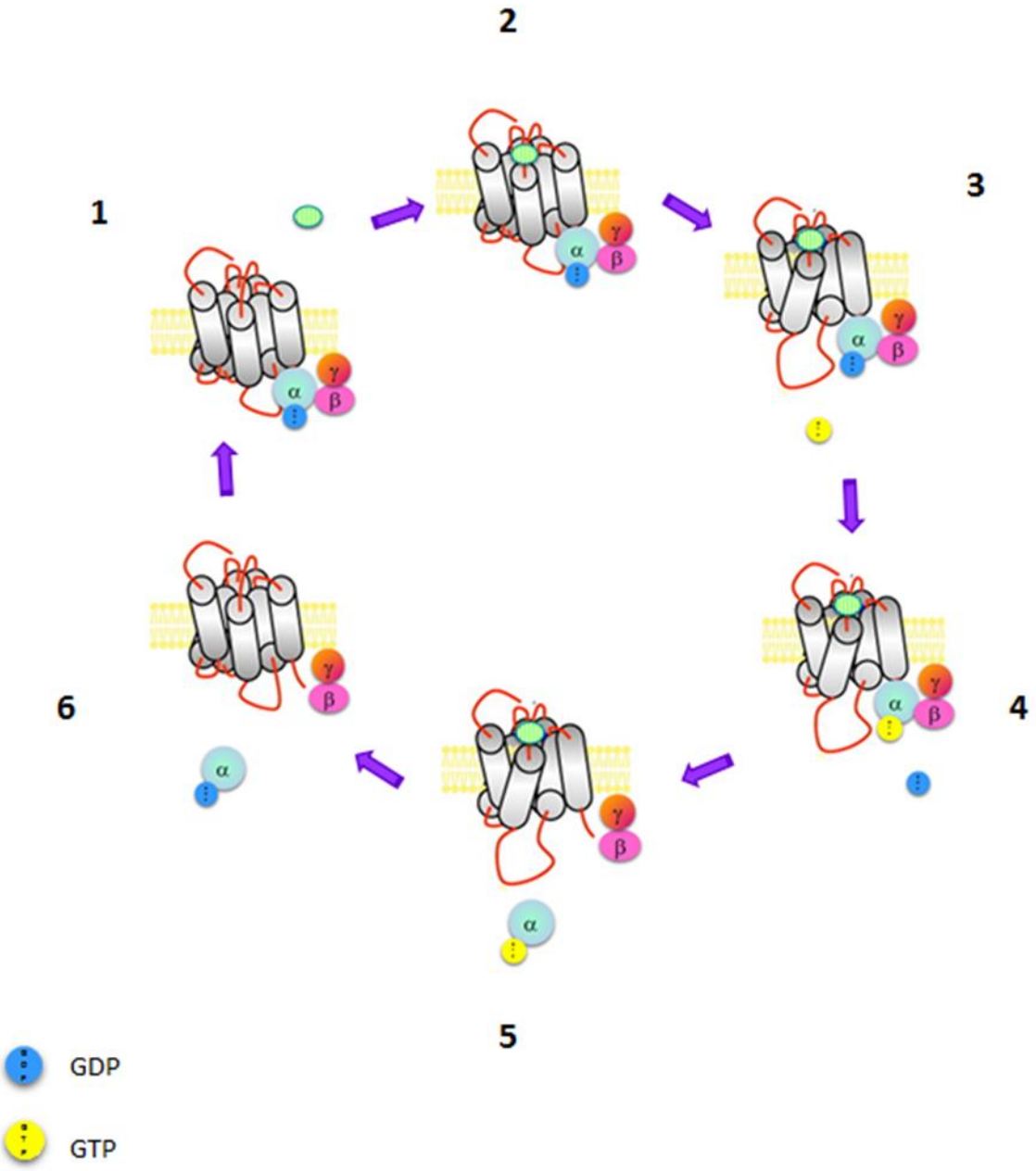

Figure 1.1

Activation cycle of G proteins. The ligand (in green) binds and activates the GPCR. GDP (in blue) is exchanged for GTP (in yellow) on the α subunit. The GTP-bound α subunit dissociates from the βγ complex and the GPCR. The free α subunit and the βγ complex then modulate activity of effectors.

Figure 1.2

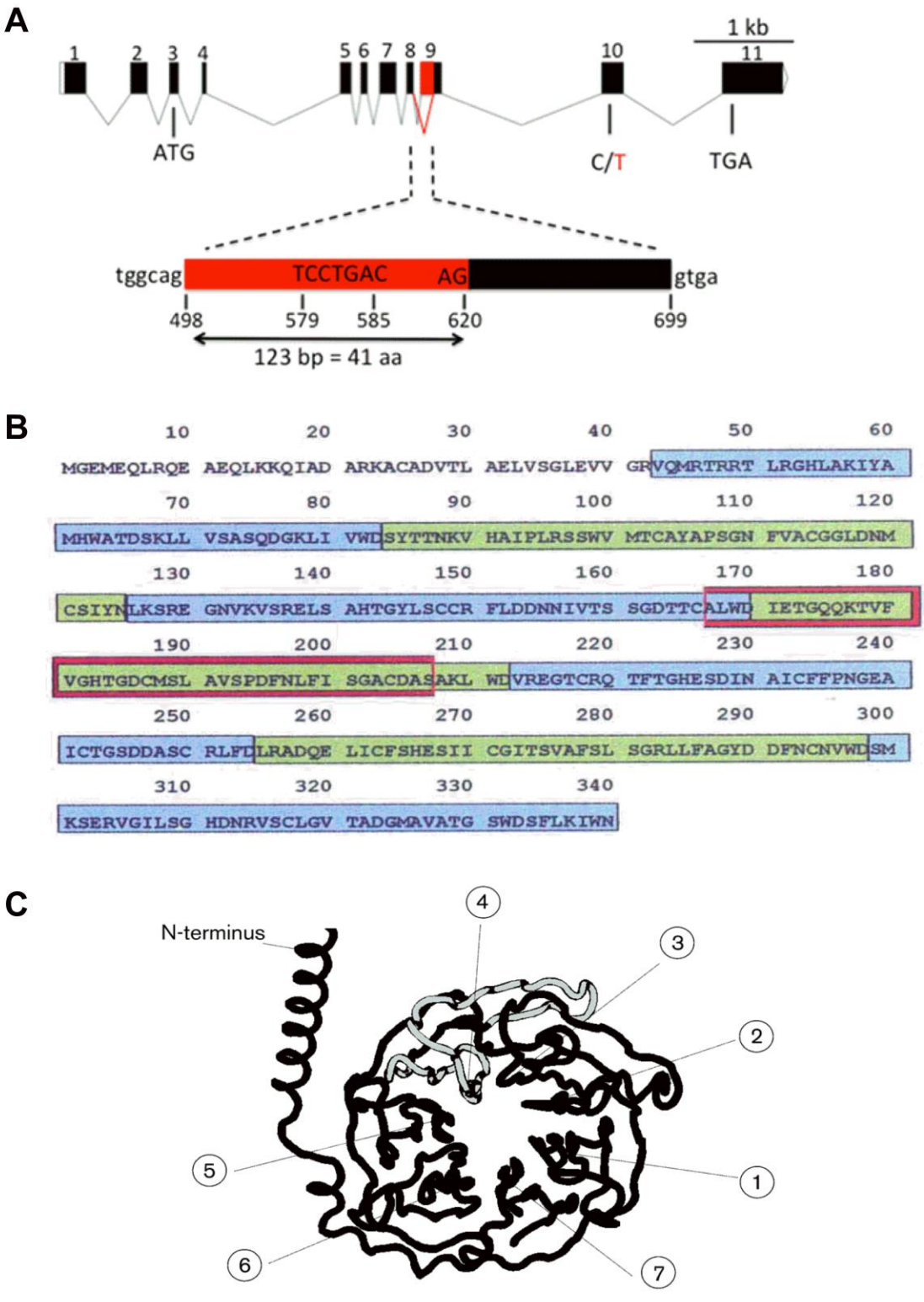
A
1 kb
1 2 3 4 5 6 7 8 9 10 11
ATG
C/T
TGA
tggcag TCCTGAC AG gtga
498 579 585 620 699
123 bp = 41 aa
B
10 20 30 40 50 60
MGEMEQLRQE AEQLKKQIAD ARKACADVTL AELVSGLEVV GRVQMRTRRT LRGHLAKIYA
70 80 90 100 110 120
MHWATDSKLL VSASQDGKLI VWDSYTTNKV HAIPLRSSWV MTCAYAPSGN FVACGGLDNM
130 140 150 160 170 180
CSIYNLKSRE GNVKVSRELS AHTGYLSCCR FLDDNNIVTS SGDTTCALWD IETGQQKTVF
190 200 210 220 230 240
VGHTGDCMSL AVSPDFNLFI SGACDASAKL WDVREGTCRQ TFTGHESDIN AICFFPNGEA
250 260 270 280 290 300
ICTGSDDASC RLFDLRADQE LICFSHESII CGITSVAFSL SGRLLFAGYD DFNCNVWDSM
310 320 330 340
KSERVGILSG HDNRVSCLGV TADGMAVATG SWDSFLKIWN
C
N-terminus
1
2
3
4
5
6
7

Figure 1.2

Structure of *GNB3* and splice variant *GNB3*-s. (A) C825T polymorphism in exon 10 is associated with alternative splicing of exon 9. The 123-bp deletion (red) results from a cryptic branch donor site (nt 579-585) and a cryptic branch acceptor site (nt 619-620). (B) Amino acid sequence of human Gβ3. There are seven WD repeat domains marked alternatively as blue or green. The deleted part in Gβ3-s is marked in red. (Siffert et al., 1998) (C) Structure of Gβ3. The seven WD repeat domains are labeled with numbers. The WD domain deleted in Gβ3-s is in grey. (Rosskopf et al., 2002)

Chapter 2

Mouse model implicates *GNB3* duplication in a childhood obesity syndrome

This chapter was published in part as: Ian S. Goldlust, Karen E. Hermetz, Lisa M. Catalano, Richard T. Barfield, Rebecca Cozad, Grace Wynn, Alev Cagla Ozdemir, Karen N. Conneely, Jennifer G. Mulle, Shikha Dharamrup, Madhuri R. Hegde, Katherine H. Kim, Brad Angle, Alison Colley, Amy E. Webb, Erik C. Thorland, Jay W. Ellison, Jill A. Rosenfeld, Blake C. Ballif, Lisa G. Shaffer, Laurie A. Demmer, Unique Rare Chromosome Disorder Support Group, and M. Katharine Rudd. Mouse model implicates *GNB3* duplication in a childhood obesity syndrome. Proc Natl Acad Sci U S A. 2013 Sep 10;110(37):14990-4. doi: 10.1073/pnas.1305999110. Epub 2013 Aug 26. Author contributions: I.S.G., K.E.H., and M.K.R. designed research; I.S.G., K.E.H., R.C., G.W., A.C.O., and S.D. performed research; I.S.G., K.E.H., L.M.C., R.T.B., G.W., A.C.O., K.N.C., J.G.M., M.R.H., K.H.K., B.A., A.C., A.E.W., E.C.T., J.W.E., J.A.R., B.C.B., L.G.S., L.A.D., U.R.C.D.S.G., and M.K.R. analyzed data; I.S.G. and M.K.R. wrote the paper; and L.M.C., K.H.K., B.A., A.C., A.E.W., E.C.T., J.W.E., J.A.R., B.C.B., L.G.S., L.A.D., U.R.C.D.S.G., and M.K.R. recruited and clinically assessed subjects.

Abstract

Obesity is a highly heritable condition and a risk factor for other diseases, including type 2 diabetes, cardiovascular disease, hypertension, and cancer. Recently, genomic copy number variation (CNV) has been implicated in cases of early onset obesity that may be comorbid with intellectual disability. Here, we describe a recurrent CNV that causes a syndrome associated with intellectual disability, seizures, macrocephaly, and obesity. This unbalanced chromosome translocation leads to duplication of over 100 genes on chromosome 12, including the obesity candidate gene *G protein β3* (*GNB3*). We generated a transgenic mouse model that carries an extra copy of *GNB3*, weighs significantly more than its WT littermates, and has excess intraabdominal fat accumulation. *GNB3* is highly expressed in the brain, consistent with G-protein signaling involved in satiety and/or metabolism. These functional data connect *GNB3* duplication and overexpression to elevated body mass index and provide evidence for a genetic syndrome caused by a recurrent CNV.

Introduction

Body weight exhibits a heritability of ~70% (Feinleib et al., 1977; Moll et al., 1991; Stunkard et al., 1990), with both rare and common alleles contributing to obesity. Few cases of obesity are explained by mutations in single genes, with most confined to the well-known leptin/melanocortin pathway (Blakemore and Froguel, 2010; Choquet and Meyre, 2011a). Genome-wide association studies (GWASs) have identified alleles that confer a small risk for elevated body mass index (BMI) and other measures of obesity, and some common variants involve candidate genes that are highly expressed in the

central nervous system (Bradfield et al., 2012; Speliotes et al., 2010; Thorleifsson et al., 2009; Willer et al., 2009). However, the functional mechanism by which most GWAS loci contribute to obesity is unknown.

Recently, large deletions and duplications that represent copy number variation (CNV) have been linked to early onset obesity in children (Bachmann-Gagescu et al., 2010; Bochukova et al., 2010; Glessner et al., 2010; Walters et al., 2010; Wheeler et al., 2013). Rare CNVs have proven to be highly penetrant in familial and spontaneous cases of obesity that are sometimes concomitant with intellectual disability (ID) and/or other neurodevelopmental disorders. Rare but recurrent CNVs are particularly useful to pinpoint critical regions or candidate genes, because their shared genotype can be correlated with a common phenotype. For example, recurrent deletions of 16p11.2 are enriched in multiple obesity cohorts vs. controls (Bachmann-Gagescu et al., 2010; Bochukova et al., 2010; Walters et al., 2010).

Mouse models have been instrumental in unraveling the genetic mechanisms and signaling pathways involved in obesity, which are critical for the development of therapeutics. Notably, ob/ob mutant mice that lack leptin are morbidly obese and exhibit other features, including hyperphagia, infertility, decreased immune function, and energy and body temperature dysfunction (Coleman, 1978; Friedman and Halaas, 1998). In humans, congenital leptin deficiency causes early onset hyperphagia, hypogonadism, impaired immunity, and severe obesity (Montague et al., 1997). For both ob/ob mice and leptin-deficient humans, leptin replacement ameliorates many of these symptoms (Coppari and Bjørbæk, 2012; Farooqi et al., 1999; Paz-Filho et al., 2011). Mouse models of other metabolic disorders have also proven insightful in teasing apart the physiological

effects of genes involved in obesity (Burns et al., 2010; Lacaria et al., 2012; Ren et al., 2005; Yeung et al., 2013).

Here, we report a syndrome caused by a recurrent chromosomal translocation associated with obesity as well as ID, seizures, macrocephaly, and eczema. Moreover, we have recapitulated the obesity phenotype in a transgenic mouse model and identified the gene responsible for elevated weight gain. This CNV duplication causes a highly penetrant form of early onset obesity.

Results

Genomic Disorder Is Caused by a Recurrent Unbalanced Chromosome Translocation. We recruited seven unrelated patients with a previous diagnosis of an unbalanced translocation between chromosomes 8 and 12 and fine-mapped the breakpoints. All seven subjects share the same genomic rearrangement, resulting in a 7.0-Mb loss of 8p and an 8.5-Mb gain of 12p (Figure 2.1). There are 23 and 107 RefSeq genes within the 8p deletion and 12p duplication, respectively. In each unbalanced translocation der(8)t(8;12)(p23.1;p13.31), which for brevity, we refer to as der(8)t(8;12), the breakpoints are in segmental duplications shared between chromosome bands 8p23.1 and 12p13.31, spanning ~280 kb (Figure 2.2 and 2.3). Recurrent translocations between paralogous segments of the genome are consistent with rearrangement by nonallelic homologous recombination (NAHR) (Giglio et al., 2002; Hermetz et al., 2012; Luo et al., 2011; Ou et al., 2011; Robberecht et al., 2013; South et al., 2008).

Children with the der(8)t(8;12) exhibit developmental delays, ID, seizures, macrocephaly, eczema, and mild dysmorphic features (Figure 2.4, Table 2.1 and 2.2).

Notably, six of seven children with the unbalanced translocation are obese, with BMI values above the 95th percentile (Figure 2.5, Table 2.1). Typically, the weight gain occurs in the first few years of life and continues into adulthood, even when on restricted diets. Subjects 1–4, 6, and 7 have a clinical diagnosis of obesity based on height and weight measurements. To rule out overgrowth, which is characterized as height 2–3 SDs greater than the mean for age and sex (Verge and Mowat, 2010; Visser et al., 2009), we analyzed the heights of children with the der(8)t(8;12) and found that none met the clinical criteria (Table 2.2).

Obesity Candidate Gene G protein β3 Is Duplicated. Among 107 genes duplicated in children with the unbalanced translocation, one gene of particular note is *G protein β3* (*GNB3*). Polymorphisms in *GNB3* are associated with hypertension, diabetes, and obesity (Klenke et al., 2011). The most studied polymorphism is a cytosine-to-thymine change (c.825C > T, commonly known as C825T) in exon 10 of *GNB3* that is synonymous at the amino acid level (TCC to TCT Serine). However, the T haplotype is linked to a shorter in-frame splice variant, *GNB3*-s, which lacks part of exon 9 (Siffert et al., 1998). Although total mRNA expression and protein levels are not significantly altered by the C825T polymorphism (Siffert et al., 1998; Sun et al., 2005), cell culture assays have shown that cells derived from CT heterozygotes or TT homozygotes have increased activation of G proteins compared with CC homozygotes (Siffert et al., 1998). We reasoned that an extra copy of *GNB3* because of the der (8)t(8;12) could, like the C825T polymorphism, alter G protein signaling and confer increased risk of obesity.

Mouse Model of GNB3 Duplication Recapitulates Obesity Phenotype. To test this hypothesis, we developed BAC transgenic mice that carry an extra copy of human *GNB3*.

The BAC insert sequence is 184 kb and contains 14 genes from 12p13.31, including the T variant of *GNB3*. We confirmed the BAC insertion by FISH and array comparative genome hybridization (Figure 2.6) and bred founders with wild-type animals to generate offspring. Starting at weaning, we weighed 30 transgenic (*GNB3*/+) and 22 wild-type (+/+) littermates derived from a single founder (Line 5) (Figure 2.7). Taqman quantitative PCR assays revealed two copies of the BAC in *GNB3*/+ mice (Figure 2.8). We used a linear mixed model to analyze the longitudinal effects of the presence of the BAC transgene on mouse weight. The weight of the mice is significantly associated with transgene genotype (P = 0.00199). On average, male and female *GNB3*/+ mice are 4.1–7.5% and 6.0–14.3% heavier, respectively, than their +/+ littermates from age 7 wk (Figure 2.7). We found similar weight differences between +/+ and *GNB3*/+ animals from two other transgenic founder lines (Lines 3 and 4) (Figure 2.9), ruling out insertional effects of the transgene. Furthermore, we dissected and weighed gonadal white adipose tissue (WAT) in *GNB3*/+ and +/+ littermates. WAT percent (WAT/body weight) of *GNB3*/+ mice is significantly greater than +/+ mice in females (P = 0.0122) and males (P < 0.0001; Student's *t*-test) (Figure 2.10A).

To measure transgenic *GNB3* and endogenous *Gnb3* expression, we performed quantitative RT-PCR (qRT-PCR). Using RNA from brains of *GNB3*/+ and +/+ littermates, we detect human *GNB3* expression from *GNB3*/+ but not +/+ mice. In addition, human *GNB3* expression is significantly greater than endogenous *Gnb3*, as measured by cycle threshold (Ct) values from multiple primer pairs (Figure 2.10B). These qRT-PCR experiments measure total *GNB3* and *Gnb3* transcript levels rather than the relative contributions of full-length transcripts and splice variants; however, these

data are consistent with overexpression of *GNB3* from the human transgene in *GNB3*/+ mice. Because of the similarity between the β-subunits of G proteins, we cannot distinguish GNB3 from related proteins by Western blot. Using a GNB-common antibody, we detected high levels of protein in mouse brain and adipose tissues (Figure 2.11 and 2.12). However, we cannot specifically measure GNB3 abundance in +/+ vs. *GNB3*/+ animals, because the antibody is predicted to detect multiple human and mouse β-subunits.

To confirm that *GNB3* is responsible for the obesity phenotype in transgenic animals, we replaced *GNB3* with a neomycin resistance gene to recombineer a construct that retains the other 13 genes in the BAC but not *GNB3* (Δ*GNB3*). We generated Δ*GNB3* transgenic mice and compared the weights of Δ*GNB3*/+ and +/+ littermates. Δ*GNB3*/+ mice have three copies of the BAC transgene (Figure 2.8). The weight of the mice is not significantly associated with the transgenic Δ*GNB3*/+ genotype (P = 0.104) (Figure 2.7B). To rule out the unlikely possibility that the entire Δ*GNB3* construct was silenced, we also measured expression of *MLF2*, another human gene on the BAC. We performed qRT-PCR to amplify *GNB3*, *Gnb3*, *MLF2*, and *Mlf2* transcripts in brains from Δ*GNB3*/+ and +/+ littermates (Figure 2.10B). *MLF2* is expressed at similar levels in the brains of Δ*GNB3*/+ and *GNB3*/+ animals, consistent with normal expression from the Δ*GNB3* BAC. These data support our hypothesis that duplication of *GNB3* is responsible for the obesity phenotype.

Translocation Formation and Incidence. The unbalanced translocation between chromosomes 8 and 12 is rare; it may be inherited from a parent with the balanced translocation, or it may be a new (de novo) event in the proband. We analyzed the

inheritance of the der(8)t(8;12) by FISH and found that four rearrangements were de novo and three rearrangements were inherited from a mother who carries the balanced translocation (Figure 2.4). To determine the parental origin of the four de novo rearrangements, we performed genome-wide SNP genotyping using the Affymetrix 6.0 platform. All four de novo translocations were derived from the maternal chromosomes 8 and 12, consistent with a maternal bias in this NAHR-mediated translocation.

Copies of the segmental duplications that mediate the translocation between chromosomes 8 and 12 are also present on the short arm of chromosome 4. A recurrent translocation between chromosomes 4 and 8, also mediated by NAHR, is a well-known genomic rearrangement that, when inherited in an unbalanced fashion, causes Wolf–Hirschhorn syndrome [der(4)t(4;8)] (Giglio et al., 2002; Wheeler et al., 1995) or a milder ID syndrome [der(8)t(4;8)] (Tranebjaerg et al., 1984). Familial studies have shown that the translocation between chromosomes 4 and 8 always originates maternally (Giglio et al., 2002). Because of the homology between segmental duplications on chromosomes 4, 8, and 12, recurrent translocations between chromosomes 4 and 12 are also possible. There is one report of a der(4)t(4;12) unbalanced translocation in a child with ID, macrosomy, macrocephaly, dysmorphic features, and epilepsy (Benussi et al., 2009).

Given the incidence of the der(8)t(8;12), we would expect to find children with the reciprocal unbalanced translocation resulting in 8p trisomy and 12p monosomy. However, the unbalanced der(12)t(8;12) is not reported in large studies of pathogenic CNV, including the Unique Rare Chromosome Disorder Support Group database, the Database of Chromosomal Imbalance and Phenotype in Humans using Ensembl Resources, the International Standards for Cytogenomic Arrays Consortium, or Signature

Genomic Laboratories (Cooper et al., 2011; Firth et al., 2009; Kaminsky et al., 2011). Individuals with the der(12)t(8;12) are likely missing from CNV studies due to embryonic lethality caused by heterozygous loss of many genes on 12p. Trisomy for portions of 12p has been reported previously in children with ID and epilepsy (Segel et al., 2006). However, children with large deletions of 12p are absent from the literature, consistent with a chromosome rearrangement incompatible with life.

Discussion

Although the der(8)t(8;12) unbalanced translocation has been previously reported in three children with ID (Margari et al., 2012; Ou et al., 2011; Segel et al., 2006), our finding connects this genomic rearrangement with ID, seizures, macrocephaly, eczema, and obesity in multiple individuals and suggests that, like other recurrent CNVs (Mefford and Eichler, 2009), the der(8)t(8;12) translocation constitutes a unique genomic syndrome. As is the case for the recurrent translocation between chromosomes 4 and 8, all of the de novo der(8)t(8;12) translocations are maternally derived. Because NAHR occurs during meiosis (Lupski, 2004; Turner et al., 2008), this maternal bias in translocation formation could suggest a higher risk for aberrant interchromosomal recombination during female meioses. Additional studies of der(8)t(8;12) families are necessary to investigate this maternal bias in a larger cohort.

The der(8)t(8;12) unbalanced translocation is one of several newly discovered CNVs associated with obesity. Collectively, such CNVs contribute to the missing heritability of obesity that is not explained by rare single-gene mutations or more common variants identified by GWASs. Polymorphisms in *GNB3* have been recognized

as a risk factor for obesity and related disorders; however, this study connects *GNB3* gene duplication to a highly penetrant form of obesity. Furthermore, our mouse model of *GNB3* duplication recapitulates the obesity phenotype and reveals overexpression of *GNB3* in the brains of transgenic animals. In both transgenic mice and humans with the der(8)t (8;12), *GNB3* duplication leads to moderate elevation in body weight. Control experiments with Δ*GNB3* mice confirm that *GNB3* is largely responsible for the weight gain phenotype; however, we cannot rule out additional subtle effects from other genes within the CNV. It is possible that smaller duplications, including *GNB3* and/or variation in *GNB3* expression, are also associated with childhood obesity. However, small duplications of *GNB3* have not been described in databases of clinically recognized CNVs (Cooper et al., 2011; Firth et al., 2009; Kaminsky et al., 2011). The absence of small *GNB3* duplications is not surprising, because most children referred for clinical cytogenetic testing are referred for neurodevelopmental disorders rather than isolated obesity.

We have linked the obesity phenotype to 1 of ~130 genes deleted or duplicated as part of the der(8)t(8;12) unbalanced translocation, but it is important to point out that there are many genes on 8p and/or 12p that could be responsible for other syndromic features, including ID, seizures, macrocephaly, eczema, and dysmorphic facies. Nevertheless, our studies connect *GNB3* gene dosage to obesity and provide a model of the functional significance of *GNB3* in BMI. Rare CNVs that include G protein-coupled receptor genes are enriched in cases of early onset obesity, and pathway analysis has revealed gene networks involving *GNB3* (Wheeler et al., 2013). As in our study, these CNV data suggest that G proteins play an important role in the genetics of obesity. We

anticipate that human and mouse studies of *GNB3* duplication and risk alleles will lead to a better understanding of cell signaling, physiology, and behaviors involved in childhood obesity. Additional investigation into *GNB3*-related pathways may point to novel therapeutics for the growing obesity epidemic.

Materials and Methods

Human Subjects. This study was approved by the Emory University Institutional Review Board. We recruited subjects from the Unique Rare Chromosome Disorder Support Group (www.rarechromo.org) and clinical cytogenetics laboratories. Samples, photos, and clinical information were obtained with informed consent per our human subjects protocol. We received peripheral blood and/or DNA samples from subjects and their parents. Samples from families 1–5 were EBV-transformed to create lymphoblastoid cell lines using standard methods.

Array Comparative Genome Hybridization. We used two custom oligonucleotide arrays for mouse and human experiments; both array designs are available on request (Agilent Technologies). We extracted genomic DNA from cell lines and peripheral blood samples using the Gentra Puregene DNA Extraction Kit. Subject DNA was cohybridized with reference DNA (from cell line GM10851 or GM15510) to a 4 × 44,000 array, with oligonucleotide probes spaced, on average, every 75 kb throughout the genome (Figure 2.1); the unique identifier (AMADID) for the design is 016267 (Baldwin et al., 2008). To confirm the BAC insertion in transgenic mice, we cohybridized genomic DNA from *G protein β3*/+ (*GNB3*/+) and wild-type (+/+) animals to a 4 × 180,000 array. The higher-

resolution 4 × 180,000 array targets chromosomes 8p23.1 and 12p13.31 with a mean probe spacing of one oligonucleotide per 250 bp (AMADID 031255).

Arrays were scanned using the Agilent High-Resolution C Scanner, and signal intensities were evaluated using Feature Extraction Version 9.5.1.1 software (Agilent Technologies). We used Genomic Workbench 5.0 software to analyze the array data and call breakpoints.

Translocation Breakpoint Sequencing. We designed PCR primers to amplify the translocation junction between chromosomes 8 and 12 in subjects with the der(8)t(8;12). Primers 8.1 (5′-GTGTAAGACGTCGATACGATACGGCACTTC-3′) and 12.4 (5′-GAACCCGATGTCAACAACAC-3′) amplify an ~1-kb band in subject 4. Primer 12.4 was designed to be specific for chromosome 12p13.31, but primer 8.1 anneals to multiple sites within the distal repeat (REPD) segmental duplications in 8p23.1 (Ou et al., 2011). Amplicons were TA-cloned and end-sequenced from the plasmid vector using standard methods. The junction sequence is shown in (Figure 2.3).

C825T Genotyping. All probands and their family members were genotyped for the C825T polymorphism using a previously described restriction enzyme assay (Nikitin et al., 2007). Briefly, a 260-bp PCR amplicon was amplified by primer GNB3-1 (5′-CCTTACCCACACGCTCAGAC-3′) and antisense primer GNB3-2 (5′-GTCTGATCCCTGACCCACTT-3′) and digested with *BsaJI* (R0536S; NEB), resulting in two fragments of 166 and 94 bp for the C allele and an uncut 260-bp fragment for the

T allele (Figure 2.13).

Pyrosequencing. We genotyped the three GNB3 alleles in subjects 1–7 for the C825T polymorphism by pyrosequencing. We performed PCR with a forward primer (5′-CATCTGCGGCATCACGTC-3′) and a biotinylated reverse primer (5′-biotin CGTCGTAGCCAGCGAATAGTAGG-3′); 50-μL reactions contained 10 pmol each primer and 20–40 ng genomic DNA. PCR conditions were as follows: 95 °C for 10 min; 50 cycles at 95 °C for 15 s, 57 °C for 30 s, and 72 °C for 15 s; 72 °C for 5 min; and 4 °C hold. PCR products were sequenced with primer 5′-CATCTGCGGCATCAC-3′ on the PSQ 96MA machine according to manufacturer's instructions (Qiagen). Pyrosequencing experiments were performed in triplicate. We calculated the T:C ratio for the C825T SNP using peak heights, taking into consideration the invariant cytosine nucleotide immediately 5′ of the C825T SNP. The anticipated ratios for trisomic genotypes (including the three copies of the 5′ C added to the peak height of the C at position 825) are as follows: CCC, 0:6; CCT, 1:5; CTT, 2:4; and TTT, 3:3. Raw peak height values and T:C ratios are listed in Table 2.3.

Parent-of-Origin Studies. Parent of origin was determined by analyzing genomic DNA from subjects and their parents on the Affymetrix Human Genome-Wide SNP Array 6.0. Genotyping was performed with the Birdseed algorithm in the Affymetrix Power Tools software package. We analyzed informative SNPs in the trisomic region of 12p by SNP cluster graphs to determine the parental origin of the additional allele. In the monosomic

region of 8p, parent of origin was determined by inferring the origin of the missing allele in the proband.

Transgenic Mice. To generate transgenic animals, we selected a human BAC with a 184-kb insert (RP11-578M14). RP11-578M14 includes 14 RefSeq genes: *GNB3*, *MLF2*, *CD4*, *PTMS*, *LAG3*, *COPS7A*, *GPR162*, *LEPREL2*, *CDCA3*, *USP5*, *TPI1*, *SPSB2*, *RPL13P5*, and *DSTNP2*. BAC DNA was prepared with the HiSpeed Plasmid Maxi Kit (12663; Qiagen) with the following modifications. After the eluent was collected from the HiSpeed Tip, it was precipitated using 0.7 volumes isopropanol and centrifuged immediately at 15,000 × g for 30 min at 4 °C. The pellet was washed with 15 mL 70% ethanol in water and centrifuged at 15,000 × g for 10 min at 4 °C. The pellet was then air dried for 10 min, resuspended in 100 μL ddH20, and left to rehydrate overnight at 65 °C.

We recombineered the Δ*GNB3* BAC using the Quick and Easy BAC Modification Kit (Gene Bridges) following the manufacturer's instructions. Forward (5′-GCCTGGGAGCAGCGTGCGGGCCTTCCCTCCACTTGAAATCCGTTGCCCGCTG GACAGCAAGCGAACCGGAATTGC-3′) and reverse (5′-ACCTGGGTCTTTTTGGA-ACAGAAGAGAGTAGAAGGCAAACATCACAGATGTCAGAAGAACTCGTCAAG AAGGCG-3′) oligonucleotides target *GNB3* for replacement with neomycin. After recombineering, we confirmed deletion of *GNB3* by sequencing across the *GNB3*–neomycin junctions.

To prepare DNA for pronuclear injection, 10 μg RP11-578M14 and Δ*GNB3* BAC DNA were linearized using 20 units *AscI* (R0558S; NEB) at 37 °C for 2 h. Linearized BAC was separated on a CHEF Mapper XA Pulsed Field Electrophoresis System

(BioRad) with the following conditions: 1% low-melting point agarose, 6 V/cm, 14 °C, 24 h, switch times ramped linearly from 1 to 25 s. The MidRange PFG Marker I (N3551S; NEB) was used to confirm the size of the linear BAC. The appropriate band was excised from the gel, digested with the recommended amount of β-agarase I (M0392S; NEB) according to the manufacturer's instructions, and concentrated in a vacuum concentrator to ∼100 μL. The DNA was dialyzed overnight on a 0.025-μm drop dialysis filter (9004–70-0; Millipore) in polyamine buffer (10 mM Tris·HCl, pH 7.5, 0.1 mM EDTA, 30 μM spermine, 70 μM spermidine, 100 mM NaCl).

DNA concentration was adjusted to 0.4–0.8 ng/μL with polyamine buffer for microinjection into fertilized eggs collected from FVB mice (Charles River Laboratories). Intact microinjected eggs were transferred to the oviducts of pseudopregnant recipients. To identify transgenic founders, 5-mm tail biopsies were collected for DNA extraction when the potential founders were 12 d old. Ear pieces were collected for those mice that were genotyped positive from initial screening for additional confirmation.

Genotyping for founders and offspring was performed in duplicate by Transnetyx using quantitative PCR to detect the presence or absence of a BAC-specific sequence in each sample. The quantitative PCR probe targets the 5′BAC end sequence of human BAC RP11-578M14; this sequence is present in *GNB3* and Δ*GNB3* transgenic mice.

Five transgenic founder animals were generated for the *GNB3* BAC construct (RP11-578M14). One founder line (Line 5) was followed for the purposes of this study, two founder lines (Lines 3 and 4) were expanded in smaller numbers of F1 offspring, and two founder lines (Lines 1 and 2) did not produce transgenic offspring before dying. One

founder line was generated for the Δ*GNB3* construct. Mice were maintained in compliance with the Institutional Animal Care and Use Committee at Emory University. Mice were maintained on a regular laboratory rodent diet (Purina LabDiet 5001) and weighed three times a week (typically Monday, Wednesday, and Friday). All mice were housed in static microisolator cages in an Association for Assessment and Accreditation of Laboratory Animal Care (AAALAC)-accredited facility in accordance with the National Research Council's Guide for the Care and Use of Laboratory Animals. Animal rooms were climate-controlled to provide temperatures of 22–23 °C on a 12-h light/dark cycle (lights on at 0700 h).

BAC Copy Number Analysis. DNA was extracted from mouse tails using standard conditions, and DNA concentration was measured using a Qubit Fluorometer (Life Technologies). Taqman Copy Number assays (PN 4397425; Life Technologies) were performed in quadruplicate for each primer set following the manufacturer's instructions. Custom primers were designed by Life Technologies to amplify the vector of the RP11-578M14 BAC (forward: 5′-CGTTTATTCTACACTGACTATTCCGGTAA-3′; reverse: 5′-CTCCGTTGATTTTGAGTGTGTCATC-3′; reporter: 5′-ACGGCAAACAAAGCCT-GACAAC-3′) and amplified in parallel with mouse *Tfrc* reference primers (4458366; Life Technologies). Fifteen-microliter reactions were performed in 384-well plates with 10 ng genomic DNA and the following PCR conditions: 95 °C for 10 min and 40 cycles at 95 °C for 15 s and 60 °C for 60 s using the 7900 HT Fast Real-Time PCR System as per the manufacturer's protocol (PN 4397425; Life Technologies). BAC copy number was analyzed with CopyCaller software (PN 4412907; Life Technologies).

RNA Isolation. Mouse brains were harvested and immediately stored in 10 volumes Allprotect Tissue Reagent (76405; Qiagen). Samples were homogenized using the Omni THQ Digital Tissue Homogenizer (Omni International) and processed using the RNeasy Lipid Tissue Mini Kit (74804; Qiagen) according to the manufacturer's instructions with the optional on-column DNase digestion step. Samples were stored at −80 °C until needed.

Quantitative RT-PCR. RNA was reverse-transcribed into cDNA using the High Capacity cDNA Synthesis Kit according to the manufacturer's instructions (4368814; Applied Biosystems). Reverse transcription conditions were as follows: 25 °C for 10 min; 37 °C for 120 min; 85 °C for 5 s; and 4 °C hold. The cDNA was amplified by real-time PCR in triplicate using an ABI 7900HT Fast Real-time PCR System (Applied Biosystems). Taqman primers and probes were purchased from Applied Biosystems (Hs01564092_m1 for exons 4 and 5 of *GNB3*, Mm00516380_g1 for exons 2 and 3 of *Gnb3*, Mm00516381_m1 for exons 3 and 4 of *Gnb3*, Hs01088031_g1 for exons 3 and 4 of *MLF2*, Mm01185203_g1 for exons 7 and 8 of *Mlf2*, and 4352341E for *Actb*) and run according to the manufacturer's instructions. The Taqman primers are specific for mouse or human orthologs (Figure 2.10). The cycling conditions were as follows: 50 °C for 2 min; 95 °C for 10 min; and 40 cycles at 95 °C for 15 s and 60 °C for 1 min.

FISH. FISH studies of subjects and their parents were performed in clinical cytogenetics laboratories to detect balanced and unbalanced translocations between chromosomes 8

and 12. FISH was performed on metaphase chromosomes from human lymphocytes using standard techniques.

FISH was also performed on mouse chromosomes to detect the insertion of BAC RP11-578M14 in *GNB3*/+ animals. Kidneys from a *GNB3*/+ and a +/+ animal were dissected and cultured separately as described previously (McGraw et al., 2010). Briefly, kidneys were manually minced with scalpels, resuspended in 0.25% collagenase B in PBS, and incubated at 37 °C for 1 h. Each culture was resuspended in 10 mL complete DMEM media and grown for 1–2 wk. Metaphase chromosomes were prepared and hybridized with BACs RP11-578M14 and RP23-384O24 using standard techniques.

Western Blot Analysis. Protein was extracted from brain and adipose tissues from 4- and 35-wk-old mice using lysis buffer of 50 mM Hepes, 150 mM NaCl2, 10% glycerol, and 1% Triton-X-100 (pH 7.5) with the recommended amount of complete protease inhibitors (11873580001; Roche Applied Science). Adipose and whole-brain tissues were homogenized using the Omni THQ digital tissue homogenizer (Omni International), lysed for 1 h at 4 °C, and cleared two times by centrifugation at 18,000 × g for 20 min; 10 μg total protein were separated by SDS/PAGE on a 4–20% polyacrylamide gel and transferred to a PVDF membrane using the TransBlot Turbo Transfer System (BioRad). In addition, human adipose tissue lysate (XBL-11048; ProSci) and two commercially available normal mouse tissue blots were blotted with the same conditions below (1561 and 1562; ProSci) (Figure 2.11 and 2.12).

Membranes were blocked for 1 h at room temperature with 5% blotting-grade blocker (170–6404; BioRad) and dissolved in Trisbuffered saline with Tween. Western

blot analysis was performed with a rabbit polyclonal antibody to GNB3 that reacts with mouse, rat, and human GNB proteins (ab72409; Abcam). The primary antibody was diluted 1:300 in 5% blotting-grade blocker and incubated overnight at 4 °C; an HRP-conjugated goat antirabbit IgG secondary antibody (ab6721; Abcam) was diluted 1:3,000 in 5% blotting-grade blocker and incubated for 1 h at room temperature. Protein concentrations were determined by Bio-Rad protein assay (500–0006; BioRad) and confirmed by probing with an antibody to HSP90 (1:1,000 dilution, ab90555; Abcam). Bands were detected using enhanced chemiluminescent reagent (RPN2132; GE Healthcare) according to the manufacturers' instructions, and images were captured using a ChemiDoc XRS+ System (BioRad).

Detailed Phenotypic Information. Phenotypic information for subjects 1–7 is given in Table 2.1. Additional clinical information is described below.

Subject 1. Subject 1 was born to a 33-y-old G1P0 mother after a normal pregnancy. The subject had a short period of failure to thrive because of oral hypotonia that did not allow her to breastfeed. After she switched to formula, she gained weight, and by 5 mo of age, she was obese. She had severe generalized hypotonia that has improved with age, although she still tires easily. Subject 1 has been described as having an immature gait and a wide-based clumsy gait. Her eye examination revealed amblyopia, strabismus, and exophoria. She is very outgoing, friendly, happy, and social; she never stops talking. She has mild to moderate intellectual disability, with an intelligence quotient (IQ) of 55. Her dysmorphic features include ptosis, a narrow, higharched palate, strong sideways lateral

tongue thrust, macroglossia, crooked teeth, late erupting teeth, and foot deformities (varus and valgus). Additionally, she has nocturnal enuresis, impaired hearing, mitral valve prolapse, Wolff–Parkinson–White syndrome, a pineal gland cyst, constipation, poor body temperature regulation, and left hemiparesis. Her first tonic–clonic seizure occurred at 26 mo of age. At that time, she began taking phenobarbital and had intermittent seizure breakthroughs (approximately one major seizure episode every 2 y). At 14 y old, she started Tegretol but had a breakthrough seizure episode. She then started taking Carbatrol XR. She is now taking Carbatrol XR and Topamax. She is also taking doxycycline for acne, lactulose solution for constipation, Diastat for emergency seizures, ketoconazole shampoo and Taclonex scalp for seborrheic dermatitis of the scalp, clindamycin phosphate for acne, Lamisil, calcium citrate, and a multivitamin.

Subject 2. Subject 2 was born to a 33-y-old G1P0 woman after a pregnancy that was complicated by preterm labor at 27 wk gestation that resolved with bed rest. He rolled over at 6 months, stood while holding before 1 y of age, crawled after his first birthday, and sat alone/pulled to stand before 18 mo of age. He was walking by 16 mo of age. His first word was at 7.5 mo of age. Between 2.5 and 3.5 y of age, subject 2 had three febrile seizures. At age 5 y, he had a complex partial seizure. His last febrile seizure was at age 9 y. He had a tonic–clonic seizure at age 13.5 y. Typically, he has one absence seizure per week. His gait can be unsteady when his muscle tone is low or when he is loose-jointed or tired. At age 13.5 y, he was working at a first grade level for math and a second grade level for reading. His dysmorphic features include hypertelorism, mildly down slanting eyes with mild ptosis, prominent nasal bridge, high-arched palate, bilateral fifth finger

clinodactyly, macrocephaly, rounded facies, telecanthus, inverted nipples, and a beaked nose. Additionally, he has flat feet, heat intolerance, echogenic kidneys, daytime enuresis, asthma, astigmatism, gastrointestinal reflux since infancy, constipation, vasovagal episodes, dental crowding, and eczema that is exacerbated by eating tomatoes. His medications include coenzyme Q, carnitine, Flovent, Intal, Ventolin, Similac Junior, magnesium, zinc, and fish oil. He takes Lamictal (since age 10.5 y), Trileptil, Keppra, and Frisium for seizures and Diastat for emergency seizures. He also takes Allegra, Rhinacort, QVAR, Glycolax, and Ativa.

Subject 3. Subject 3 was born to a G1P0 mother with a history of bipolar disorder and schizophrenia. During pregnancy, his mother was treated with Zoloft and Prozac. He is the only child of both of his parents and was reported to be a happy baby. Subject 3 crawled at ~3 y, walked at approximately 4.5 y, and started to speak at approximately 4.5 y. At age 11 y and 8 mo, he was learning the curriculum of a kindergarten level. He had febrile seizures during his first year of life as well as a prolonged seizure at 3 y of age. He had one tonic–clonic seizure at age 7 y. Generally, he has absence seizures several times daily. He has hypotonia and an awkward and wide-based gait. He wears a helmet because of his poor coordination. His eye examination revealed exotropia, iris disorders, refractive amblyopia, and astigmatism. His dysmorphic features include a small mouth, dental crowding, prominent eyebrows, and a large forehead. Additionally, he has aggressive behavior and obsessive–compulsive disorder. He continues to have problems with bowel movements and constipation. He tends to have croup during an upper

respiratory illness. His medications include Paxil, which was discontinued at 11 y and 3 mo, Trilepltal for seizures, Abilify for aggression, and Strattera for hyperactivity.

Subject 4. Subject 4 was born to a G3P1021 mother. No pregnancy or birth history was reported. Subject 4 was hypotonic as an infant. She is mildly dysmorphic with prominent cheeks and facial fullness. At age 7 y, she functioned at the developmental level of age 3.5 y. She has generalized seizures in addition to daily head bobbing and staring spells that began between ages 4 and 6 y. Her eye problems include intermittent left exotropia. MRI revealed a stable pineal cyst. She takes Keppra for seizures, which was tapered and discontinued at age 9 y. At 10 y old, her weight remains significantly greater than 2 SDs above normal.

Subject 5. Subject 5 was born to a G1P0 mother. At age 5 y and 8 mo, he had a cognitive age of ~2 y and 9 mo. He walked late and wears leg splints. He tires quickly and has a tendency to fall over, but his stamina and walking skills are continuing to improve. He has poor muscle tone and had his Achilles tendons lengthened. Subject 5's eczema was severe when younger, but it has improved with age. He is quite social and enjoys being around people, especially family. He has a high arched palate. Since infancy, he has taken Epaderm for his eczema. For the last couple of years, he uses Hyoscine patches to control excess saliva. At one time, he blanked out for a short period, but he has not been formally diagnosed with a seizure disorder.

Subject 6. Subject 6 was born to a G1P0 mother after an uncomplicated pregnancy. He has a younger sister who is developing normally. His developmental delays were noticed at 9 mo of age when he was not crawling and seemed to be dragging his left leg. He walked unassisted at 3 y and 2 mo. Subject 6 has three to five absence seizures daily, and he had a generalized seizure at 3.5 y. He has problems with coordination and a clumsy gait. His dysmorphic features include coarse facies, periobital puffiness, and a prominent lower lip. He has left hemiparesis and speech articulation problems. MRI showed chronic significantly diffusely decreased cerebral hemispheric white matter volume, thinning of the corpus callosum, and a right frontoparietal porencephalic cyst adjacent to the body of the right lateral ventricle. He has taken Keppra since his generalized seizure at 3.5 y.

Subject 7. Subject 7 had slow developmental progress with therapeutic interventions and no regressions. She has poor coordination and a broad-based gait. Her eye problems include bilateral alternating exotropia and delayed visual development. She has a history of eczema, especially during the first year of life. Her facial dysmorphic features noted are round face, broad cheeks, flat broad nasal bridge, epicanthal folds, short nose with small alae nasi, microganthia, and posterior rotated ears that are not low set with a simple upper helical pattern. She has recurrent respiratory infections with left lower lobe pneumonia and a lung abscess. She has herpes simplex infection on her skin. She has taken Lactobact and Valaciclovir in the past.

GNB3 Genotyping. Children with the der(8)t(8;12) have three copies of *GNB3*, which may correspond to the C or T haplotype. It is possible that more copies of the T haplotype

exacerbate weight gain. To probe this possibility, we genotyped the C825T polymorphism in the three *GNB3* alleles of children with the der (8)t(8;12) using two complementary approaches: a restriction site assay and pyrosequencing (Figure 2.13 and Table 2.3). We found no obvious correlation between *GNB3* genotype and body mass index in our seven subjects (Table 2.1); this observation could be confounded by differences in age and sex in a small number of individuals.

Statistical Analysis. To analyze the longitudinal effect of the BAC transgenes on mouse weight, we used the R package *nlme* to model weight (grams) as a linear function of presence/absence of the transgene, sex, age [log(days)], litter, and a mouse-specific random effect to account for the repeated observations of each mouse. The P value corresponding to presence/absence of the transgene was used to assess significance of the association between the transgene and mouse weight in the presence of the other variables.

Figure 2.1

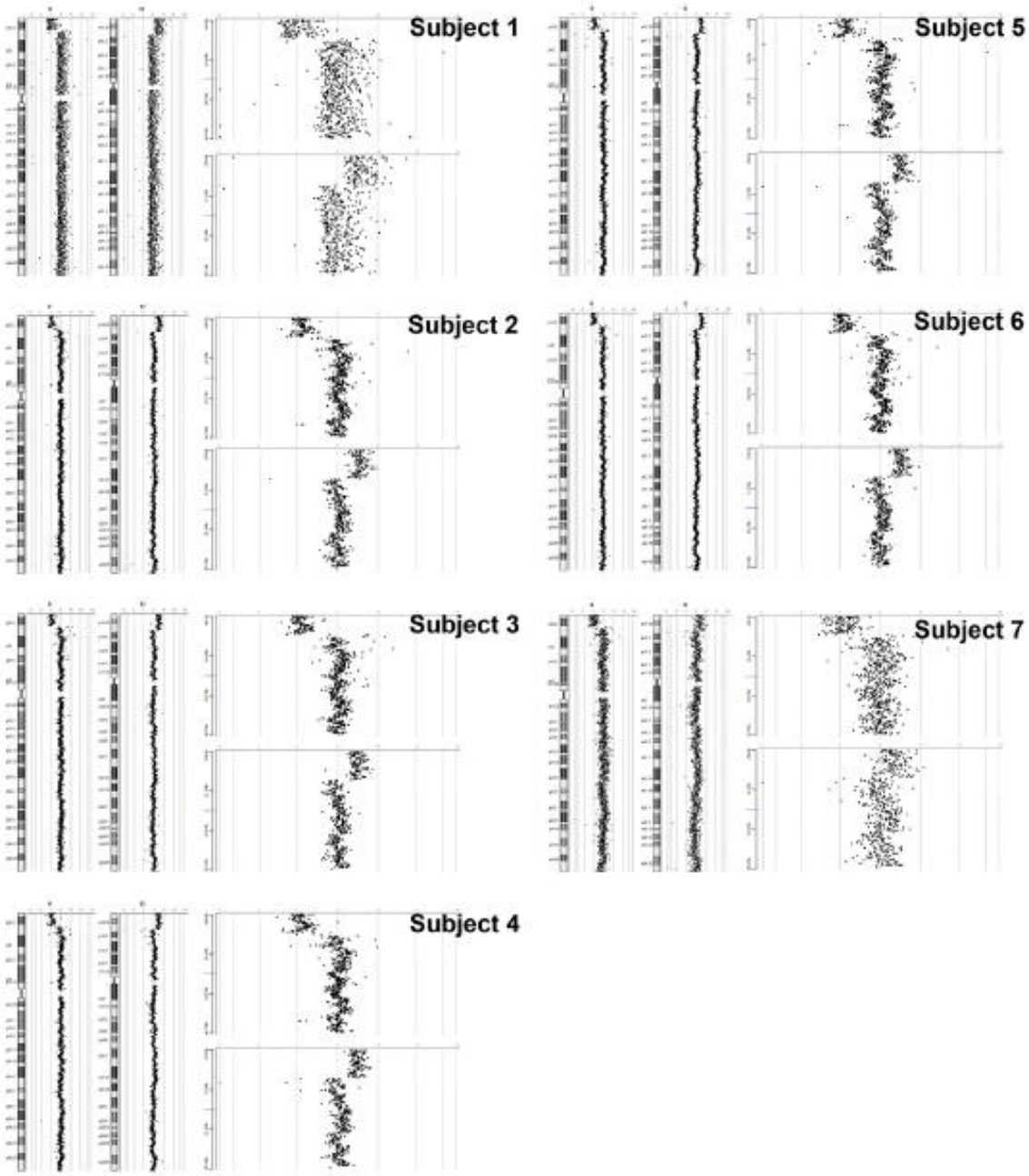
Subject 1
Subject 5
Subject 2
Subject 6
Subject 3
Subject 7
Subject 4

Figure 2.1

Array comparative genome hybridization of genomic DNA from subjects 1–7 using a 4 × 44,000 array (AMADID 016267). Log2 ratios of oligonucleotide signal intensities are shown as dots. (*Left*) The views of chromosomes 8 and 12 and (*Right*) the zoomed-in views of the breakpoints reveal a 7.0-Mb loss of 8p and an 8.5-Mb gain of 12p in all seven subjects.

Figure 2.2

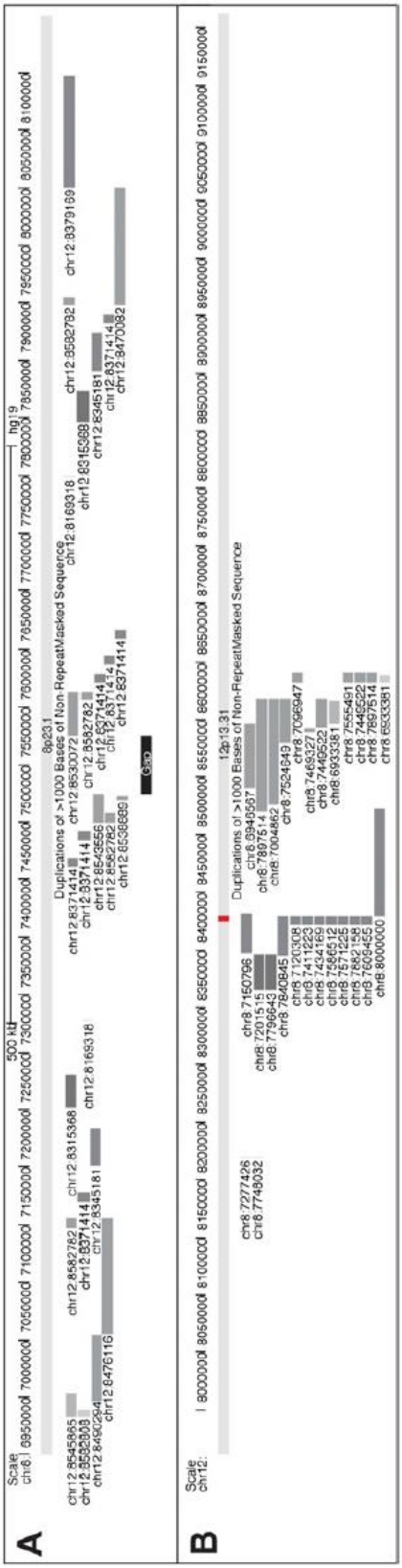
A
Scale
chr8:
500 kb
hg19
Duplications of >1000 Bases of Non-RepeatMasked Sequence
8p23.1
Gap
B
Scale
chr12:
Duplications of >1000 Bases of Non-RepeatMasked Sequence
12p13.31
Gap

Figure 2.2

Organization of segmental duplications on chromosomes (A) 8p23.1 and (B) 12p13.31. Segmental duplications shared by 8p23.1 and 12p13.31 are shown as gray boxes labeled with the coordinates of the paralogous chromosomal segment. The red box indicates the 12p side of the translocation junction in subject 4; the 8p side of the junction maps to several loci in 8p23.1. This figure was made using the postscript output function of the University of California, Santa Cruz (UCSC) browser (http://genome.ucsc.edu/).

Figure 2.3

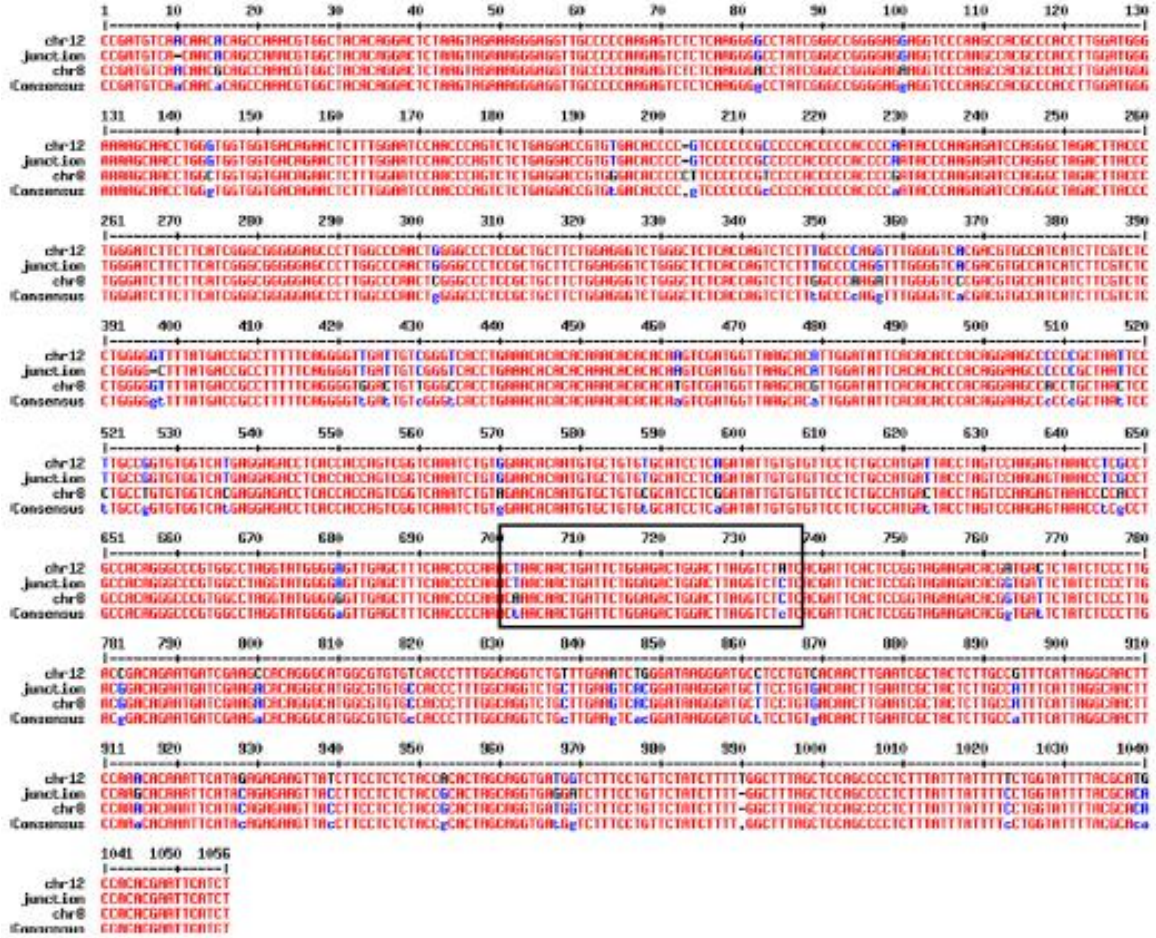

Figure 2.3

Translocation junction sequence from subject 4. The 1,056-bp junction sequence is aligned to chr12:8377049–8378103 and chr8:7432148–7433202 of the hg19/GRCh37 reference genome using MultAlin (http://multalin.toulouse.inra.fr/multalin/). SNPs depicted in blue and black delineate the chromosome 8 and 12 sides of the junction, respectively. We narrowed the site of recombination to a 34-bp region between chromosome 12- and 8-specific SNPs (shown boxed). Subject 4's translocation junction is ~2.5 kb proximal of the 12p translocation junction published in the work by Ou et al. (Ou et al., 2011).

Figure 2.4

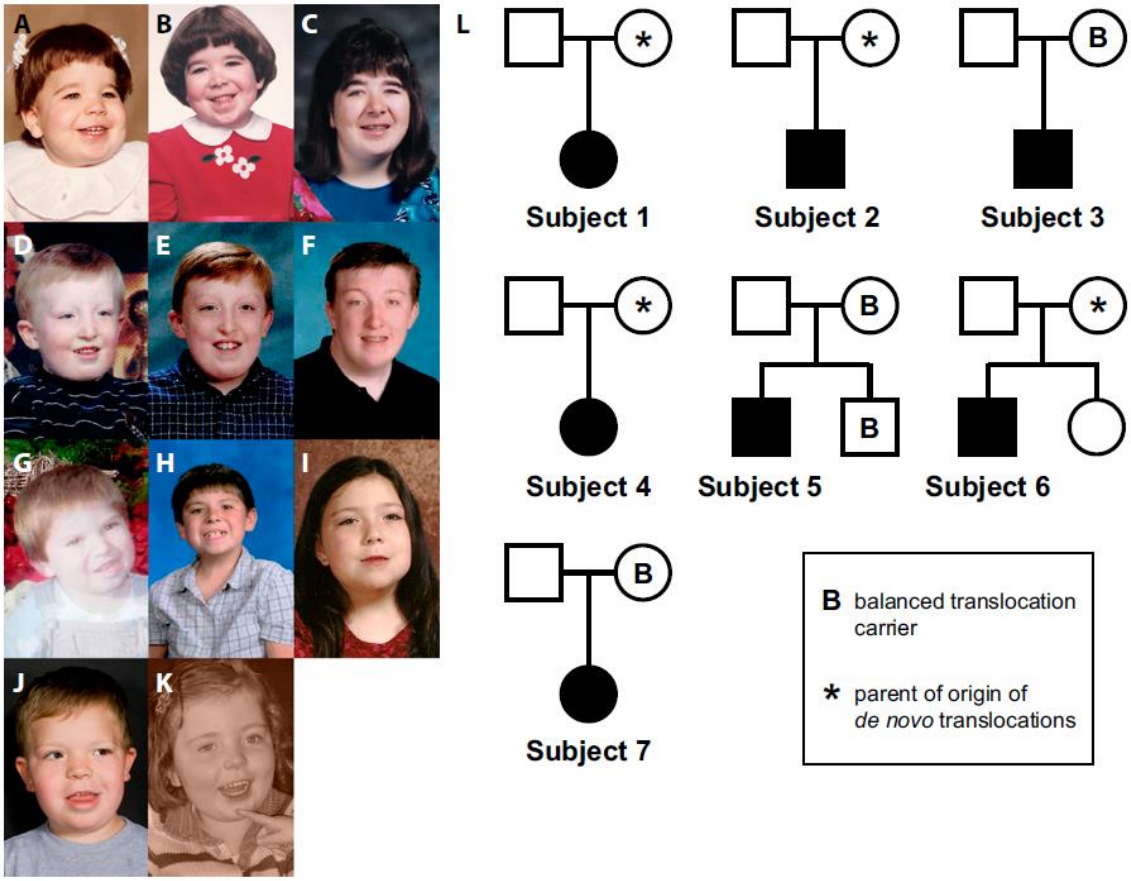
A
B
C
D
E
F
G
H
I
J
K
L
Subject 1
Subject 2
Subject 3
Subject 4
Subject 5
Subject 6
Subject 7
B balanced translocation carrier
* parent of origin of de novo translocations

Figure 2.4

Children with the der(8)t(8;12) exhibit features including a thin upper lip, short nose, periorbital fullness, malar hypoplasia, narrow palpebral fissures, high forehead, and prominent chin. Facial features of subject 1 at (A) 22 mo, (B) 5 y, and (C) 13 y; subject 2 at (D) 4 y, (E) 11 y, and (F) 15 y; subject 3 at (G) 4 y and (H) 11 y; (I) subject 4 at 9 y; (J) subject 6 at 4 y; and (K) subject 7 at 5 y are shown. (L) Pedigrees of 7 families. Filled symbols indicate affected individuals with the unbalanced translocation.

Figure 2.5

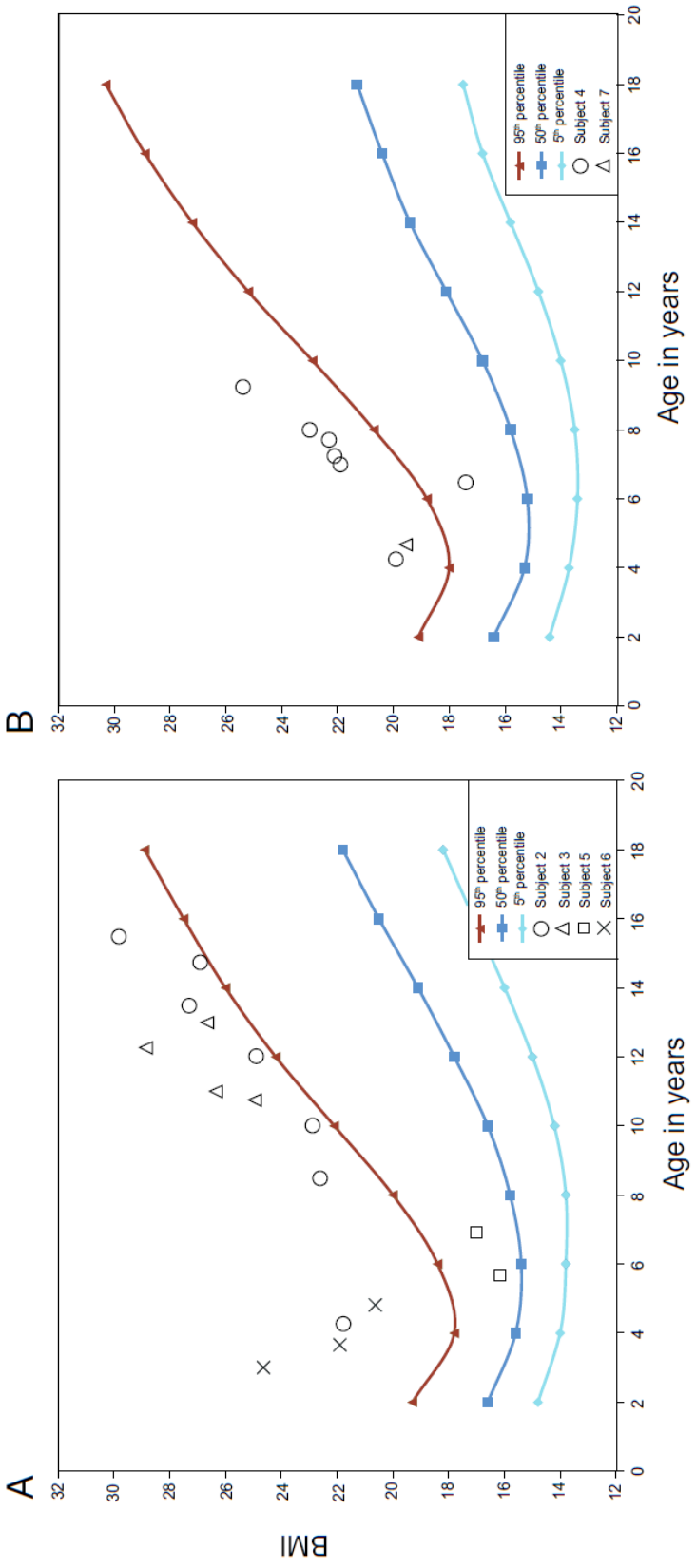
A
B
BMI
Age in years
Age in years
95th percentile
50th percentile
5th percentile
Subject 2
Subject 3
Subject 5
Subject 6
95th percentile
50th percentile
5th percentile
Subject 4
Subject 7

Figure 2.5

BMI for (A) male and (B) female subjects. The 5th, 50th, and 95th BMI percentile curves for boys and girls from the Centers for Disease Control and Prevention are plotted. BMI values were calculated using the reported height and weight with a childhood BMI calculator (Flegal et al., 2002).

Figure 2.6

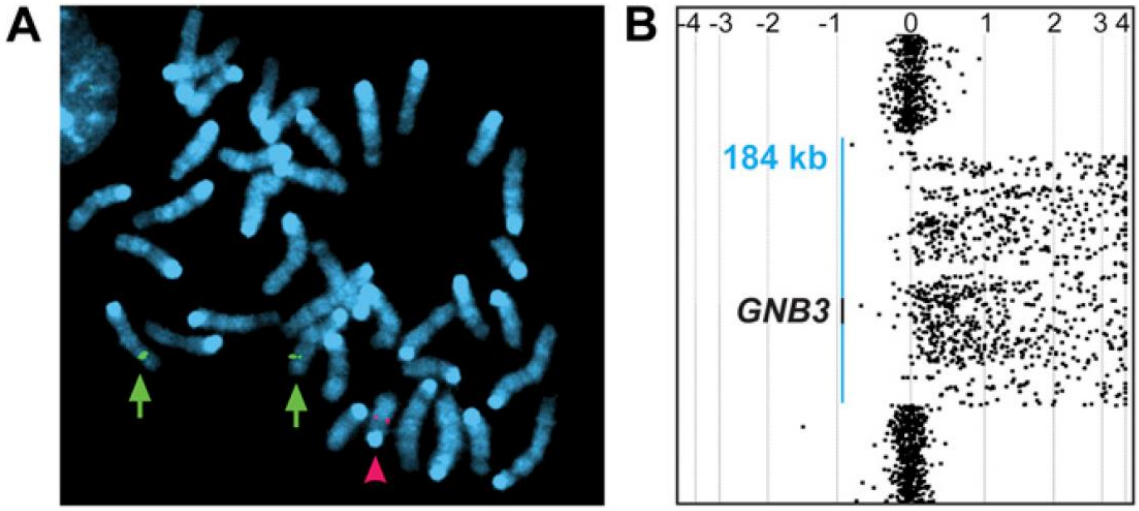

Figure 2.6

Transgenic mouse model of *GNB3* duplication. (A) FISH of chromosomes prepared from a *GNB3*/+ animal. BAC RP11-578M14 (red) hybridizes to the transgene insertion site (arrowhead), and RP23-384O24 (green) hybridizes to the endogenous Gnb3 locus (arrows). (B) Array comparative genome hybridization of a *GNB3*/+ vs. a +/+ animal on a high-resolution array covering human chromosome 12p. Log2 ratios of oligonucleotide signal intensities are shown as dots; ratios are labeled at the top of the image. The 184-kb human BAC inserted completely, which is shown by the positive shift in signal intensity. The location of *GNB3* within the BAC is indicated (black line).

Figure 2.7

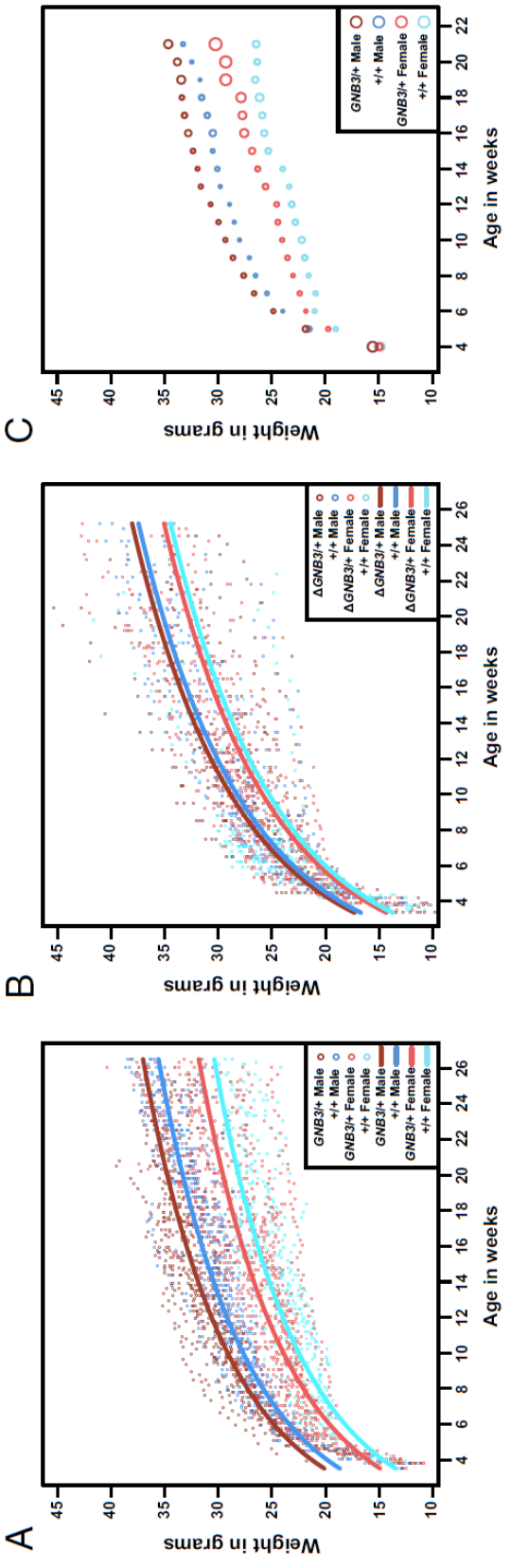
A
B
C
Weight in grams
Age in weeks
GNB3j/+ Male
+/+ Male
GNB3j/+ Female
+/+ Female
ΔGNB3j/+ Male
ΔGNB3j/+ Female

Figure 2.7

Plots of mouse weight by age; (A) 52 (14 *GNB3*/+ male, 13 +/+ male, 16 *GNB3*/+ female, and 9 +/+ female mice) and (B) 91 (25 Δ*GNB3*/+ male, 31 +/+ male, 20 Δ*GNB3*/+ female, and 15 +/+ female mice) mice were weighed three times a week beginning at weaning. Each dot represents the weight of a single mouse at a given age. Lines indicate predicted mouse weight by age based on presence/absence of the transgene and mouse sex. (C) Weight gain of *GNB3*/+ and +/+ animals. Circles depict average weekly values of mouse weight ± SEM.

Figure 2.8

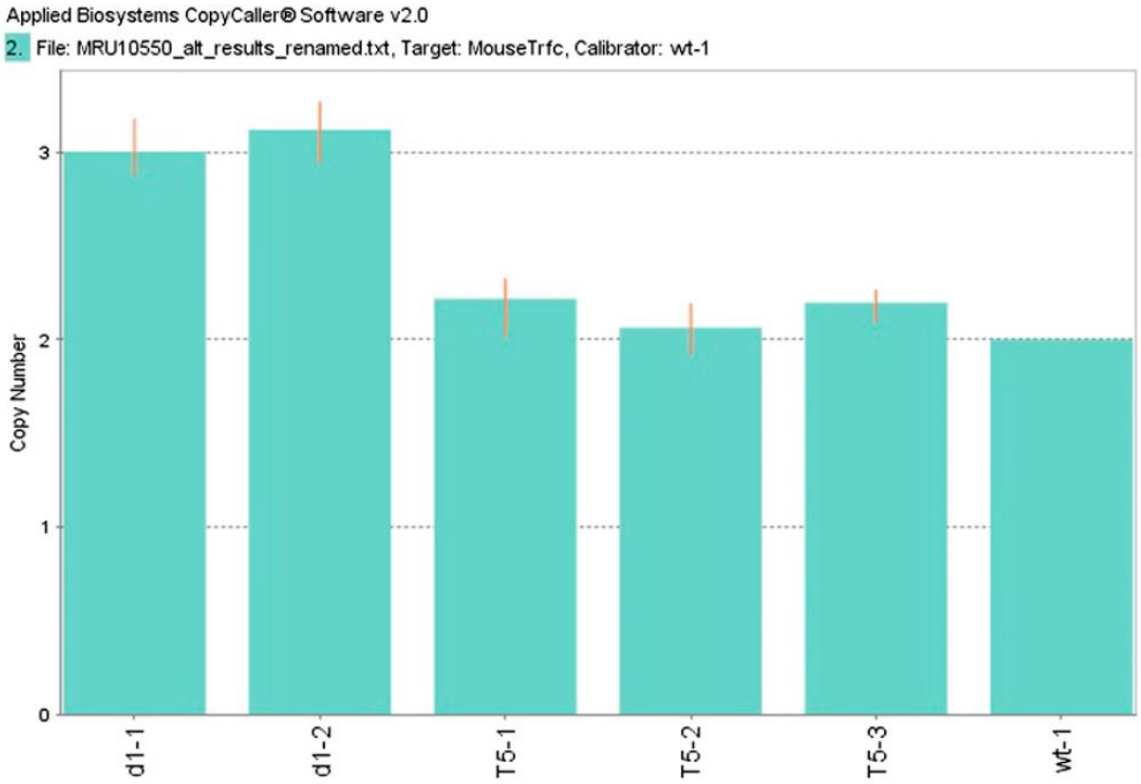
Applied Biosystems CopyCaller® Software v2.0
2. File: MRU10550_alt_results_renamed.txt, Target: MouseTrfc, Calibrator: wt-1
Copy Number
3
2
1
0
d1-1
d1-2
T5-1
T5-2
T5-3
wt-1

Figure 2.8

BAC copy number. Taqman quantitative PCR primers amplify the RP11-578M14 BAC in *GNB3*/+ (T) and Δ*GNB3*/+ (d) mice. Copy number of the BAC was determined using ΔΔcycle threshold values of the BAC and Tfrc control and calculated using CopyCaller software (Life Technologies). Quantitative PCR was performed in quadruplicate; the mean copy number is shown with error bars representing the minimum and maximum values of four experiments per sample. The BAC was stably transmitted from parent to offspring in Δ*GNB3* line 1 (d1-1 to d1-2) and *GNB3* line 5 (T5-1 to T5-2 to T5-3).

Figure 2.9

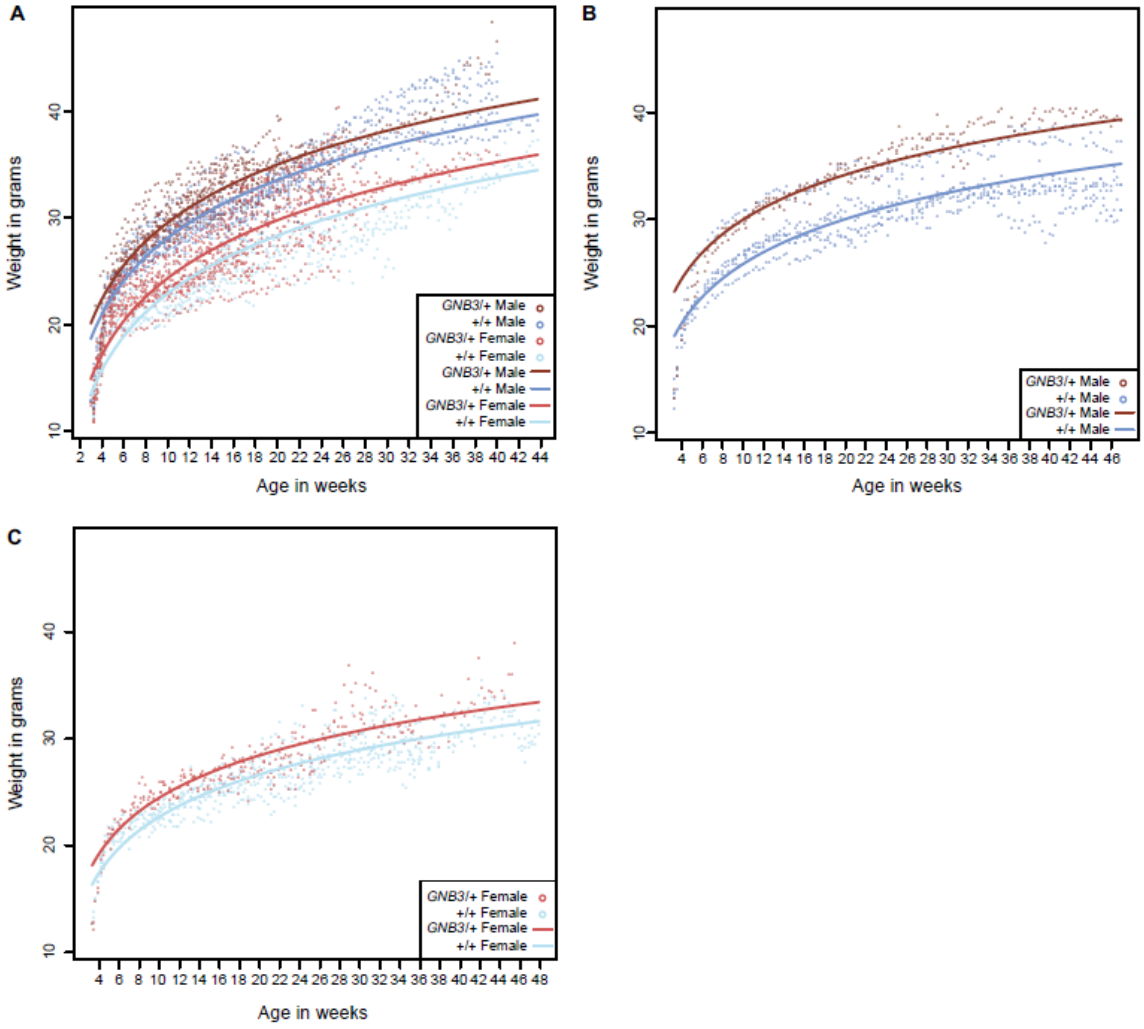
A
Weight in grams
Age in weeks
GNB3/+ Male
+/+ Male
GNB3/+ Female
+/+ Female
GNB3/+ Male
+/+ Male
GNB3/+ Female
+/+ Female
B
Weight in grams
Age in weeks
GNB3/+ Male
+/+ Male
GNB3/+ Male
+/+ Male
C
Weight in grams
Age in weeks
GNB3/+ Female
+/+ Female
GNB3/+ Female
+/+ Female

Figure 2.9

Plots of mouse weight by age. Mice were weighed three times a week for varying lengths of time. Each dot represents the weight of a single mouse at a given age. Lines indicate predicted mouse weight by age based on presence/absence of the transgene and mouse sex: (A) 30 *GNB3*/+ and 22 +/+ mice from Founder Line 5, (B) 2 *GNB3*/+ and 5 +/+ male mice from Founder Line 3, and (C) 3 *GNB3*/+ and 8 +/+ female mice from Founder Line 4. We used a linear mixed model to analyze the longitudinal effects of the presence of the BAC transgene on mouse weight. The weight of the mice is significantly associated with transgene genotype in Founder Lines 5 (P = 0.00199), 3 (P = 0.0487), and 4 (P = 0.00689).

Figure 2.10

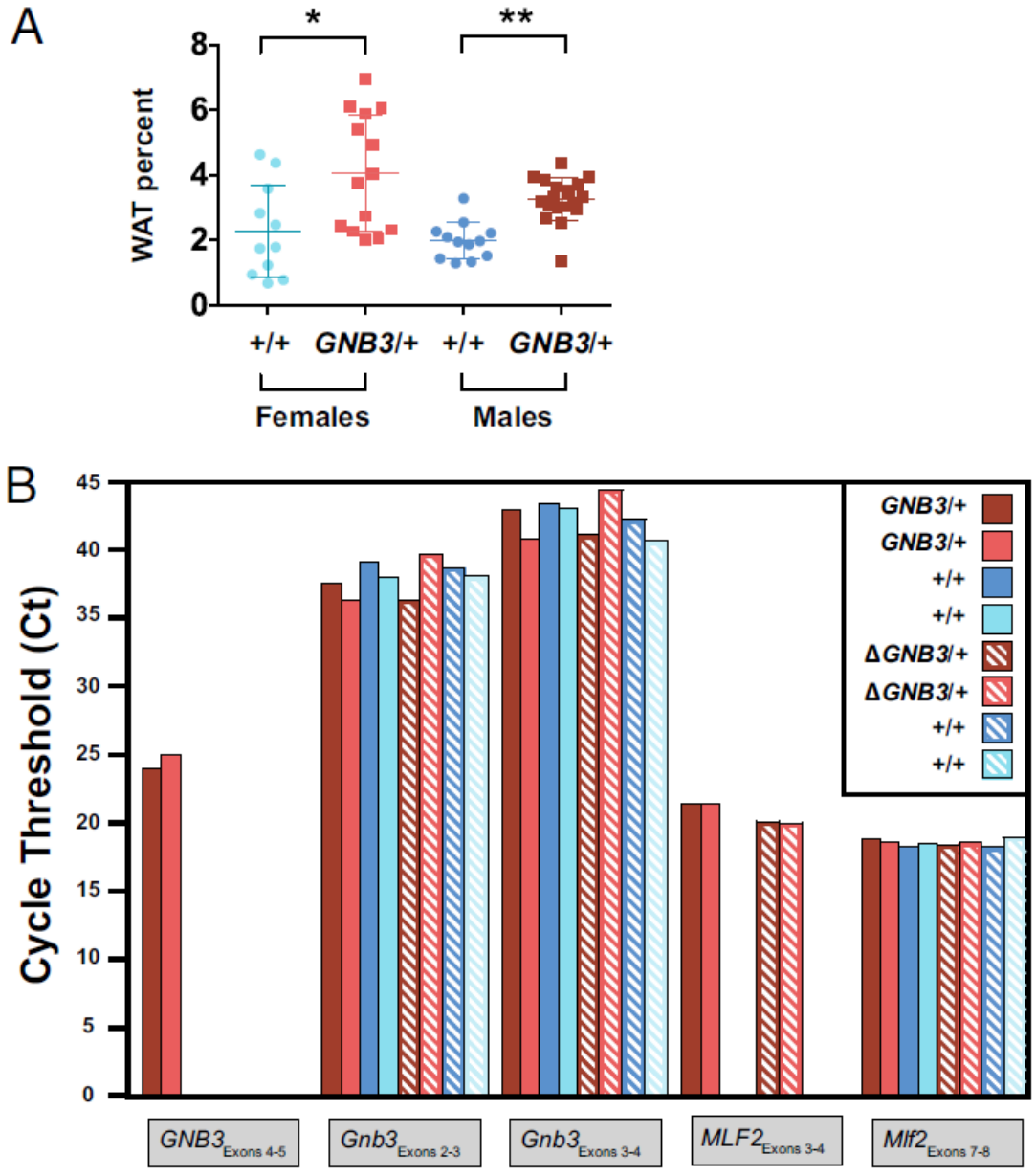
A
*
**
WAT percent
8
6
4
2
0
+/+
GNB3/+
+/+
GNB3/+
Females
Males
B
Cycle Threshold (Ct)
45
40
35
30
25
20
15
10
5
0
GNB3/+
GNB3/+
+/+
+/+
ΔGNB3/+
ΔGNB3/+
+/+
+/+
GNB3 Exons 4-5
Gnb3 Exons 2-3
Gnb3 Exons 3-4
MLF2 Exons 3-4
Mlf2 Exons 7-8

Figure 2.10

Gonadal WAT percent of mice and transgenic *GNB3* and endogenous *Gnb3* expression. (A) Gonadal WAT was extracted from 20-wk-old mice (19 *GNB3*/+ male, 12 +/+ male, 14 *GNB3*/+ female, and 11 +/+ female mice) and weighed to calculate WAT percent. *GNB3*/+ WAT percent is significantly greater than +/+ WAT percent in *females ($P = 0.0122$) and **males ($P < 0.0001$; Student's *t*-test). (B) *GNB3* is highly expressed in *GNB3*/+ brains. Mean Ct values from qRT-PCR of human *GNB3*, mouse *Gnb3*, human *MLF2*, and mouse *Mlf2* transcripts in whole brains from eight 8-wk-oldmale mice are plotted. Data from *GNB3*/+ and +/+ littermates are shown as solid bars; data from Δ*GNB3*/+ and +/+ littermates are shown as hatched bars. Lower Ct values correspond to greater gene expression; the absence of Ct data indicates no detection of transcript. All qRT-PCR experiments were performed in triplicate with an internal mouse β-actin (*Actb*) control. SEM for 40 *Actb* triplicates was ± 0.05 Ct; maximum SEM for other transcripts was ± 0.31 Ct.

Figure 2.11

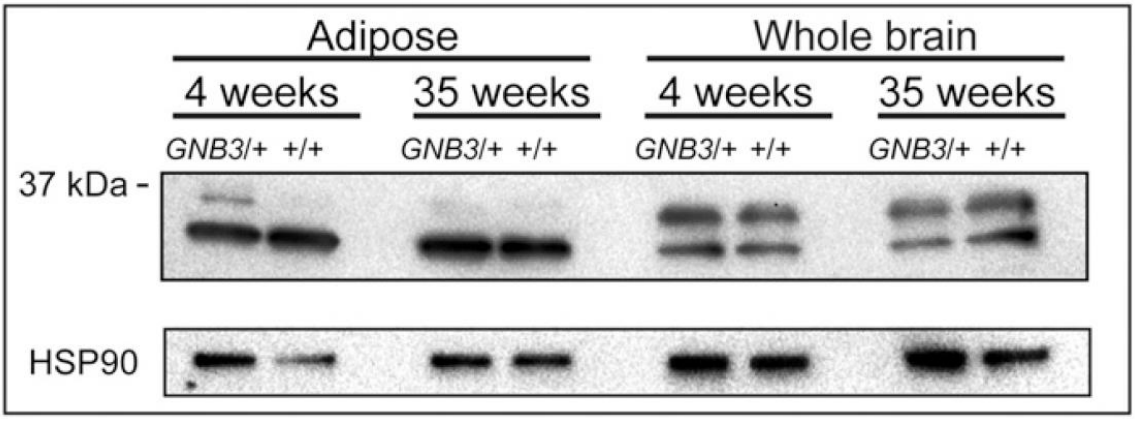
Adipose
Whole brain
4 weeks
35 weeks
4 weeks
35 weeks
GNB3/+ +/+
GNB3/+ +/+
GNB3/+ +/+
GNB3/+ +/+
37 kDa -
HSP90

Figure 2.11

Western blot of GNB proteins in brain and adipose tissue from 4- and 35-wk-old GNB3/+ mice and +/+ littermates. This antibody does not distinguish various β-subunits of G proteins and is not specific for GNB3. The location of the 37-kDa marker is shown. (*Lower*) The blot was probed with an HSP90 antibody as a loading control.

Figure 2.12

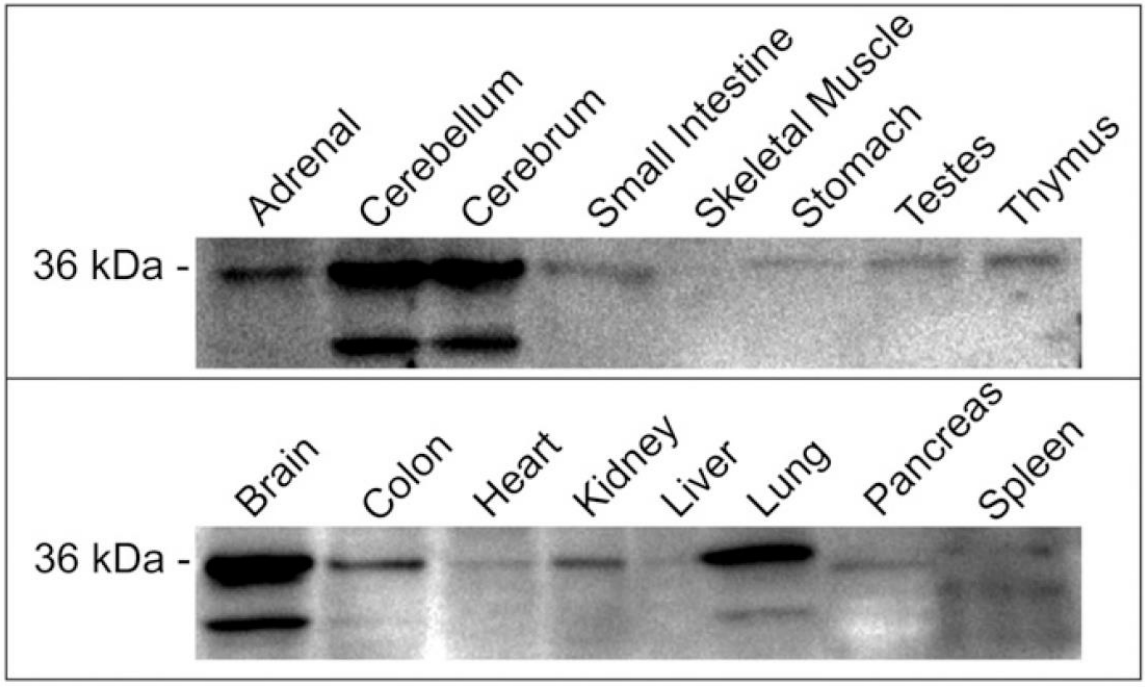
Adrenal
Cerebellum
Cerebrum
Small Intestine
Skeletal Muscle
Stomach
Testes
Thymus
36 kDa -
Brain
Colon
Heart
Kidney
Liver
Lung
Pancreas
Spleen
36 kDa -

Figure 2.12

Western blot of tissue panel from normal mice. Same GNB antibody as in Figure 2.11 was used. (*Upper*) Mouse Normal Tissue Blot II (1562; ProSci). (*Lower*) Mouse Normal Tissue Blot I (1561; ProSci). Both mouse tissue blots have 15 μg total cellular protein per lane and were blotted with the conditions described in Materials and Methods. Tissues are labeled above the lanes. The location of the 36-kDa marker is shown; 37- and 32-kDa GNB isoforms are detected in some tissues.

Figure 2.13

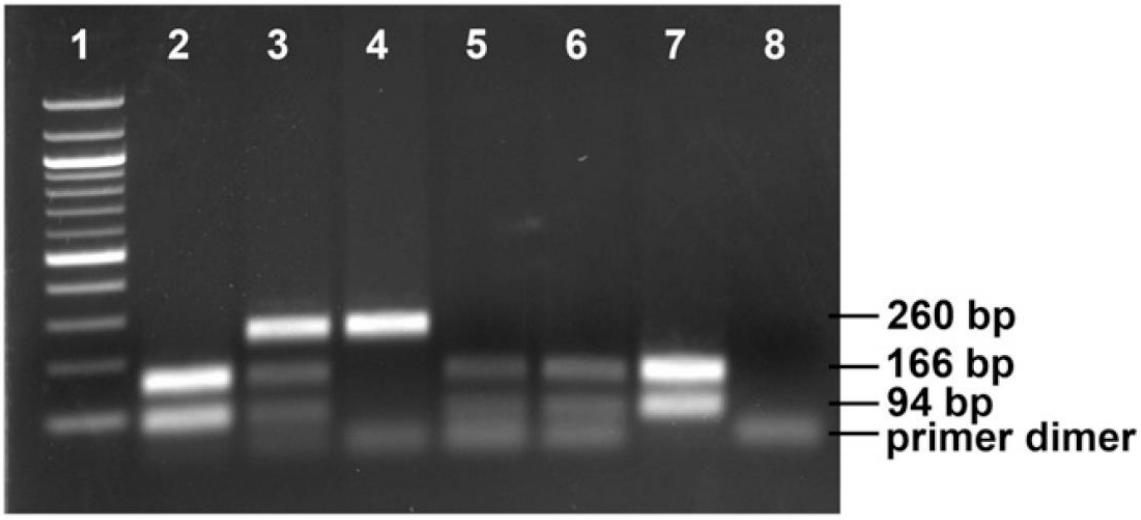

Figure 2.13

Restriction site assay for the C825T polymorphism. The uncut T allele is 260 bp, and the C allele digests into two bands of 94 and 166 bp. Primer dimer is present at the bottom of the lanes. Lanes are as described: lane 1, 100-bp ladder (N3231S; NEB); lane 2, CC control; lane 3, CT control; lane 4, subject 4 (TTT); lane 5, subject 2 (CCC); lane 6, mother of subject 2 (CC); lane 7, father of subject 2 (CC); and lane 8, PCR water control.

Table 2.1

Subject	Age	*GNB3*	Height (cm; %)	Weight (kg; %)	BMI (%)	HC (cm; %)	DD	S	H	DF	G	PC	O	E	SP	DP
1	29 y, 0 mo	CCT	167.6	85.3	30.4	57.2	+	+	+	+	+	+	+	+	+	+
2	15 y, 6 mo	CCC	174 (50)	90.2 (>95)	29.8 (>95)	61.5 (>98)	+	+	+	+	−	N	+	+	+	+
3	11 y, 8 mo	CCC	137.5 (10–25)	49.8 (90–95)	26.3 (>95)	57 (>98)	+	+	+	+	+	+	+	+	+	+
4	8 y, 0 mo	TTT	135 (90)	42 (>95)	23.0 (>95)	55 (>98)	+	+	+	+	−	N	+	+	−	−
5	6 y, 11 mo	CCC	114.3 (10–25)	22.2 (50)	17 (50–75)	55.9 (>98)	+	−	+	+	−	+	−	+	+	+
6	4 y, 10 mo	CTT	115 (90–95)	27.3 (>95)	20.6 (>95)	52 (90–98)	+	+	−	+	+	+	N	−	+	−
7	4 y, 8 mo	CCT	115.5 (>95)	26 (>95)	19.5 (>95)	52 (90–98)	+	−	−	+	+	+	+	+	+	−
							7/7	5/7	5/7	7/7	4/7	5/5	5/6	6/7	6/7	4/7

Table 2.1

Clinical features of subjects. Listed are age at assessment, *GNB3* genotype (Figure 2.13, Table 2.3), height, weight, BMI, head circumference (HC), and percentiles (%). Subject 1 is an adult; her measurements do not fall within childhood growth percentiles. Subjects exhibit features (+) including developmental delay (DD), seizure (S), hypotonia (H), dysmorphic features (DF), abnormal gait (G), poor coordination (PC), ocular problems (O), eczema (E), social personality (SP), and dental/palate abnormalities (DP). Features not formally evaluated (N) or not present (−) are indicated. Detailed clinical information is located in Materials and Methods.

Table 2.2

Subject	Age (y)	Head circumference (cm)	Weight (kg)	Height (cm)	Age-matched mean height (cm)	+2 SD	+3 SD
1	29	57.2	85.3	167.6			
2	4.25	54.5	25	107	105.0041	113.6145	117.9197
2	8.25	56.5		133			
2	8.5		40				
2	10	59	48.5	145.5			
2	12	60	63	159			
2	13.5	60.8	79	170			
2	14.75		80	172.5			
2	15.5		90	174			
2	18	59					
3	10.75		46	136			
3	11	57	49.8	137.5			
3	12.25		58	142			
3	13		56	145			
4	4.25		25	112	104.4786	113.3238	117.7464
4	4.75		28				
4	6.5		37	127			
4	7	54.5	38	130			
4	7.25	54.5		131			
4	7.75		40	134			
4	8	55	42	135			
4	9.25		52	143			
5	5.67		20	111			
5	6.92	55.9	22.2	114.3			
6	3	51	22.9	96.5	96.0835	103.4973	107.2042
6	3.67		24.8	106.4	101.0374	109.1244	113.1679
6	4.83	52	27.3	115.1	108.8689	117.9921	122.5537
7	4.67	52	26	115.5	107.2788	116.5004	121.1112

Table 2.2

Measurements from clinic visits. Age- and sex-matched mean heights +2 and +3 SDs for children under 5 y were reported by the World Health Organization (WHO Multicentre Growth Reference Study Group, 2006). None of the subjects' heights exceed 2 SDs above the mean; thus, they do not have an overgrowth phenotype (Verge and Mowat, 2010; Visser et al., 2009).

Table 2.3

Subject	C peak height	T peak height	T/C ratio	Genotype
CC control	61.84	0.7	0.011319534	CC
CC control	82.16	0.47	0.005720545	CC
CC control	85.65	12.78	0.149211909	CC
CT control	41.61	16.44	0.395097332	CT
CT control	56.04	24.37	0.434867951	CT
CT control	44.74	18.13	0.405230219	CT
Subject 1	58.69	17.15	0.292213324	CCT
Subject 1	62.45	17.65	0.282626101	CCT
Subject 1	68.05	18.36	0.269801616	CCT
Mother of subject 1	62.96	0.3	0.00476493	CC
Mother of subject 1	95.74	0.58	0.006058074	CC
Mother of subject 1	84.38	0.66	0.007821759	CC
Subject 2	103.33	1.31	0.012677828	CCC
Subject 2	85.76	0.37	0.004314366	CCC
Subject 2	96.68	0.52	0.005378568	CCC
Father of subject 2	87.63	0.29	0.003309369	CC
Father of subject 2	81.2	0.4	0.004926108	CC
Father of subject 2	99.78	1.08	0.010823812	CC
Mother of subject 2	83.83	1.32	0.015746153	CC
Mother of subject 2	91.48	0.78	0.008526454	CC
Mother of subject 2	90.92	0.39	0.004289485	CC
Subject 3	67.47	0.31	0.004594635	CCC
Subject 3	77.15	0.23	0.002981205	CCC
Subject 3	85.48	0.53	0.006200281	CCC
Subject 4	36.42	30.57	0.83937397	TTT
Subject 4	45.14	41.85	0.92711564	TTT
Subject 4	44.73	40.76	0.911245249	TTT
Father of subject 4	52.9	21.72	0.410586011	CT
Father of subject 4	52.75	23.69	0.449099526	CT
Father of subject 4	56.02	23.79	0.424669761	CT
Mother of subject 4	51.09	20.6	0.403210022	CT
Mother of subject 4	56.27	26.6	0.47272081	CT
Mother of subject 4	57.91	24.34	0.420307374	CT
Subject 5	91.6	0.25	0.002729258	CCC
Subject 5	93.97	0.79	0.008406938	CCC
Subject 5	81.44	0.38	0.004666012	CCC
Father of subject 5	56.29	0.43	0.007639012	CC
Father of subject 5	92.93	0.46	0.004949962	CC
Father of subject 5	84.48	0.4	0.004734848	CC
Mother of subject 5	91.58	0.31	0.003385019	CC
Mother of subject 5	77.34	0.32	0.004137574	CC
Mother of subject 5	81.97	0.2	0.002439917	CC
Brother of subject 5	71.31	0.36	0.00504838	CC
Brother of subject 5	82.28	0.67	0.008142927	CC
Brother of subject 5	89.55	0.37	0.00413177	CC
Subject 6	51.72	32.14	0.621423047	CTT
Subject 6	51.4	32.19	0.626264591	CTT
Subject 6	58.04	32.35	0.557374225	CTT
Father of subject 6	84.72	0.58	0.006846081	CC
Father of subject 6	78.52	0.6	0.007641365	CC
Father of subject 6	93.88	0.52	0.005538986	CC
Mother of subject 6	52.12	38.77	0.743860322	TT
Mother of subject 6	80.61	42.24	0.524004466	TT
Mother of subject 6	65.02	41.77	0.642417718	TT
Subject 7	70.57	19.19	0.271928582	CCT
Subject 7	81.15	27.42	0.337892791	CCT
Subject 7	68.29	20.3	0.297261678	CCT
Father of subject 7	58.19	24	0.412442	CT
Father of subject 7	60.04	25.6	0.426382412	CT
Father of subject 7	59.51	27.19	0.456898	CT
Mother of subject 7	100.05	1.16	0.011594203	CC
Mother of subject 7	85.51	0.44	0.005145597	CC
Mother of subject 7	91.09	0.27	0.002964101	CC

Table 2.3

C825T genotypes determined by pyrosequencing.

Chapter 3

GNB3 overexpression causes obesity and metabolic syndrome

This chapter was submitted in part as: Alev Cagla Ozdemir, Grace M. Wynn, Aimee Vester, M. Neale Weitzmann, Gretchen N. Neigh, Shanthi Srinivasan, and M. Katharine Rudd. *GNB3* overexpression causes obesity and metabolic syndrome. *PLOS ONE*. 2017. A.C.O. designed the study, performed the experiments, collected, analyzed and interpreted the data, prepared the figures, and wrote the manuscript. G.M.W. performed the experiments, collected, analyzed and interpreted the data. A.V. and G.N.N. were responsible for the behavioral studies. M.N.W. helped with DXA. S.S. provided metabolic cages and contributed to discussion. M.K.R. designed the study and reviewed and edited the manuscript.

Abstract

The G-protein beta subunit 3 (*GNB3*) gene has been implicated in obesity risk; however, the molecular mechanism of *GNB3*-related disease is unknown. *GNB3* duplication is responsible for a syndromic form of childhood obesity, and an activating DNA sequence variant (C825T) in *GNB3* is also associated with obesity. To test the hypothesis that *GNB3* overexpression causes obesity, we created bacterial artificial chromosome (BAC) transgenic mice that carry an extra copy of the human *GNB3* risk allele. Here we show that *GNB3*-T/+ mice have increased adiposity, but not greater food intake or a defect in satiety. *GNB3*-T/+ mice have elevated fasting plasma glucose, insulin, and C-peptide, as well as glucose intolerance, indicating type 2 diabetes. Fasting plasma leptin, triglycerides, cholesterol and phospholipids are elevated, suggesting metabolic syndrome. Based on a battery of behavioral tests, *GNB3*-T/+ mice did not exhibit anxiety- or depressive-like phenotypes. *GNB3*-T/+ and wild-type animals have similar activity levels and heat production; however, *GNB3*-T/+ mice exhibit dysregulation of acute thermogenesis. Finally, uncoupling protein 1 (*Ucp1*) expression is significantly lower in white adipose tissue (WAT) in *GNB3*-T/+ mice, suggestive of WAT remodeling that could lead to impaired cellular thermogenesis. Taken together, our study provides the first functional link between *GNB3* and obesity, and presents insight into novel pathways that could be applied to combat obesity and type 2 diabetes.

Introduction

Obesity is a chronic disease associated with significant morbidity and mortality, affecting over 600 million adults globally (World Health Organization, 2016a). Furthermore,

obesity is an important risk factor for metabolic conditions such as type 2 diabetes mellitus, insulin resistance, dyslipidemia, and cardiovascular problems including hypertension, cardiovascular disease, and congestive heart failure, as well as certain cancers (Chan et al., 1994; Haslam and James, 2005; O'Rahilly, 2009). Obesity is a highly heritable trait – twin and adoption studies estimate that over 70% of the variance in BMI is attributed to genetic factors (Stunkard et al., 1986b, 1990). Since the identification of leptin (*LEP*) as the first obesity gene (Zhang et al., 1994), several other Mendelian forms of non-syndromic obesity have been discovered (Blakemore and Froguel, 2010; Crowley, 2008; Sabin et al., 2011). Along with monogenic forms of obesity, genetic disorders like Prader-Willi and Bardet-Biedl syndromes include obesity as a significant phenotype (Sabin et al., 2011). Moreover, genome-wide association studies have identified alleles that contribute to common forms of obesity (Choquet and Meyre, 2011a). Though many genetic causes of obesity have been discovered, additional genes are necessary to explain the "missing heritability" in obesity (Choquet and Meyre, 2011b; Xia and Grant, 2013).

We recently described a syndrome associated with obesity, seizures, and intellectual disability in individuals with an unbalanced chromosome translocation that leads to an 8.5-megabase (Mb) duplication of chromosome 12 and a 7.0-Mb deletion of chromosome 8 (Goldlust et al., 2013). One of the duplicated genes on chromosome 12 is the obesity candidate gene *GNB3*, which encodes the G-protein β3 subunit. Specific *in vivo* interactions of the Gβ subunits with other Gα and Gγ subunits are unknown (Krumins and Gilman, 2006; Poon et al., 2009). However, a silent cytosine to thymine (C825T) polymorphism in *GNB3* is associated with hypertension and obesity (Klenke et

al., 2011). This variant, located in exon 10 of *GNB3*, does not alter the amino acid sequence; however, the T-allele is associated with alternative splicing of exon 9 and encodes a splice variant (*GNB3*-s) with a 123-bp in-frame deletion (Siffert et al., 1998). The T-allele is also associated with increased signal transduction by activation of G-proteins in human cells (Siffert et al., 1998). *GNB3*-s produces a functional protein; yet, the properties of *GNB3*-s that enhance activation of G-proteins in unknown. Since Gβ subunits are important mediators of transmembrane signaling (Ford et al., 1998), *GNB3*-s could enhance signal transduction in a variety of tissues. How the *GNB3*-T allele, the associated splice variant, and increased G-protein signal transduction contribute to obesity risk are not understood.

Though *Gnb3* knock-out does not alter body weight in mice (Ye et al., 2014), our human data suggested that *GNB3* duplication leads to obesity. To model *GNB3* overexpression, we created transgenic mice carrying the T variant of human *GNB3* (Goldlust et al., 2013). In addition to the two endogenous copies of *Gnb3*, *GNB3*-T/+ mice carry two copies of human *GNB3*-T. Previous work from our group demonstrated that heterozygous *GNB3* transgenic mice weigh significantly more than sex- and age-matched wild-type (WT) littermates and that *GNB3*-T is highly expressed in the brain (Goldlust et al., 2013). Here, we build upon these findings and establish that *GNB3* overexpression causes increased adiposity, glucose intolerance, metabolic syndrome and dysregulation of acute thermogenesis in mice even though food intake, satiety, activity levels, energy expenditure, and behavioral phenotypes are similar to that of WT animals.

Results

Transgenic GNB3 expression in brain and adipose tissue. In this study, we refer to mice heterozygous for the human BAC transgene as *GNB3*-T/+. To determine the expression levels of human *GNB3* and endogenous *Gnb3* we performed quantitative RT-PCR in RNA from whole brain, olfactory bulb, hypothalamus, and cerebellum of 5-week-old *GNB3*-T/+ and WT mice. As expected, we did not detect human *GNB3* in WT mice. Notably, human *GNB3* expression was ~1000-fold greater than endogenous *Gnb3* in whole brain, olfactory bulb, hypothalamus and cerebellum of *GNB3*-T/+ mice as calculated by delta cycle threshold values (Figure 3.1A). We also detected expression of human *GNB3* and endogenous *Gnb3* in adipose tissue from 20-week-old *GNB3*-T/+ and WT mice. Human *GNB3* expression was 4-fold greater than endogenous *Gnb3* in gonadal WAT (gWAT), and 50-fold greater than endogenous *Gnb3* in iWAT and BAT (Figure 3.1B).

Greater adiposity in GNB3-T/+ mice. In our previous studies, we found that *GNB3*-T/+ mice weighed significantly more than WT littermates starting at age 6-7 weeks onwards (Goldlust et al., 2013). We chose two ages, 5 weeks and 20 weeks, to evaluate the phenotypes of mice before and after obesity onset (Figure 3.2A-B) and weighed gWAT and iWAT as representative of visceral and subcutaneous WAT depots, respectively (Table 3.1). At 5 weeks, *GNB3*-T/+ and WT mice had similar gWAT%, iWAT%, BAT%, and liver% (Figure 3.3A-D). However, at 20 weeks, female and male *GNB3*-T/+ mice had greater gWAT%, iWAT%, and BAT%, but similar liver% compared to WT (Figure 3.2C-F). H&E staining revealed *GNB3*-T/+ adipocytes were 50% larger in gWAT (Figure 3.2G) and 27% larger in iWAT (Figure 3.2H) depots compared to WT. To further investigate body composition, we performed dual-energy X-ray absorptiometry

(DXA) on *GNB3*-T/+ and WT mice. Though lean mass of *GNB3*-T/+ and WT mice was the same at 5 and 20 weeks (Figure 3.2I, Figure 3.3), fat mass was increased in male and female *GNB3*-T/+ mice at 20 weeks (Figure 3.2J).

GNB3-T/+ mice have metabolic syndrome. Next, we investigated the metabolic profiles of *GNB3*-T/+ mice prior to and during obesity. At 20-weeks-old, female and male *GNB3*-T/+ mice had elevated fasting blood glucose, fasting plasma insulin, and C-peptide compared to WT (Figure 3.4). However, at 5 weeks, fasting blood glucose was greater only in female *GNB3*-T/+ mice, but both female and male *GNB3*-T/+ mice had elevated fasting plasma insulin (Figure 3.5A-B). Lipid profiling revealed that at 5 weeks, fasting plasma leptin, triglycerides, and cholesterol were similar for *GNB3*-T/+ mice and WT in both sexes (Figure 3.5D-F). Phospholipids were elevated, and non-esterified fatty acids (NEFA) were lower in female *GNB3*-T/+ mice, while in males both were similar to WT (Figure 3.5G-H). At 20 weeks, *GNB3*-T/+ mice had higher fasting plasma leptin, triglycerides, cholesterol, and phospholipids; however, NEFA were similar for *GNB3*-T/+ mice and WT (Figure 3.4).

To evaluate the impact of *GNB3* overexpression on glucose metabolism, we subjected mice to a glucose tolerance test (GTT) prior to and during obesity. At 5 weeks of age, *GNB3*-T/+ and WT mice have similar glucose tolerance (Figure 3.5I-J). However, at 20 weeks, as indicated by glycemia levels and calculations of area under the curve (AUC), female and male *GNB3*-T/+ mice exhibited glucose intolerance (Figure 3.4I-J). To follow up these findings, we assessed insulin sensitivity at 20 weeks old via insulin tolerance test (ITT). For both sexes, insulin sensitivity was similar between *GNB3*-T/+ and WT mice (Figure 3.4K-L).

Further metabolic profiling revealed that prior to obesity, fasting plasma glucagon, resistin and gastric inhibitory polypeptide (GIP) were not significantly different in *GNB3*-T/+ and WT mice (Figure 3.6A,C,E). At 20 weeks of age, resistin was elevated only in male *GNB3*-T/+ mice, while *GNB3*-T/+ glucagon and GIP levels were not different than WT in either sex (Figure 3.6B,D,F). Inflammatory marker IL-6, TNF-alpha and MCP-1 levels in fasting plasma were similar between *GNB3*-T/+ and WT mice prior to and during obesity (Figure 3.6G-L). Growth hormone (GH), thyroid stimulating hormone (TSH), follicle stimulating hormone (FSH), luteinizing hormone (LH), prolactin, and adrenocorticotropic hormone (ACTH) levels were similar between *GNB3*-T/+ and WT mice at 5 weeks. However, at 20 weeks, GH, TSH, FSH, LH and prolactin were lower in obese *GNB3*-T/+ male mice (Figure 3.7). It is important to note that GH secretion is pulsatile, so we measured GH at the same time point each day to minimize variation.

No significant difference detected between GNB3-T/+ and WT mice in food intake and activity levels. The increased adiposity and total body weight in *GNB3*-T/+ mice could be due to greater food intake, lack of activity, or a metabolic defect in energy expenditure. To investigate these possibilities, we measured food consumption at ages 5, 10, 15, 20 and 25 weeks (Figure 3.8A). At each time point, food intake was not significantly different between *GNB3*-T/+ and WT mice. Prior to obesity, fasting plasma ghrelin was lower, but PYY and amylin were elevated in male *GNB3*-T/+ mice; no difference was detected between *GNB3*-T/+ and WT females (Figure 3.9A-C). At 20 weeks of age, *GNB3*-T/+ fasting plasma ghrelin and PYY levels were similar to WT, while amylin was elevated in *GNB3*-T/+ mice (Figure 3.8), suggesting proper satiety.

Next, we measured locomotor activity in *GNB3*-T/+ mice over the course of three days. Horizontal and vertical activity levels during day and night cycles were not significantly different between *GNB3*-T/+ and WT mice at 5 weeks (Figure 3.9D-F) or 20 weeks of age (Figure 3.8E-G). In addition, there was no significant difference in total distance moved, frequency of center zone entrances, time spent in the center zone, or latency to center zone between the *GNB3*-T/+ and WT mice in open field testing (Figure 3.8H-K). This suggests that there is not a general locomotor defect in *GNB3*-T/+ mice, or an anxiety-like phenotype that would affect locomotor activity.

Energy expenditure and Ucp1 expression in GNB3-T/+ mice. Since food intake and locomotor activity were similar between *GNB3*-T/+ and WT mice, we next considered energy expenditure. Using metabolic cages, we measured VO_2, heat production, and respiratory exchange ratio (RER) in male mice. At 5 weeks old, VO_2, heat and RER measurements are similar in *GNB3*-T/+ and WT mice (Figure 3.10A-C). Once obese, *GNB3*-T/+ mice consume less oxygen, though the difference is not statistically significant. Heat production and RER in *GNB3*-T/+ mice are comparable to WT (Figure 3.11).

To further probe differences in energy expenditure, we performed an acute cold challenge at 4°C for 75 minutes and monitored the core body temperature of mice. Prior to obesity, *GNB3*-T/+ and WT mice dropped their core body temperatures at a similar rate during acute cold stress (Figure 3.10D). However, at 20 weeks old, *GNB3*-T/+ mice had significantly lower core body temperature compared to WT (Figure 3.11D). Since failure to maintain body temperature during acute cold exposure could be related to BAT function, we measured citrate synthase, a marker of mitochondrial activity (Rong et al.,

2007). Citrate synthase activity was comparable in BAT and iWAT from 20-week-old *GNB3*-T/+ and WT mice (Figure 3.11E-F).

Gene expression in GNB3-T/+ mice. We measured expression of oxidative phosphorylation, mitochondria, and white, beige, and brown adipocyte markers by quantitative RT-PCR in BAT, iWAT, and gWAT, and calculated the fold change between *GNB3*-T/+ and WT mice. Leptin expression was increased in BAT, iWAT and gWAT. Adipogenic markers *Pparg* and *Adipoq* were elevated in iWAT (Figure 3.12A). Beige adipocyte markers *Tbx1*, *Cd137*, and *Tmem26* (Figure 3.12B) as well as brown adipocyte markers *Eva1* and *Hspb7* had lower expression in BAT. *Eva1* expression was also lower in iWAT and gWAT, while *Hspb7* expression was elevated in gWAT (Figure 3.12C). Expression of *Ucp1*, a marker of brown and beige adipocytes, was lower most dramatically in iWAT. Additionally, iWAT *Prdm16* and *Pgc1a* expression were elevated, while *Cidea* expression was lower (Figure 3.12D). Mitochondrial genes *Cpt1a*, *Cpt2* and *Cox7a* were equally expressed in BAT. *Cpt1a* was elevated in iWAT and gWAT, while *Cox7a* was lower in iWAT but elevated in gWAT (Figure 3.12E).

Discussion

The mechanism of *GNB3*-related disease is only beginning to be understood, yet G-proteins are excellent candidates for a role in obesity (Wettschureck and Offermanns, 2005). By transducing extracellular signals, membrane-spanning G-protein coupled receptors activate G-protein αβγ heterotrimers (Bourne, 1997). Activated Gα, Gβ, and Gγ subunits are critical molecules that transmit signals to intracellular signaling pathways (Neves et al., 2002). G-protein mediated signaling, by combinations of different Gα, Gβ,

and Gγ subunit isoforms, controls diverse cellular and organismal functions such as differentiation, sensation, growth, and homeostasis (Wettschureck and Offermanns, 2005). Mutations in some G-protein subunit genes lead to abnormal signal transduction (Lania et al., 2001; Offermanns and Simon, 1998). For example, impaired taste sensation, defects in metabolism, and a variety of endocrine disorders are caused by mutations in different human Gα subunits (Lania et al., 2001; Moxham and Malbon, 1996; Wettschureck and Offermanns, 2005).

In our transgenic model, *GNB3* overexpression is associated with obesity, type 2 diabetes, and metabolic syndrome that presents without hyperphagia or reduced locomotion. Specifically, we find fat accumulation in visceral and subcutaneous WAT depots as well as in BAT. The lean mass of *GNB3*-T/+ and WT mice is the same, indicating that the difference in weight is strictly due to fat mass. Even though livers of *GNB3*-T/+ mice weighed more than WT, when normalized to total body weight (liver %), this difference was not significant.

GNB3-T/+ mice have glucose intolerance and type 2 diabetes are apparent at 20 weeks in *GNB3*-T/+ mice, indicated by elevated fasting plasma glucose levels and GTT response. Though *GNB3*-T/+ mice did not have glucose intolerance prior to obesity, 5-week old female *GNB3*-T/+ mice had elevated fasting blood glucose, and both female and male *GNB3*-T/+ mice had elevated fasting plasma insulin. This could indicate the beginning stage of impaired glucose metabolism prior to obesity. However, *GNB3*-T/+ mice do not respond to the ITT like other mouse models of type 2 diabetes, indicating a milder phenotype.

GH was reduced in obese *GNB3*-T/+ mice, consistent with lower circulating GH in obese humans (Scacchi et al., 1999). Another pituitary hormone, TSH, was also reduced in obese *GNB3*-T/+ mice at 20 weeks. Thyroid hormones control multiple physiological systems and have an important role in regulating basal metabolic rate, lipolysis, as well as the differentiation process in the adipose tissue (Obregon, 2014). FSH, LH and prolactin are reduced in obese male *GNB3*-T/+ mice at 20 weeks, which could indicate hypogonadotropic hypogonadism (Teerds et al., 2011).

Obesity is caused by an energy imbalance between calories consumed and calories expended. The increased adiposity in *GNB3*-T/+ mice could be due to increased calorie intake, reduced activity, or a defect in metabolism that results in lower energy expenditure. Our results from food intake measurements and levels of fasting ghrelin, PYY, and amylin hormones revealed that hyperphagia or a satiety defect are not responsible. Novelty suppressed feeding tests also show no significant difference in the amount of sucrose eaten, latency to feed, or total feeding time between the *GNB3*-T/+ and WT mice, indicating that anxiety-like feeding behaviors are not involved in *GNB3*-related obesity (see supplementary material). *GNB3*-T/+ and WT mice do not have a statistically significant difference in locomotor activity or oxygen consumption. However, it is possible that subtle differences in locomotion and/or oxygen consumption could contribute to increased adiposity. Future energy expenditure experiments conducted at thermoneutrality and/or brown fat induction experiments could shed light on the effects of *GNB3* overexpression. Further, behavioral assessments indicate that there are no substantial anxiety- or depressive-like phenotypes in *GNB3*-T/+ mice, and that these

affective phenotypes are unlikely to add to the relationship between *GNB3* overexpression and obesity.

Ucp1 expression in adipose tissues provides a clue to the underlying defect in *GNB3*-T/+ mice. Ucp1 in mitochondria dissipates chemical energy in the form of heat, mainly in BAT, through a process called nonshivering thermogenesis (Cannon and Nedergaard, 2004). Recently, BAT has become a therapeutic target in obesity and metabolic disorders. Ucp1-ablated mice are obese and have type 2 diabetes, though this only occurs when living at thermoneutrality (Feldmann et al., 2009). In addition to classic brown fat, white fat depots contain $UCP1^{+}$ cells (Cousin et al., 1992; Ghorbani and Himms-Hagen, 1997; Guerra et al., 1998; Himms-Hagen et al., 2000; Xue et al., 2005) known as beige (Wu et al., 2012) or brown-white (brite) adipocytes (Petrovic et al., 2010). Beige cells and classic brown adipocytes have distinctly different molecular signatures (Wu et al., 2012) and developmental origins (Seale et al., 2008). Adult humans have $UCP1^{+}$ adipose tissue which has a gene expression pattern more similar to beige cells than to classic brown cells in the mouse (Wu et al., 2012). Though *GNB3* overexpression alters the gene expression profiles of both BAT and WAT, *GNB3* appears to have the greatest effect in beige-cell containing iWAT.

BAT in *GNB3*-T/+ mice has lower expression of beige and brown adipocyte markers. Additionally, *GNB3*-T/+ mice showed markedly worsened beige adipocyte function in subcutaneous fat pads as indicated by lower levels of *Ucp1* in iWAT. Subcutaneous adipose tissue in *GNB3*-T/+ mice acquired properties of visceral fat indicated by elevated expression of adipogenic markers, *Pparg* and *Adipoq*. Overall, *GNB3* overexpression stimulates a conversion of subcutaneous WAT, particularly in the

inguinal depot, into a less $UCP1^+$ and a less beige but whiter tissue. We show that this white-like remodeling of iWAT and loss of brown and beige properties in BAT is accompanied by increased adiposity in mice fed normal chow. Together, these data implicate *GNB3* overexpression in impaired WAT and BAT, and for the first time provide a functional link between *GNB3* and obesity pathogenesis. However, the specific causes of *GNB3*-related obesity remain to be determined. Future studies of *GNB3* overexpression are needed to dissect the molecular mechanisms by which *GNB3* alters adipose tissue metabolism, signaling, and energy expenditure.

Materials and Methods

Animals. Mice were housed in a 22–23 °C climate controlled room on a 12-h light/dark cycle (lights on at 0700 h), in static micro-isolator cages with free access to water and standard rodent chow (Purina LabDiet 5001). Mice rooms were in an Association for Assessment and Accreditation of Laboratory Animal Care (AAALAC)-accredited facility in accordance with the National Research Council's Guide for the Care and Use of Laboratory Animals. All animal studies were performed according to protocols approved by the Institutional Animal Care and Use Committee at Emory University. The BAC transgenic *GNB3*-T/+ mice were developed on a FVB background as previously described (Goldlust et al., 2013). Mice were weighed once a week or once every 5 weeks from weaning to 25 weeks of age. Mice were euthanized by isoflurane.

Food intake. Littermate mice were housed in groups of 2-3, separated by sex and genotype. Mice had free access to water and chow in cages that were supplied with a pre-

weighed amount of food. For three days, the remaining food in the cage was weighed every 12 hours at ages 5, 10, 15, 20 and 25 weeks. Mice were acclimated to the cages for at least 24 hours before measuring food intake. Per mouse food consumption was calculated by dividing the total amount of food consumed in cage (g) by the number of animals in cage.

Tissue weights. Inguinal and gonadal WAT, brown adipose tissue (BAT) and liver were dissected and weighed. Percent tissue weights were calculated by dividing tissue weight by total body weight of each mouse. Mouse length was measured from nose to anus.

Dual-energy X-ray absorptiometry (DXA). Body composition was measured using DXA scanning (Lunar PIXImus2 densitometer, GE Medical Systems) after anesthesia using isoflurane at ages 5 and 20 weeks.

Blood analysis. Five and 20-week-old mice were fasted for 6 hours. Blood glucose was measured by a glucometer (Accu-Check Aviva, Roche) from a drop of tail blood collected by milking the tail. For metabolic, lipid and hormone profiling, blood was collected by cardiac puncture following euthanasia using isoflurane. Blood collection started between 1:00 and 2:00 pm each day. Dipeptidyl peptidase-4 inhibitor (EMD Millipore Corporation, Billerica, MA, USA), aprotinin (Sigma-Aldrich, Saint Louis, MO, USA), protease inhibitor cocktail (Sigma-Aldrich, Saint Louis, MO, USA) and serine protease inhibitor (AEBSF) (Sigma-Aldrich, Saint Louis, MO, USA) were added to samples collected in tubes coated with EDTA (Becton, Dickinson and Company,

Franklin Lakes, NJ). Fasting blood plasma was separated immediately by centrifuge (1000×g) for 10 minutes at room temperature and was aliquoted and stored at −20°C. Plasma concentrations of amylin (active), C-peptide, acylated ghrelin (active), GIP (total), GLP-1 (active), glucagon, IL-6, insulin, leptin, MCP-1, PP, PYY, resistin and TNF-α were measured using MILLIPLEX MAP mouse metabolic hormone magnetic bead panel kit (MMHMAG-44K). Plasma concentrations of ACTH, FSH, GH, prolactin, TSH and LH were measured using MILLIPLEX MAP mouse pituitary magnetic bead panel kit (MPTMAG-49K) (Millipore, Billerica, MA, USA). The assays were performed according to the manufacturer's instructions. Plasma triglycerides, cholesterol, phospholipids and non-esterified fatty acids were measured at the Mouse Metabolic Phenotyping Center (Cincinnati, OH, USA).

Glucose tolerance test and insulin tolerance test. For the glucose tolerance test (GTT), 5 and 20-week-old mice were fasted for 6 hours and injected intraperitoneally with 1 mg/g D-glucose (Sigma-Aldrich, St. Louis, MO, USA). For the insulin tolerance test (ITT), 20-week-old mice were fasted for 4 hours and injected intraperitoneally with insulin (I9278 SIGMA, Sigma-Aldrich, St. Louis, MO, USA) using 0.05 units/kg (females) or 0.1 units/kg (males). Blood glucose levels were measured from the tip of the tail using a glucometer (Accu-Check Aviva, Roche) at -5, 0, 5, 10, 15, 20, 25, 30, 60, 120 min after injection for GTT, and at 0, 15, 30, 45, 60, 75, 90 min after injection for ITT, respectively.

Indirect calorimetry study. Five and 20-22 week old male mice were housed individually in metabolic chambers with free access to food and water on a 12 hour light/dark cycle, and assessed for metabolic activities using an OPTO-M3 sensor system (Oxymax, Columbus Instruments, Columbus, OH, USA). Spontaneous activity, volume of oxygen consumption (VO_2) and volume of carbon dioxide production were measured over a 72 hour collection period after 48 hours of acclimation.

Cold challenge: Rectal temperature measurement. Rectal temperature of 5 and 20 week old mice was measured using a MicroTherma 2T hand held thermometer (ThermoWorks, Lindon, UT, USA) at time 0, 15, 30, 45, 60, 75 min after placement in a 4 °C room.

Behavioral tests. We used an established repertoire of tests (Burgado et al., 2014) to examine anxiety- and depressive-like behaviors in adult *GNB3*-T/+ and WT mice. Mice were between 19-23 weeks old and behavioral tests were started between 2:00 and 3:00 pm each day. The same investigator conducted all experiments and was blinded to treatment group. Both groups were counterbalanced. Behavioral tests were conducted on subsequent days in the following order: open field testing and novelty suppressed feeding, social interaction, marble burying, novel object recognition. For all behavioral assays, 6 *GNB3*-T/+ and 6 WT subjects were used.

Open field. The open field test measures both general locomotor activity and anxiety-like behavior (Carola et al., 2002; Choleris et al., 2001; Prut and Belzung, 2003). Mice were placed in a corner of a 45x45 cm^2 square box and allowed to explore for 10 minutes. Noldus Ethovision software was used to record and analyze total distance

moved, frequency of entrance into the center zone, time spent in center zone, and latency to enter center zone.

Novelty suppressed feeding. Novelty suppressed feeding measures the latency to feed in a novel environment and is sensitive to administration of anti-depressants and anxiolytics (Fukumoto et al., 2014). Mice were tested on the same day as the open field test to ensure animals were not habituated to the environment. Three grams of sucrose pellets were placed in the center of the open field box and mice were allowed to freely explore for 10 minutes. After testing, mice were placed back in the home cage along with the sucrose pellets and were allowed to feed for an additional 5 minutes. The sucrose pellets left over were weighed and subtracted from the initial amount to determine total amount of sucrose eaten. All mice were habituated to sucrose pellets at least 24 hours before testing.

Social interaction. Social interaction is also a measure of anxiety-like behavior in mice (File, 1980; File and Seth, 2003) and was assessed with age-matched, non-littermate mice as a stimulus. The stimulus mouse was placed at the center of the open field box and the reactive mouse was placed in a corner of the open field box. Mice were allowed to interact for 10 minutes. Latency to interact and total interaction time were analyzed.

Marble burying. The marble burying test also examines anxiety-like behavior (Njung'e and Handley, 1991). Using clean mouse cages with twice the normal amount of bedding, twenty marbles were placed on top of bedding in a 4x5 pattern. Mice were placed in a corner of the box and allowed to explore for 30 minutes. After testing mice were removed and two researchers independently counted the number of marbles buried.

Novel object recognition. The novel object recognition task is used to assess learning and memory in mice (Sargolini et al., 2003; Tang et al., 1999). Testing was conducted in the open field box over three successive days. For each round of testing, mice were placed in the same corner of the open field box. Two identical objects were placed in opposite corners of the box and mice were allowed to explore freely for 10 minutes. Mice were habituated to the test set-up for one day before testing. For the no-delay test, one of the objects was replaced by a novel object immediately after. For the one-hour and 24-hour delay tests, mice were placed back in the home cage for one or 24 hours, respectively. Mice were then placed back in the box with a different novel object and allowed to explore for 10 minutes. Noldus Ethovision software was used to record and analyze number of object touches, time spent sniffing each object, latency to approach objects, total distance moved, and average velocity.

Histology. Inguinal and gonadal WAT were fixed in 10% formalin. Tissue processing, embedding, sectioning and haematoxylin and eosin (H&E) staining were performed at Emory University Winship Pathology Core Lab. Adipocyte size was measured using ImageJ software (Schneider et al., 2012).

Gene expression: Total RNA extraction, cDNA synthesis, and quantitative real-time PCR. Total RNA was extracted from fresh tissue using the RNeasy Lipid Tissue Mini kit (Qiagen, Austin, TX, USA) following manufacturer's instructions and cDNA was synthesized from total RNA using the SuperScript III First-Strand Synthesis System for RT-PCR (Invitrogen Corporation, Carlsbad, CA, USA). Quantitative real-time PCR was

performed using iQ SYBR Green Supermix (Bio-Rad Laboratories, Hercules, CA, USA) mixed with gene-specific primers on the Bio-Rad CFX96 Real-Time PCR Detection System. Expression data were normalized by the 2-[delta][delta]Ct method using *Gapdh* as an internal control. Primer sequences are listed in Table 3.2. Taqman quantitative RT-PCR was performed as described (14) to measure *GNB3* and *Gnb3* expression using *Actb* as an internal control.

Protein extraction and Western blot analysis. Inguinal WAT (iWAT) and BAT were dissected, weighed and immediately homogenized on ice in CelLytic MT Mammalian Tissue Lysis/Extraction Reagent (Sigma-Aldrich, St. Louis, MO, USA) with protease inhibitor cocktail. Total protein concentration was determined using Pierce BCA Protein Assay Kit (Pierce Biotechnology, Rockford, IL, USA).

Citrate synthase. Citrate synthase activity for iWAT and BAT extracts were measured using the Citrate Synthase Assay Kit (Sigma-Aldrich, St. Louis, MO, USA) following the manufacturer's instructions.

Statistical analysis. Statistical analyses were performed using GraphPad Prism version 6 for Mac (GraphPad Software, Inc., La Jolla, CA, USA). Data are presented as mean ± SD (or SEM where indicated). Unpaired Student's *t*-test was used to compare two groups, and one-way ANOVA was used to compare more than two groups. Comparisons with *p*-values <0.05 were considered significant.

Figure 3.1

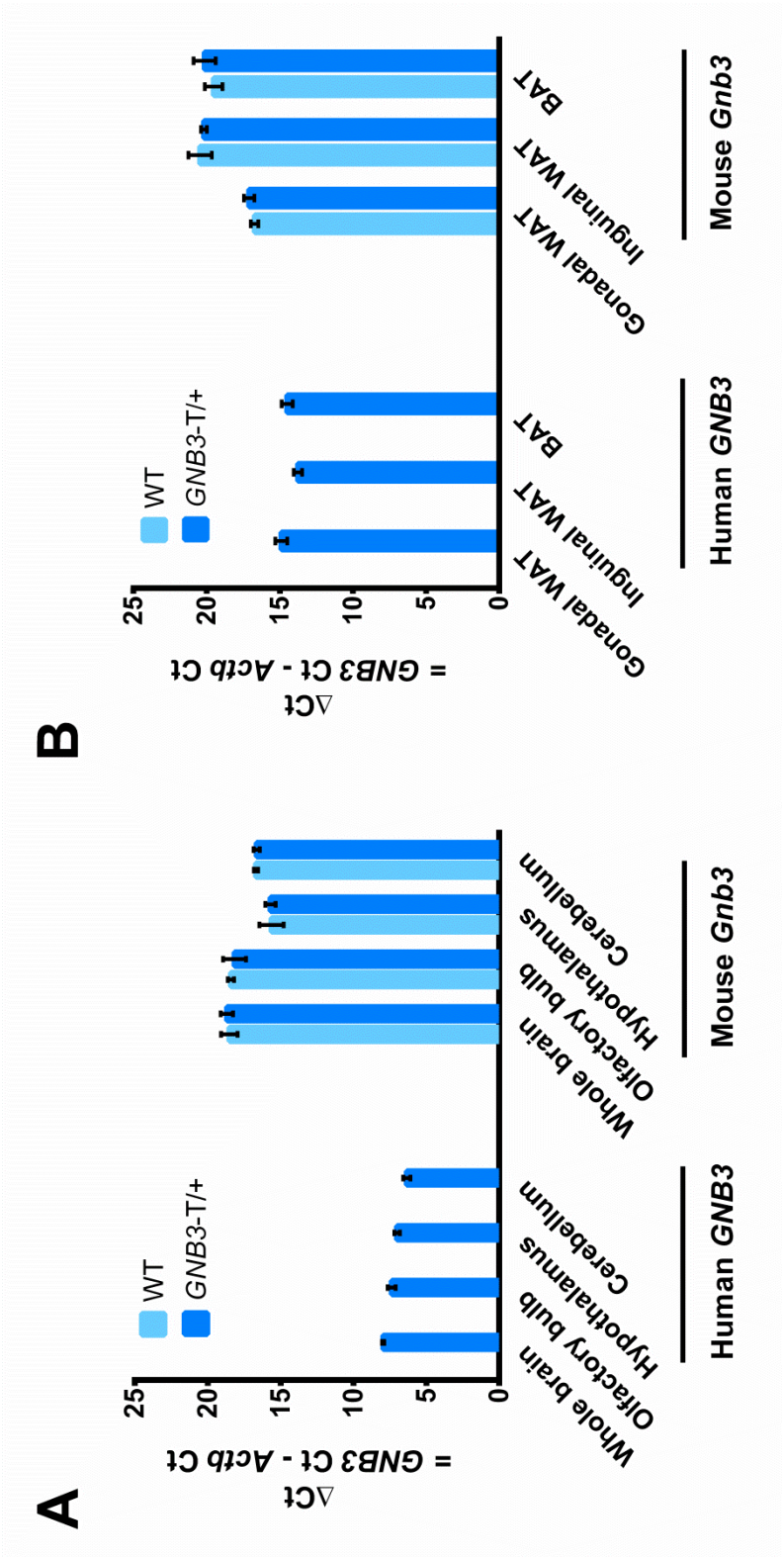
A
ΔCt
= GNB3 Ct - Actb Ct
25
20
15
10
5
0
WT
GNB3-T/+
Whole brain
Olfactory bulb
Hypothalamus
Cerebellum
Human GNB3
Whole brain
Olfactory bulb
Hypothalamus
Cerebellum
Mouse Gnb3
B
ΔCt
= GNB3 Ct - Actb Ct
25
20
15
10
5
0
WT
GNB3-T/+
Gonadal WAT
Inguinal WAT
BAT
Human GNB3
Gonadal WAT
Inguinal WAT
BAT
Mouse Gnb3

Figure 3.1

Transgenic *GNB3* is highly expressed in the brain, at levels greater than endogenous *Gnb3*. (A) Transgenic human *GNB3* and mouse endogenous *Gnb3* gene expression in brain tissues of 5-week-old mice. (B) *GNB3* and *Gnb3* expression in gWAT, iWAT, and BAT of 20-week-old mice. n = 4 mice per group in A, n = 3 mice per group in B. 3 technical replicates for both. Ct, cycle threshold.

Figure 3.2

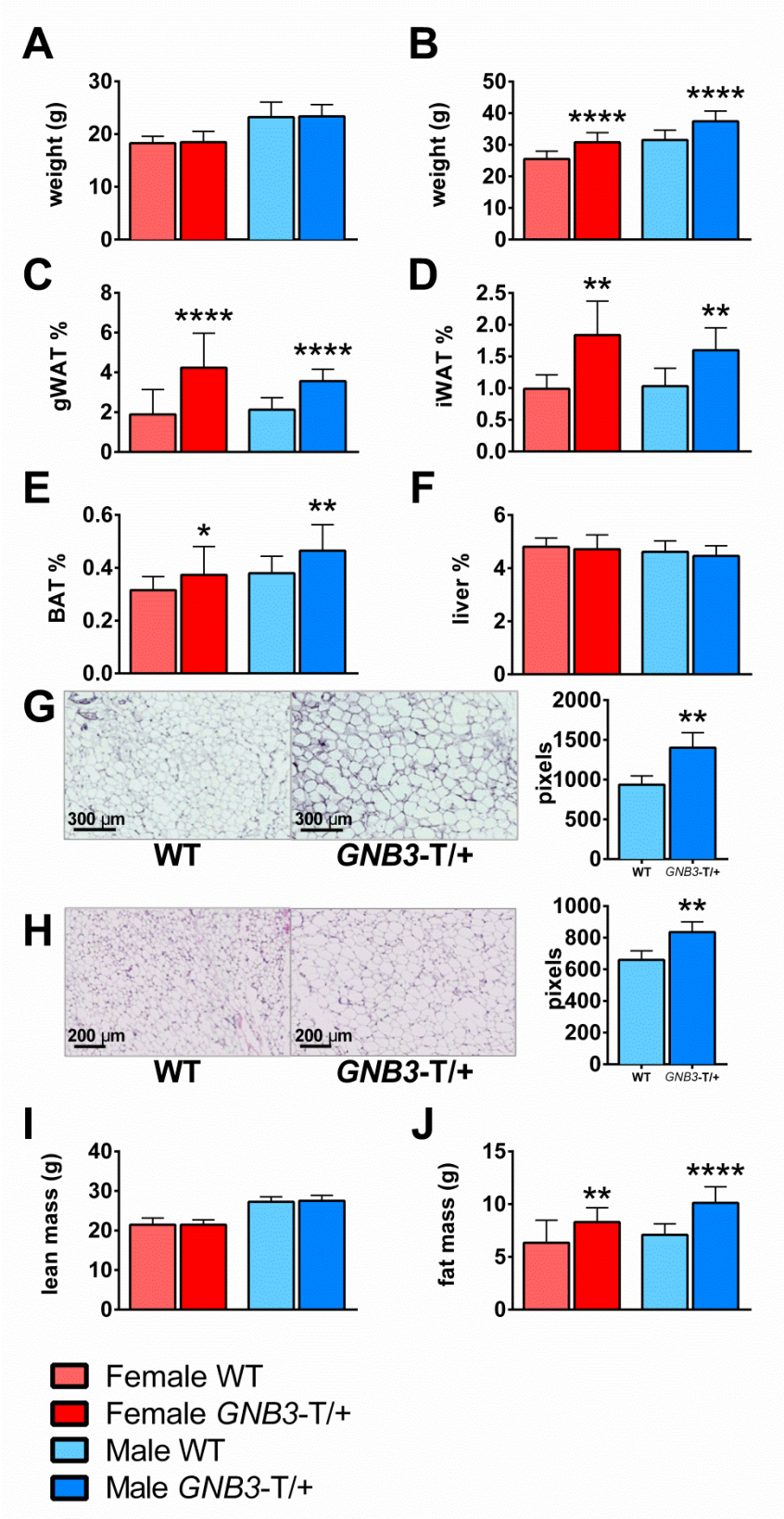
A
weight (g)
B
weight (g)
****
****
C
gWAT %
****
****
D
iWAT %
**
**
E
BAT %
*
**
F
liver %
G
300 µm
300 µm
WT
GNB3-T/+
pixels
**
WT
GNB3-T/+
H
200 µm
200 µm
WT
GNB3-T/+
pixels
**
WT
GNB3-T/+
I
lean mass (g)
J
fat mass (g)
**
****
Female WT
Female GNB3-T/+
Male WT
Male GNB3-T/+

Figure 3.2

***GNB3*-T/+ mice have greater adiposity than WT.** (A) Body weight of 5-week-old mice. (B) Body weight, (C) gWAT weight/body weight (gWAT%), (D) iWAT weight/body weight (iWAT%), (E) BAT weight/body weight (BAT%), (F) liver weight/body weight (liver%) of 20-week-old mice. (G) Representative images of 20-week-old gWAT and (H) iWAT sections stained with H&E; cell size measured in pixels to the right. (I) DXA lean mass and J. DXA fat mass of 20-week-old mice. n = 8-11 mice per group in A; n = 16-23 mice per group in B, C and E; n = 5-9 mice per group in D; n = 10-20 mice per group in F; n = 5 mice per group in G, H (five images per mouse were used to quantify adipocyte size in pixels); n = 17-20 mice per group in I, J. Data are mean ± SD. *P < 0.05, **P < 0.01, ***P < 0.001, ****P < 0.0001 vs. WT of same sex by unpaired Student's t-test.

Figure 3.3

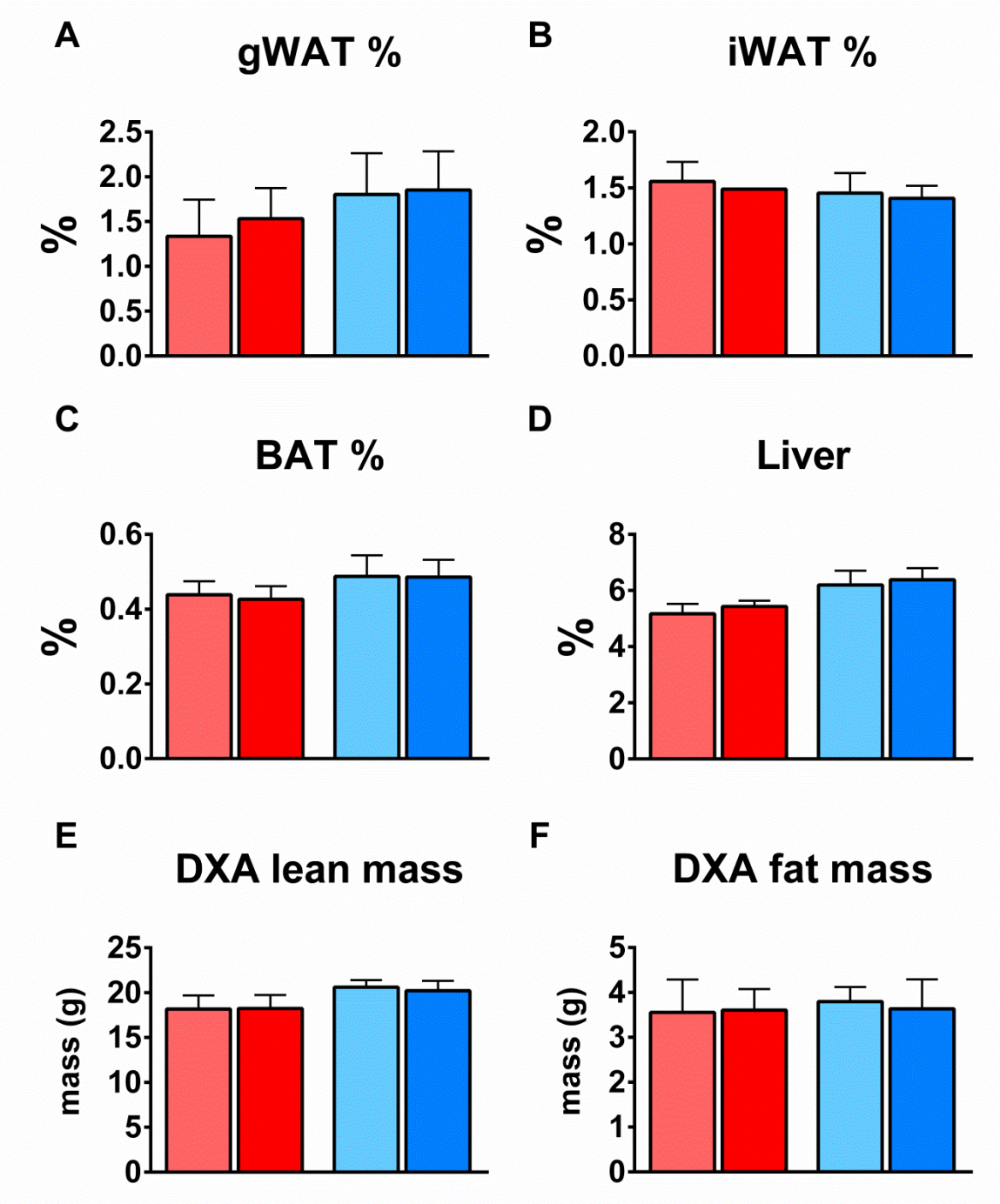
A
gWAT %
%
2.5
2.0
1.5
1.0
0.5
0.0
B
iWAT %
%
2.0
1.5
1.0
0.5
0.0
C
BAT %
%
0.6
0.4
0.2
0.0
D
Liver
%
8
6
4
2
0
E
DXA lean mass
mass (g)
25
20
15
10
5
0
F
DXA fat mass
mass (g)
5
4
3
2
1
0

Figure 3.3

Five-week-old *GNB3*-T/+ mice have similar adiposity compared to WT. (A) gWAT weight/body weight (gWAT%), (B) iWAT weight/body weight (iWAT%), (C) BAT weight/body weight (BAT%), (D) liver weight/body weight (liver%), (E) DXA lean mass and (F) DXA fat mass of 5-week-old mice. *n* = 8-11 mice per group in A, C, and D; *n* = 1-8 mice per group in B; *n* = 14-22 mice per group in E, F. Data are mean ± SD. No significant difference between *GNB3*-T/+ and WT of same sex by unpaired Student's *t*-test.

Figure 3.4

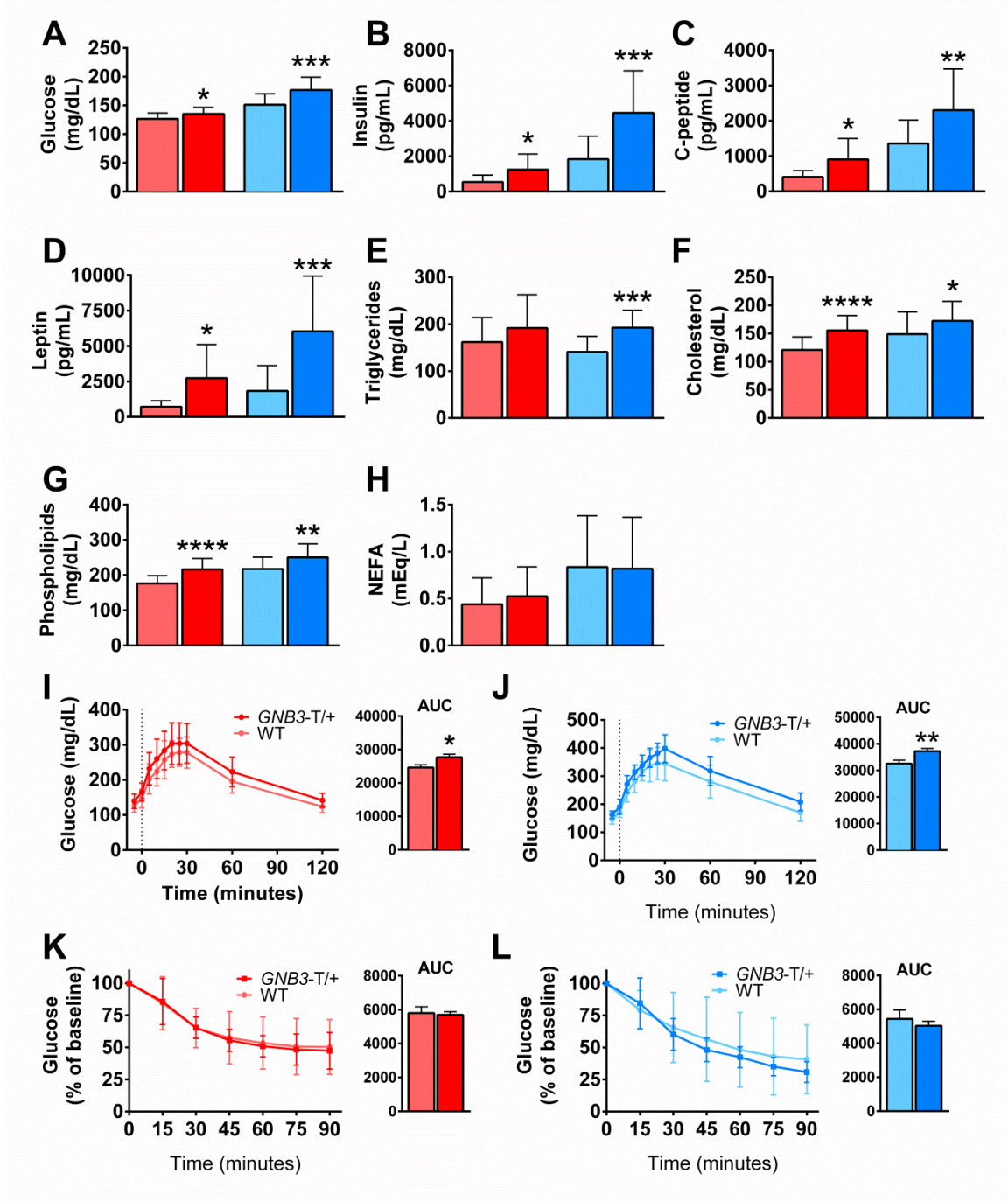
A
Glucose (mg/dL)
250
200
150
100
50
0
*
***
B
Insulin (pg/mL)
8000
6000
4000
2000
0
*
***
C
C-peptide (pg/mL)
4000
3000
2000
1000
0
*
**
D
Leptin (pg/mL)
10000
7500
5000
2500
0
*
***
E
Triglycerides (mg/dL)
300
200
100
0
***
F
Cholesterol (mg/dL)
250
200
150
100
50
0
****
*
G
Phospholipids (mg/dL)
400
300
200
100
0
****
**
H
NEFA (mEq/L)
1.5
1.0
0.5
0.0
I
Glucose (mg/dL)
400
300
200
100
0
0 30 60 90 120
Time (minutes)
GNB3-T/+
WT
AUC
40000
30000
20000
10000
0
*
J
Glucose (mg/dL)
500
400
300
200
100
0
0 30 60 90 120
Time (minutes)
GNB3-T/+
WT
AUC
50000
40000
30000
20000
10000
0
**
K
Glucose (% of baseline)
100
75
50
25
0
0 15 30 45 60 75 90
Time (minutes)
GNB3-T/+
WT
AUC
8000
6000
4000
2000
0
L
Glucose (% of baseline)
100
75
50
25
0
0 15 30 45 60 75 90
Time (minutes)
GNB3-T/+
WT
AUC
8000
6000
4000
2000
0

Figure 3.4

***GNB3*-T/+ mice have metabolic syndrome.** (A) Fasting blood glucose, (B) fasting plasma insulin, (C) C-peptide, (D) leptin, (E) triglycerides, (F) cholesterol, (G) phospholipids and (H) non-esterified fatty acids of mice. (I) GTT and areas under the curve (AUC) of female and (J) male mice. (K) ITT and AUC of female and (L) male mice. All mice are 20 weeks old. n = 15-23 mice per group in A, n = 11-20 mice per group in B-D, n = 16-25 mice per group in E-H, n = 18-22 mice per group in I, n = 17-18 mice per group in J, n = 14-16 mice per group in K, n = 10-17 mice per group in L. Data are mean ± SD. *P < 0.05, **P < 0.01, ***P < 0.001, ****P < 0.0001 vs. WT of same sex by unpaired Student's t-test.

Figure 3.5

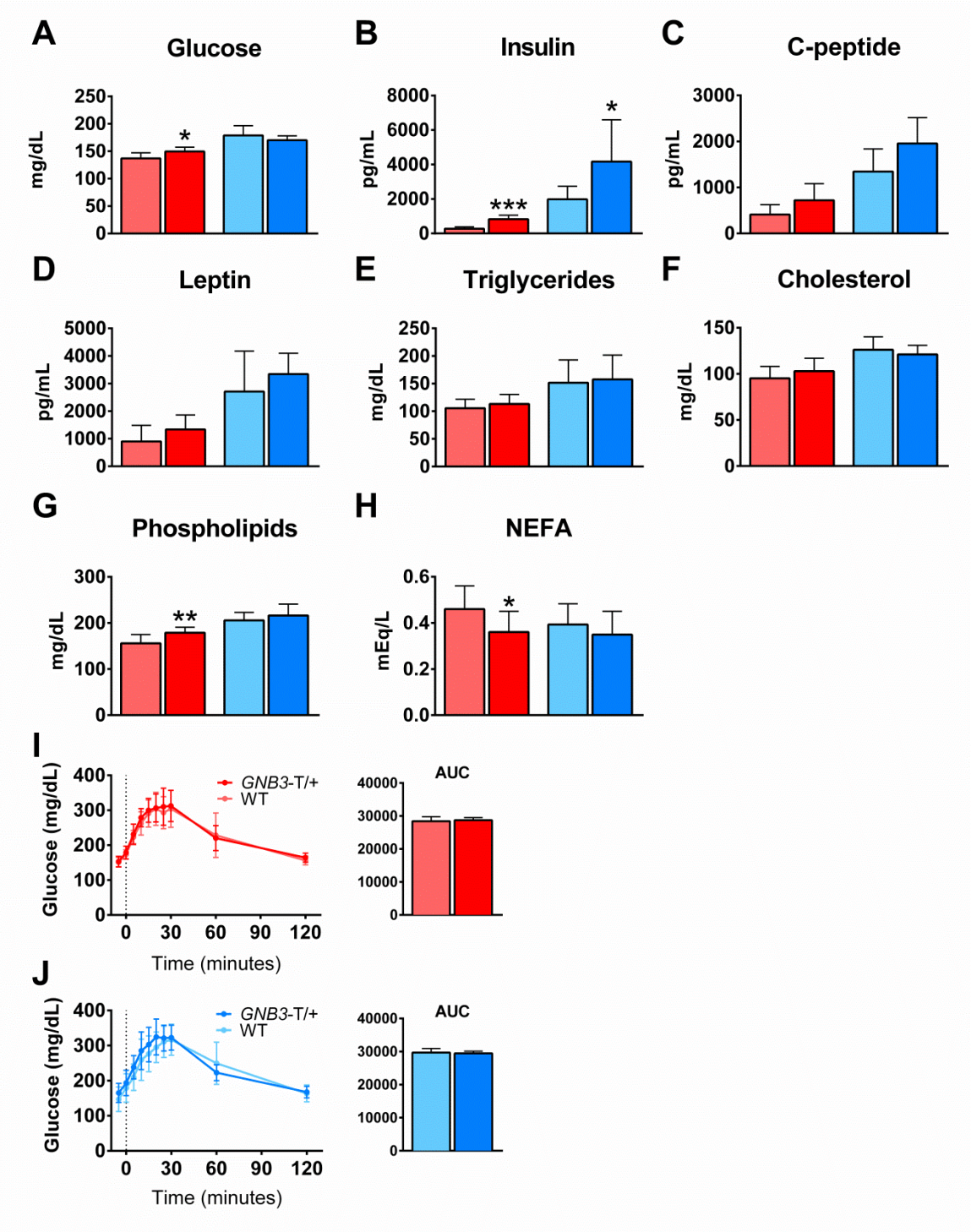
A
Glucose
mg/dL
250
200
150
100
50
0
*
B
Insulin
pg/mL
8000
6000
4000
2000
0
***
*
C
C-peptide
pg/mL
3000
2000
1000
0
D
Leptin
pg/mL
5000
4000
3000
2000
1000
0
E
Triglycerides
mg/dL
250
200
150
100
50
0
F
Cholesterol
mg/dL
150
100
50
0
G
Phospholipids
mg/dL
300
200
100
0
**
H
NEFA
mEq/L
0.6
0.4
0.2
0.0
*
I
Glucose (mg/dL)
400
300
200
100
0
GNB3-T/+
WT
0
30
60
90
120
Time (minutes)
AUC
40000
30000
20000
10000
0
J
Glucose (mg/dL)
400
300
200
100
0
GNB3-T/+
WT
0
30
60
90
120
Time (minutes)
AUC
40000
30000
20000
10000
0

Figure 3.5

***GNB3*-T/+ mice have slightly impaired glucose metabolism prior to obesity.** (A) Fasting blood glucose, (B) fasting plasma insulin, (C) C-peptide, (D) leptin, (E) triglycerides, (F) cholesterol, (G) phospholipids and (H) non-esterified fatty acids. GTT and AUC of (I) female and (J) male mice. All mice are 5 weeks old. n = 8-11 mice per group in A, n = 7 mice per group in B-D, n = 9-13 mice per group in E-H, n = 10-14 mice per group in I, n = 11-15 mice per group in J. Data are mean ± SD. *$P < 0.05$, **$P < 0.01$ vs. WT of same sex by unpaired Student's *t*-test.

Figure 3.6

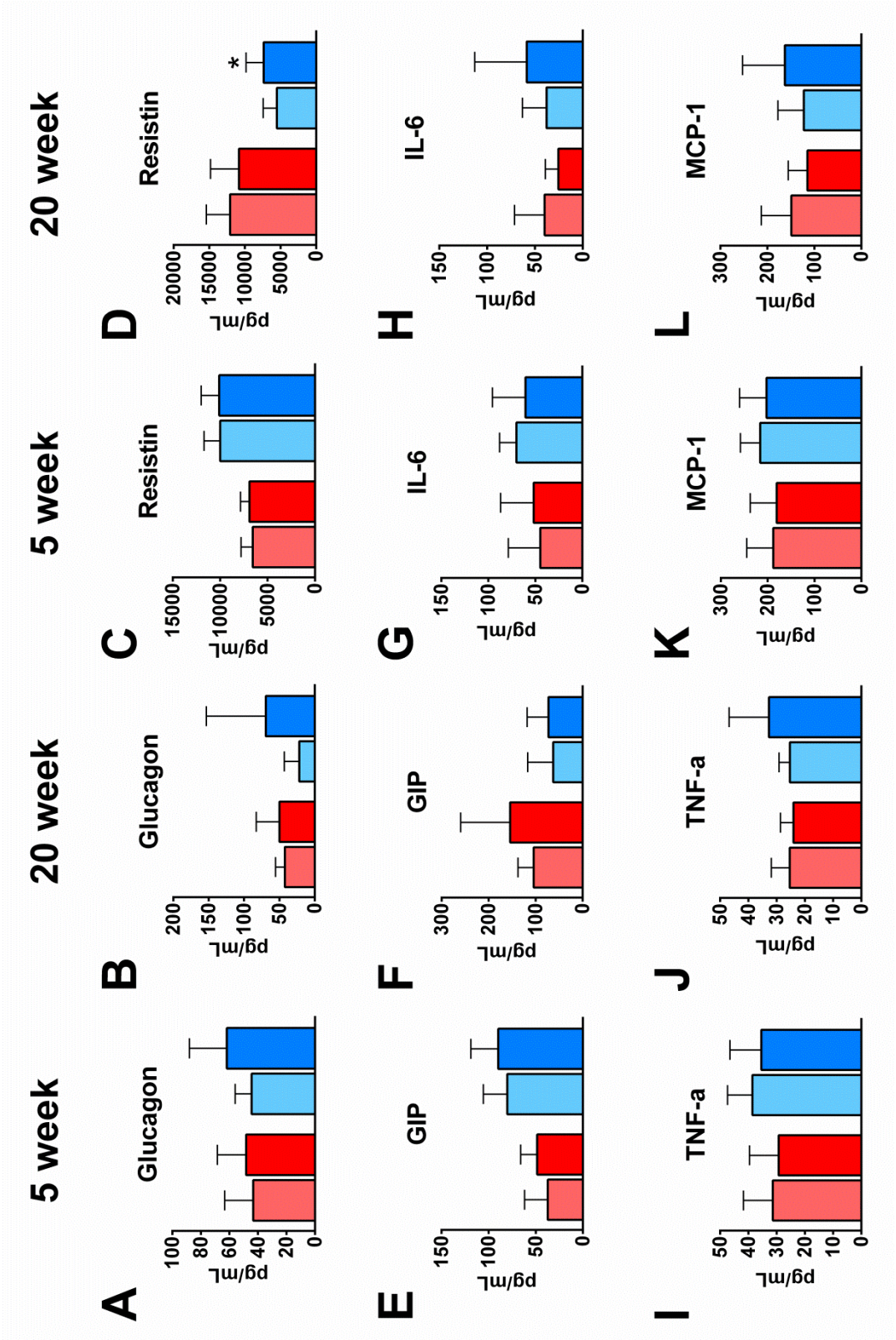
5 week
20 week
5 week
20 week
A
Glucagon
pg/mL
B
Glucagon
pg/mL
C
Resistin
pg/mL
D
Resistin
pg/mL
*
E
GIP
pg/mL
F
GIP
pg/mL
G
IL-6
pg/mL
H
IL-6
pg/mL
I
TNF-a
pg/mL
J
TNF-a
pg/mL
K
MCP-1
pg/mL
L
MCP-1
pg/mL

Figure 3.6

Panel of metabolic hormones and inflammatory markers. Male *GNB3*-T/+ mice have elevated fasting plasma resistin during obesity. (A), (B) Fasting plasma glucagon; (C), (D) resistin; (E), (F) GIP; (G), (H) IL-6; (I), (J) TNF-a; and (K), (L) MCP-1 in 5-week and 20-week-old mice, respectively. *n* = 7 mice per group in A, C, E, G, I, K; *n* = 10-13 mice per group in *B, n* = 11-20 mice per group in D, F, H, J, L. Data are mean ± SD. **P* < 0.05 vs. WT of same sex by unpaired Student's *t*-test.

Figure 3.7

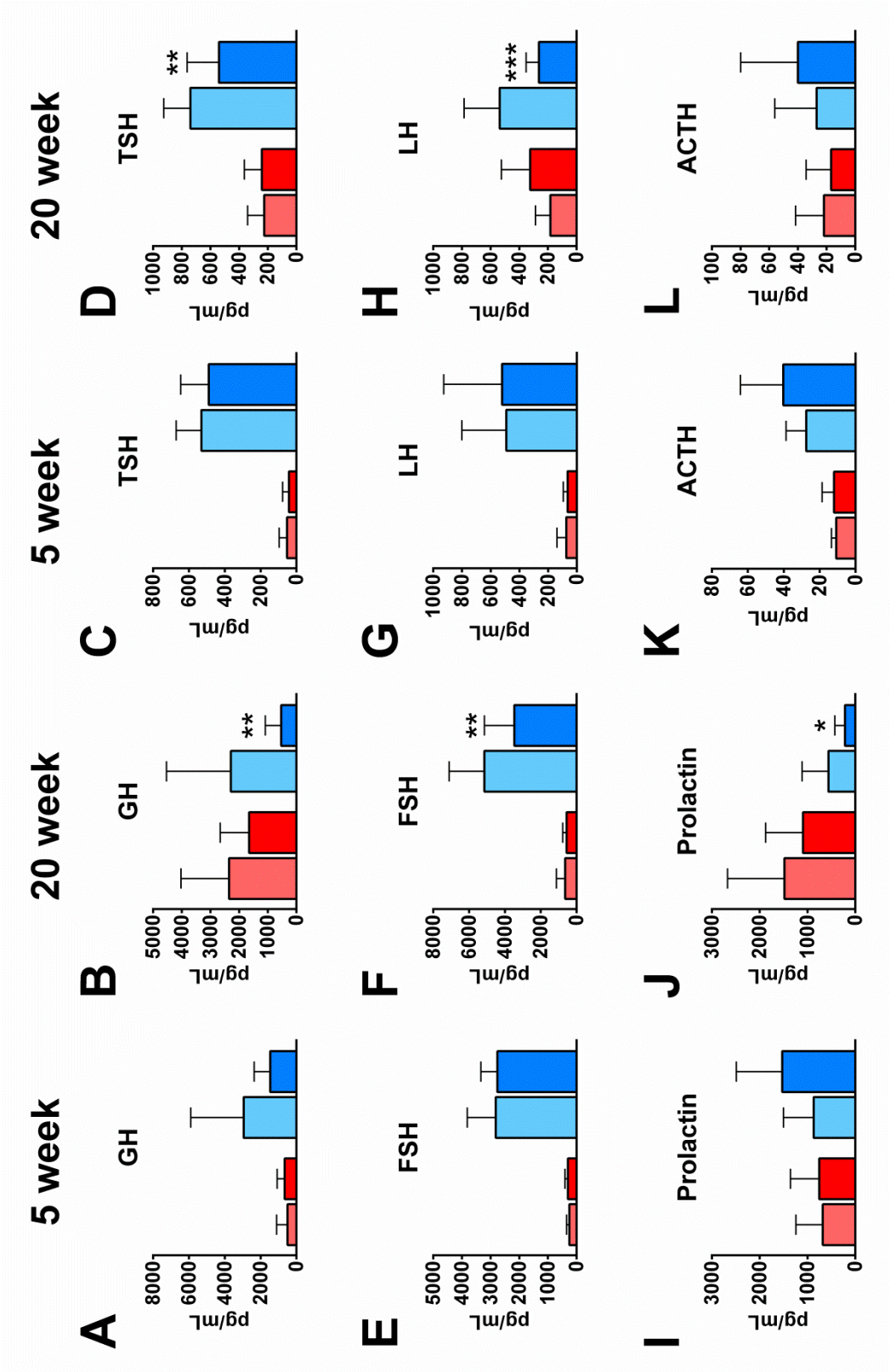
5 week
20 week
5 week
20 week
A
B
C
D
E
F
G
H
I
J
K
L
GH
GH
TSH
TSH
FSH
FSH
LH
LH
Prolactin
Prolactin
ACTH
ACTH
pg/mL
**
**
**
***
*

Figure 3.7

Panel of pituitary hormones. *GNB3*-T/+ male mice have lower GH, TSH, FSH, LH and prolactin during obesity. (A), (B) Fasting plasma growth hormone (GH); (C), (D) thyroid-stimulating hormone (TSH); (E), (F) follicle-stimulating hormone (FSH); (G), (H) luteinizing hormone (LH); (I), (J) prolactin; (K), (L) adrenocorticotropic hormone (ACTH) levels of 5 week and 20 week old mice, respectively. n = 7 mice per group in A, C, E, G, I, K; n = 11-20 mice per group in B, D, F, H, J, L. Data are mean ± SD. *P < 0.05, **P < 0.01, ***P < 0.001 vs. WT of same sex by unpaired Student's t-test.

Figure 3.8

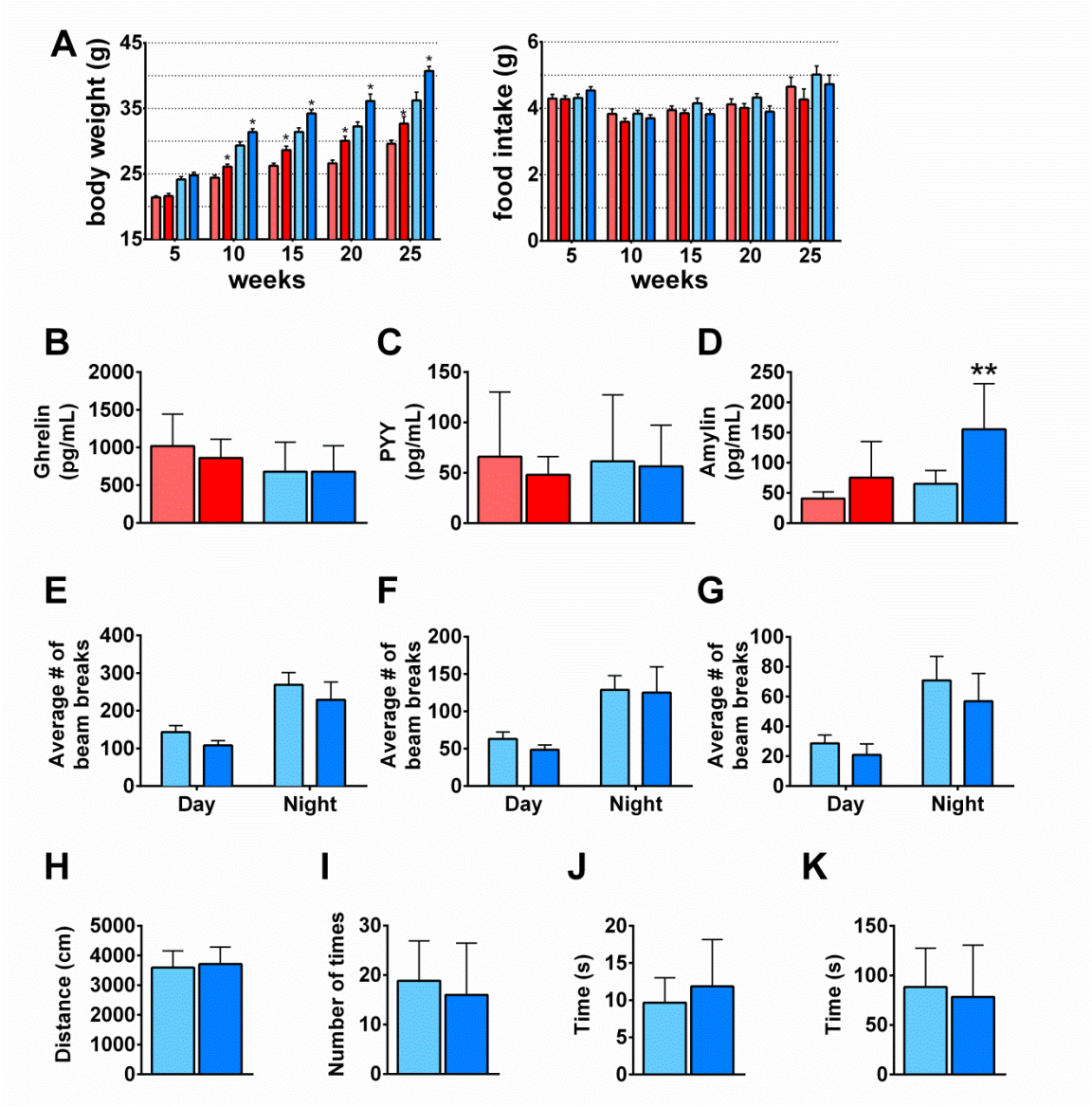
A
body weight (g)
45
35
25
15
5
10
15
20
25
weeks
food intake (g)
6
4
2
0
5
10
15
20
25
weeks
B
Ghrelin (pg/mL)
2000
1500
1000
500
0
C
PYY (pg/mL)
150
100
50
0
D
Amylin (pg/mL)
250
200
150
100
50
0
**
E
Average # of beam breaks
400
300
200
100
0
Day
Night
F
Average # of beam breaks
200
150
100
50
0
Day
Night
G
Average # of beam breaks
100
80
60
40
20
0
Day
Night
H
Distance (cm)
5000
4000
3000
2000
1000
0
I
Number of times
30
20
10
0
J
Time (s)
20
15
10
5
0
K
Time (s)
150
100
50
0

Figure 3.8

***GNB3*-T/+ mice have proper satiety, similar food intake and activity levels compared to WT.** (A) Daily amount of food consumption per mouse (right) and corresponding body weight of same mice (left) measured every 5 weeks for 25 weeks. (B) Fasting plasma ghrelin, (C) PYY, (D) amylin. (E) Total movement in X-plane, (F) horizontal ambulatory activity, and (G) vertical activity averaged over a 72-hour period. (H) Distance moved, (I) frequency of entrance into center zone, (J) time spent in center, (K) latency during open field test. Mice are 20 weeks old in B-K. n = 24-33 mice per group in A, n = 10-13 mice per group in B, n = 7-19 mice per group in C, n = 4-13 mice per group in D, n = 16-31 mice per group in E-G, n = 6-7 mice per group in H-K. Data are mean ± SD in B-D, H-K; and ± SEM in A, E-G. *$P < 0.05$, **$P < 0.01$ vs. WT of same sex by unpaired Student's *t*-test.

Figure 3.9

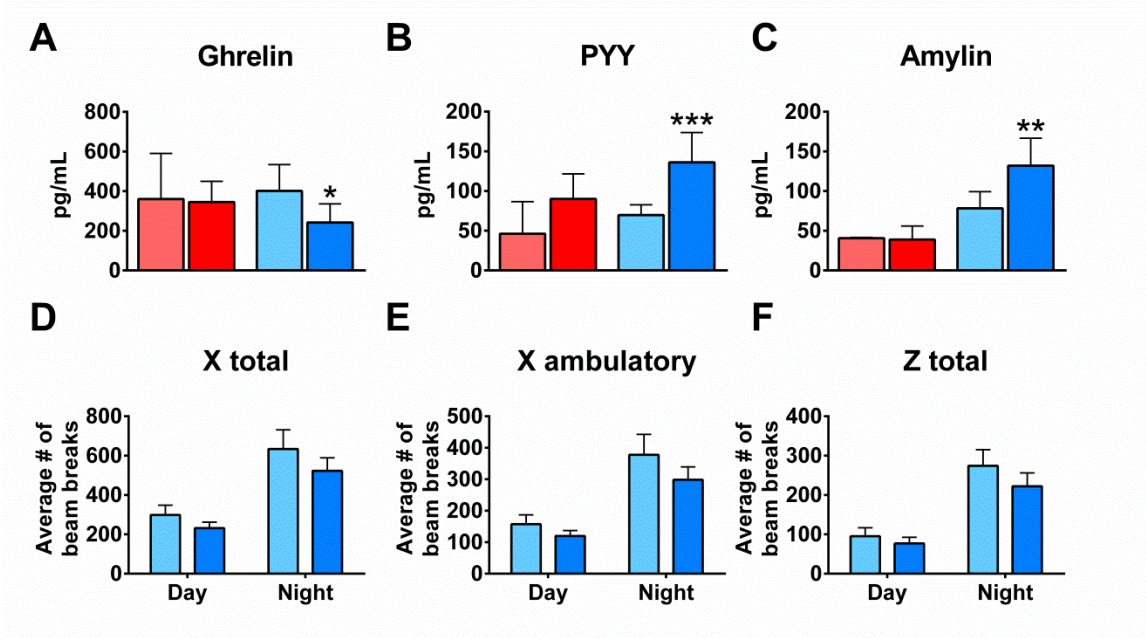
A
Ghrelin
pg/mL
800
600
400
200
0
*
B
PYY
pg/mL
200
150
100
50
0
***
C
Amylin
pg/mL
200
150
100
50
0
**
D
X total
Average # of beam breaks
800
600
400
200
0
Day
Night
E
X ambulatory
Average # of beam breaks
500
400
300
200
100
0
Day
Night
F
Z total
Average # of beam breaks
400
300
200
100
0
Day
Night

Figure 3.9

***GNB3*-T/+ mice have proper satiety and similar activity levels compared to WT prior to obesity.** (A) Fasting plasma ghrelin, (B) PYY and (C) amylin. (D) Total movement in X-plane, (E) horizontal ambulatory activity, (F) and vertical activity averaged over a 72-hour period. All mice are 5 weeks old. $n = 7$ mice per group in A-C, $n = 19$-21 mice per group in D-F. Data are mean ± SD in A-C, and ± SEM in D-F. $^{*}P < 0.05$, $^{**}P < 0.01$, $^{***}P < 0.001$ vs. WT of same sex by unpaired Student's *t*-test.

Figure 3.10

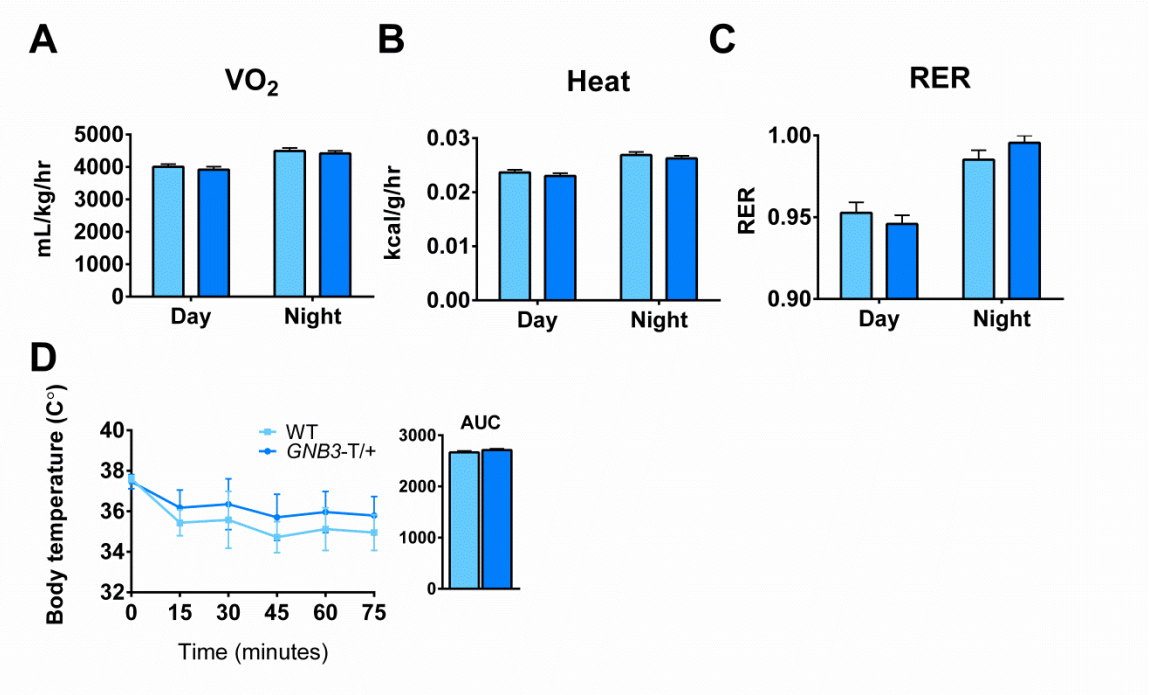
A
VO2
mL/kg/hr
5000
4000
3000
2000
1000
0
Day
Night
B
Heat
kcal/g/hr
0.03
0.02
0.01
0.00
Day
Night
C
RER
RER
1.00
0.95
0.90
Day
Night
D
Body temperature (C°)
40
38
36
34
32
0
15
30
45
60
75
Time (minutes)
WT
GNB3-T/+
AUC
3000
2000
1000
0

Figure 3.10

Oxygen consumption is similar in *GNB3*-T/+ and WT mice, and *GNB3*-T/+ mice do not have dysregulation of acute thermogenesis prior to obesity. (A) VO_2, (B) heat produced normalized over body weight, and (C) RER (VCO_2/VO_2) averaged over a 72-hour period. (D) Acute cold stress at 4°C. All mice are 5 weeks old. *n* = 19-21 mice per group in A-C, *n* = 5-8 mice per group in D. Data are mean ± SEM in A-C; and ± SD in D-F. ****$P < 0.0001$ vs. WT of same sex by unpaired Student's *t*-test.

Figure 3.11

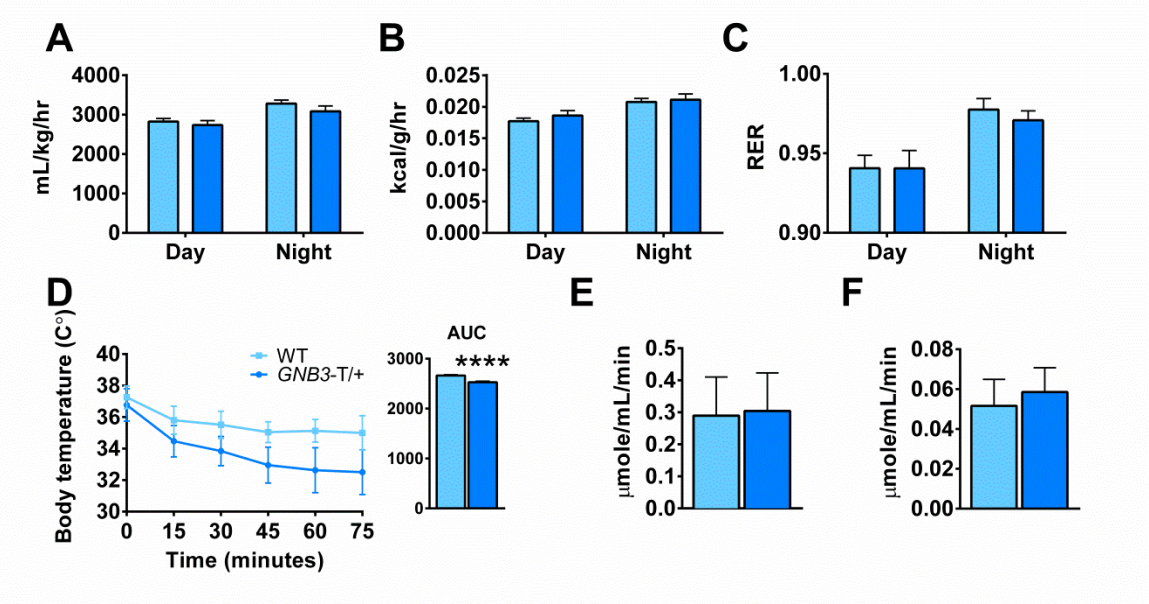
A
mL/kg/hr
4000
3000
2000
1000
0
Day
Night
B
kcal/g/hr
0.025
0.020
0.015
0.010
0.005
0.000
Day
Night
C
RER
1.00
0.95
0.90
Day
Night
D
Body temperature (C°)
40
38
36
34
32
30
WT
GNB3-T/+
0
15
30
45
60
75
Time (minutes)
AUC
****
3000
2000
1000
0
E
µmole/mL/min
0.5
0.4
0.3
0.2
0.1
0.0
F
µmole/mL/min
0.08
0.06
0.04
0.02
0.00

Figure 3.11

Oxygen consumption is similar in *GNB3*-T/+ and WT mice, but *GNB3*-T/+ mice have dysregulation of acute thermogenesis. (A) VO_2, (B) heat produced normalized over body weight, and (C) RER (VCO_2/VO_2) averaged over a 72-hour period. (D) Acute cold stress at 4°C, (E) citrate synthase activity in BAT and (F) iWAT. All mice are 20 weeks old. *n* = 16-31 mice per group in A-C, *n* = 8-14 mice per group in D, *n* = 13-14 mice per group in E, F. Data are mean ± SEM in A-C; and ± SD in D-F. ****$P < 0.0001$ vs. WT of same sex by unpaired Student's *t*-test.

Figure 3.12

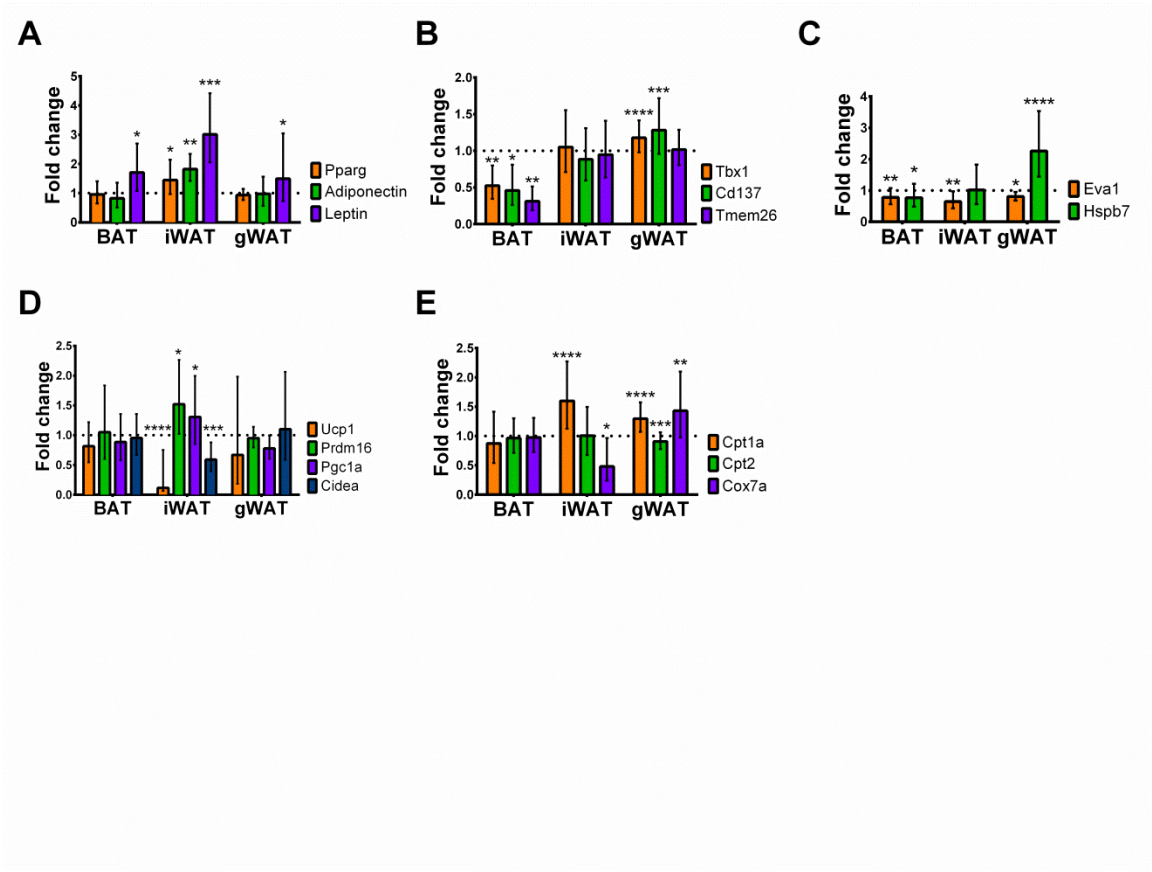
A
Fold change
BAT
iWAT
gWAT
Pparg
Adiponectin
Leptin
B
Fold change
BAT
iWAT
gWAT
Tbx1
Cd137
Tmem26
C
Fold change
BAT
iWAT
gWAT
Eva1
Hspb7
D
Fold change
BAT
iWAT
gWAT
Ucp1
Prdm16
Pgc1a
Cidea
E
Fold change
BAT
iWAT
gWAT
Cpt1a
Cpt2
Cox7a

Figure 3.12

***GNB3*-T/+ mice have lower gene expression of *Ucp1* in BAT, iWAT and gWAT, and lower gene expression of beige and brown adipocyte markers in BAT.** (A) Gene expression profiles of adipogenic, (B) beige adipocyte, (C) brown adipocyte, (D) oxidative phosphorylation, and (E) mitochondria markers in BAT, iWAT and gWAT measured by quantitative RT-PCR. Fold change is *GNB3*-T/+ versus WT, mean ± SD. All mice are 20 weeks old. $n = 3$ mice per group and experiment was repeated 3 times. *$P < 0.05$, **$P < 0.01$, ***$P < 0.001$, ****$P < 0.0001$ vs. WT of same sex by unpaired Student's *t*-test.

Table 3.1

Tissue	Age	Sex	Genotype	Average weight	SD	P	Significant?
gWAT	5 weeks	F	WT	0.2927	0.1430	0.9727	no
			GNB3-T/+	0.2947	0.08817		
		M	WT	0.4255	0.1442	0.8238	no
			GNB3-T/+	0.4384	0.1235		
	20 weeks	F	WT	0.5069	0.3776	<0.0001	****
			GNB3-T/+	1.297	0.6515		
		M	WT	0.7560	0.3061	<0.0001	****
			GNB3-T/+	1.357	0.4051		
iWAT	5 weeks	F	WT	0.3414	0.04497	n/a	n/a
			GNB3-T/+	0.3439	0.0		
		M	WT	0.3624	0.05929	0.5387	no
			GNB3-T/+	0.3463	0.03430		
	20 weeks	F	WT	0.2465	0.08008	0.0129	*
			GNB3-T/+	0.5109	0.2623		
		M	WT	0.4532	0.2509	0.1828	no
			GNB3-T/+	0.5882	0.1645		
BAT	5 weeks	F	WT	0.0799	0.008725	0.9365	no
			GNB3-T/+	0.07954	0.01043		
		M	WT	0.1091	0.02022	0.9029	no
			GNB3-T/+	0.1100	0.01396		
	20 weeks	F	WT	0.08075	0.01669	0.0015	**
			GNB3-T/+	0.1135	0.03946		
		M	WT	0.1256	0.02986	0.0010	***
			GNB3-T/+	0.1719	0.05021		
Liver	5 weeks	F	WT	0.9623	0.06720	0.1311	no
			GNB3-T/+	1.035	0.1266		
		M	WT	1.415	0.1492	0.2613	no
			GNB3-T/+	1.487	0.1427		
	20 weeks	F	WT	1.229	0.1623	0.0169	*
			GNB3-T/+	1.385	0.2046		
		M	WT	1.423	0.2294	0.0157	*
			GNB3-T/+	1.633	0.1983		

*$P < 0.05$, **$P < 0.01$, ***$P < 0.001$, ****$P < 0.0001$ vs. WT of same sex by unpaired Student's *t*-test.

Table 3.1

Absolute weights (g) of dissected adipose tissues and liver.

Table 3.2

Gene	Forward primer (5'→3')	Reverse primer (5'→3')
Adipoq	GGAACTTGTGCAGGTTGGAT	CCTTCAGCTCCTGTCATTCC
Cd137 (or *Tnfrsf9*)	ATAGGTGGACAGCCGAACTG	GCCTGCAGTCCTTTTCACAT
Cidea	TGACATTCATGGGATTGCAG	TAACCAGGCCAGTTGTGATG
Cox7a1	CCGACAATGACCTCCCAGTA	ACTTCTTGTGGGGGAAGGAG
Cpt1a	GCTGCACTCCTGGAAGAAGA	GGTGTCTAGGGTCCGATTGA
Cpt2	CGGCCCTTAAGTGCTGTCT	TGGCTGTCATTCAAGAGAGG
Eva1 (or *Mpzl2*)	TGTGCTTCCACTTCTCCTGA	AGTTAGCGCATCTCCCACAG
Gapdh	TTGTGATGGGTGTGAACCACGA	TCTTCTGGGTGGCAGTGATGG
Hspb7	TCACCACCTTCAACAACCAC	GTGAGGCTACCATCCTCTCG
Lep	CAAGACCATTGTCACCAGGA	TCATTGGCTATCTGCAGCAC
Pparg	CAGGCCTCATGAAGAACCTT	GGATCCGGCAGTTAAGATCA
Ppargc1a	TTGCCCAGATCTTCCTGAAC	TCTGTGAGAACCGCTAGCAA
Prdm16	GAGAAGTTCTGCGTGGATGC	AGGCACCTTCTTTCACATGC
Tbx1	TGTGGGACGAGTTCAATCAG	TGTCATCTACGGGCACAAAG
Tmem26	CTTTCTCCGGCCATCTTTGT	TGGGATGACAGGGTTTGATT
Ucp1	GGCAAAAACAGAAGGATTGC	TAAGCCGGCTGAGATCTTGT

Abbreviations:

Adipoq: adiponectin

Cd137 (or *Tnfrsf9*): tumor necrosis factor receptor superfamily, member 9

Cidea: cell death-inducing DNA fragmentation factor, alpha subunit-like effector A

Cox7a1: cytochrome c oxidase subunit VIIa 1

Cpt1a: carnitine palmitoyltransferase 1a, liver

Cpt2: carnitine palmitoyltransferase 2

Eva1 (or *Mpzl2*): myelin protein zero-like 2

Gapdh: glyceraldehyde-3-phosphate dehydrogenase

Hspb7: heat shock protein family, member 7

Lep: leptin

Pparg: peroxisome proliferator activated receptor gamma

Ppargc1a: peroxisome proliferative activated receptor, gamma, coactivator 1 alpha

Prdm16: PR domain containing 16

Tbx1: T-box 1

Tmem26: transmembrane protein 26

Ucp1: uncoupling protein 1

Table 3.2

Sequence of primers used for real-time quantitative reverse transcription PCR.

Table 3.3

Category	Test	# of mice	Measurement	Genotype	Average	SD	P
Mouse weight	Mouse weight	7	Weight (g)	WT	35.30	2.216	0.7618
		6		*GNB3*-T/+	34.77	3.880	
Anxiety/ depression-like	Novelty suppressed feeding test	7	Amount of sucrose eaten (mg)	WT	216.6	266.5	0.6432
		6		*GNB3*-T/+	152.0	214.1	
		7	Latency to approach (s)	WT	63.08	36.37	0.2897
		6		*GNB3*-T/+	93.58	61.30	
		7	Latency to feed (s)	WT	468.9	425.4	0.6554
		6		*GNB3*-T/+	381.2	206.2	
		7	Total time spent feeding (s)	WT	68.70	69.79	0.5873
		6		*GNB3*-T/+	93.33	89.12	
		7	Number of approaches	WT	31.86	10.19	0.4953
		6		*GNB3*-T/+	28.00	9.381	
	Marble burying	7	# of marbles 50% buried	WT	7.357	5.352	0.0751
		6		*GNB3*-T/+	2.750	2.132	
		7	# of marbles 67% buried	WT	5.000	4.082	0.0554
		6		*GNB3*-T/+	1.250	1.332	
	Social interaction	6	Latency to interact (s)	WT	10.78	8.767	0.7800
		6		*GNB3*-T/+	12.20	7.328	
		6	Total time interacting (s)	WT	210.4	47.88	0.4568
		6		*GNB3*-T/+	185.3	63.38	
	Open field	7	Average velocity (cm/s^2)	WT	6.160	0.7572	0.4014
		6		*GNB3*-T/+	6.538	0.8046	
		7	Time spent in border (s)	WT	463.3	188.7	0.6886
		6		*GNB3*-T/+	501.8	136.7	
Learning/ memory	Novel object recognition (Day 1 - habituation)	7	# of touches to object 1	WT	15.29	10.77	0.3650
		6		*GNB3*-T/+	21.50	12.97	
		7	# of touches to object 2	WT	18.43	8.979	0.2472
		6		*GNB3*-T/+	28.17	18.83	
		7	Time spent sniffing object 1 (s)	WT	10.24	7.053	0.2528
		6		*GNB3*-T/+	14.41	4.605	
		7	Time spent sniffing object 2 (s)	WT	11.97	8.071	0.0966
		6		*GNB3*-T/+	30.77	26.15	
		7	Latency to object 1 (s)	WT	111.1	56.22	0.1833
		6		*GNB3*-T/+	63.16	65.74	
		7	Latency to object 2 (s)	WT	101.3	118.7	0.3579
		6		*GNB3*-T/+	180.7	178.2	
		7	Distance moved (cm)	WT	3051	528.8	0.2672
		6		*GNB3*-T/+	2672	641.0	
		7	Average velocity (cm/s^2)	WT	5.259	0.7228	0.2065
		6		*GNB3*-T/+	4.621	0.9877	
	Novel object recognition (Day 2 - habituation)	7	# of touches to object 1	WT	11.14	5.336	0.5111
		6		*GNB3*-T/+	13.83	8.796	
		7	# of touches to object 2	WT	10.00	6.325	0.2507
		6		*GNB3*-T/+	16.00	11.22	
		7	Time spent sniffing object 1 (s)	WT	8.217	4.724	0.9248
		6		*GNB3*-T/+	8.573	8.364	
		7	Time spent sniffing object 2 (s)	WT	5.691	4.870	0.1664
		6		*GNB3*-T/+	10.52	6.853	
		7	Latency to object 1 (s)	WT	173.7	164.6	0.8476
		6		*GNB3*-T/+	151.9	181.0	
		7	Latency to object 2 (s)	WT	170.5	160.9	0.6543
		6		*GNB3*-T/+	135.0	105.5	
		7	Distance moved	WT	3175	499.2	0.0581

		6	(cm)	*GNB3*-T/+	2409	796.3	
		7	Average velocity (cm/s^2)	WT	5.557	0.6866	0.0435 *
		6		*GNB3*-T/+	4.261	1.315	
	Novel object recognition (No delay)	7	# of touches to familiar object	WT	9.429	4.467	0.2175
		6		*GNB3*-T/+	13.67	7.118	
		7	# of touches to novel object	WT	25.29	7.158	0.0363 *
		6		*GNB3*-T/+	16.67	5.610	
		7	Time spent sniffing familiar object (s)	WT	7.634	5.573	0.5832
		6		*GNB3*-T/+	9.547	6.637	
		7	Time spent sniffing novel object (s)	WT	22.22	12.10	0.2283
		6		*GNB3*-T/+	14.91	7.594	
		7	Latency to familiar object (s)	WT	182.1	159.0	0.5981
		6		*GNB3*-T/+	144.6	59.29	
		7	Latency to novel object (s)	WT	92.88	112.0	0.6363
		6		*GNB3*-T/+	121.3	96.29	
		7	Distance moved (cm)	WT	2594	842.3	0.2566
		6		*GNB3*-T/+	2074	700.1	
		7	Average velocity (cm/s^2)	WT	4.479	1.409	0.2547
		6		*GNB3*-T/+	3.629	1.086	
	Novel object recognition (1 hour delay)	7	# of touches to familiar object	WT	12.43	9.693	0.7744
		6		*GNB3*-T/+	14.17	11.67	
		7	# of touches to novel object	WT	13.43	6.503	0.8553
		6		*GNB3*-T/+	14.50	13.55	
		7	Time spent sniffing familiar object (s)	WT	11.45	13.05	0.6128
		6		*GNB3*-T/+	8.453	5.574	
		7	Time spent sniffing novel object (s)	WT	15.54	15.78	0.7894
		6		*GNB3*-T/+	13.39	11.93	
		7	Latency to familiar object (s)	WT	121.2	74.14	0.9892
		6		*GNB3*-T/+	121.7	53.25	
		7	Latency to novel object (s)	WT	131.7	107.5	0.9755
		6		*GNB3*-T/+	129.9	94.47	
		7	Distance moved (cm)	WT	2600	469.6	0.6772
		6		*GNB3*-T/+	2455	745.5	
		7	Average velocity (cm/s^2)	WT	4.518	0.8279	0.9788
		6		*GNB3*-T/+	4.504	1.036	
	Novel object recognition (24 hour delay)	7	# of touches to familiar object	WT	15.86	12.08	0.7294
		6		*GNB3*-T/+	18.17	11.23	
		7	# of touches to novel object	WT	29.43	17.00	0.6972
		6		*GNB3*-T/+	26.00	13.30	
		7	Time spent sniffing familiar object (s)	WT	10.25	9.741	0.9276
		6		*GNB3*-T/+	10.69	6.834	
		7	Time spent sniffing novel object (s)	WT	36.86	25.01	0.3557
		6		*GNB3*-T/+	23.37	25.30	
		7	Latency to familiar object (s)	WT	128.4	77.07	0.6903
		6		*GNB3*-T/+	108.9	95.05	
		7	Latency to novel object (s)	WT	71.85	84.80	0.8849
		6		*GNB3*-T/+	66.03	48.64	
		7	Distance moved (cm)	WT	3089	853.1	0.4710
		6		*GNB3*-T/+	2772	637.0	
		7	Average velocity (cm/s^2)	WT	5.352	1.385	0.4848
		6		*GNB3*-T/+	4.848	1.075	

Table 3.3

Summary of behavioral assessment of *GNB3*-T/+ mice. *GNB3*-T/+ mice and WT littermates were subjected to behavioral tests in order to evaluate anxiety/depressive-like behaviors and learning and memory.

Chapter 4

GNB3 alleles and expression levels dictate severity of obesity

Abstract

As described in the previous chapter, mice that overexpress the T risk allele of human *GNB3* are obese with impaired glucose tolerance. We created BAC transgenic mice that overexpress the non-risk C allele of *GNB3* and mouse *Gnb3*. Mice that overexpress *GNB3*-C weigh less than their WT littermates, but have elevated fasting blood lipids. Mice that overexpress mouse *Gnb3* are heavier than their WT littermates, but this phenotype depends on BAC copy number. Thus, overexpression of *GNB3*-C is protective for weight, while overexpression of *GNB3*-T and mouse *Gnb3* lead to weight gain in mice.

Introduction

Obesity is a highly heritable disease of excess fat accumulation, and a major public health issue globally, with a prevalence that has been increasing at an alarming rate since the 1970s (Finkelstein et al., 2012; World Health Organization, 2016a). Obesity is a major risk factor for type 2 diabetes, hypertension, cardiovascular disease and certain types of cancer (Chan et al., 1994; McMillan et al., 2006; World Health Organization, 2016a). Several genes or loci are associated with obesity (Locke et al., 2015; Xia and Grant, 2013). However, the current list only explains a minor portion of the apparent heritability, and many more genes need to be identified to explain the missing heritability (Xia and Grant, 2013).

We hypothesized that an extra copy of *GNB3* confers a risk for obesity, like the C825T polymorphism. To test this, we created bacterial artificial chromosome (BAC) transgenic mice carrying the human risk allele of *GNB3* (*GNB3*-T) (Goldlust et al., 2013).

Heterozygous *GNB3*-T mice are heavier, have greater adiposity and fat mass, impaired glucose tolerance, metabolic syndrome, while having similar food intake and activity levels compared to their WT littermates (Chapter 3). However, the particular human *GNB3* allele (T vs. C) and/or the orthologous gene (*GNB3* vs. *Gnb3*) could also play a role in the overexpression phenotype.

In this study, we created additional transgenic mouse lines with different copy numbers of BACs containing the human *GNB3*-C or mouse *Gnb3* genes. We hypothesized that *GNB3* alleles and expression levels dictate severity of obesity. Here we show that, overexpression of the *GNB3* non-risk C allele seems to protect from the increase in adiposity and the impairment of glucose tolerance seen in *GNB3*-T mice; however, it does not protect from elevated levels of fasting blood lipids. Overexpression of the mouse endogenous *Gnb3* leads to an increase in body weight and adiposity that is related to BAC copy number. These data help elucidate the roles of risk allele and gene expression in GNB3-related obesity.

Results

We created 10 different transgenic mouse founder lines using four different BACs (Figure 4.1A). The human *GNB3*-T BAC includes 14 RefSeq genes, one of which is *GNB3* with the T risk allele. The *GNB3*-Δ BAC was recombineered from the human *GNB3*-T BAC to replace *GNB3* with neomycin while the other 13 genes remain. The human *GNB3*-C BAC was derived from a different BAC library and includes one additional gene compared to the human *GNB3*-T BAC. Lastly, the mouse *Gnb3* BAC consists of 15 RefSeq genes. BAC copy number in each founder line was determined by

Taqman copy number assays (Chapter 2). A list of all the mouse lines, nomenclature and BAC copy number can be found in Table 4.1.

As described in chapter 3, we performed quantitative RT-PCR and found that transgenic *GNB3* is highly expressed in the brain. Transgenic *GNB3* expression in heterozygous *GNB3*-T mice was 293.7-fold higher than in heterozygous *GNB3*-C mice. Additionally, homozygous *GNB3*-T and *GNB3*-C mice had greater transgenic *GNB3* expression than their heterozygous littermates. Transgenic *GNB3* expression in homozygous *GNB3*-T mice was 2-fold greater than in heterozygous *GNB3*-T mice, while transgenic *GNB3* expression in homozygous *GNB3*-C mice was 5.4-fold greater than in heterozygous *GNB3*-C mice. As expected, *GNB3*-Δ mice did not express transgenic *GNB3* (Figure 4.1B). Heterozygous *GNB3*-m mice had greater endogenous *Gnb3* expression than their WT littermates (Figure 4.1C).

We also measured expression of another gene nearby to *GNB3* on the BAC, *MLF2*. Transgenic *MLF2* was expressed in *GNB3*-T mice, at levels greater than in *GNB3*-C mice. Homozygous *GNB3*-T and *GNB3*-C mice had greater transgenic *MLF2* expression than their heterozygous littermates. One of the *GNB3*-Δ lines with one copy of the BAC (*GNB3*-Δ1a) did not express transgenic *MLF2*. However, the other *GNB3*-Δ lines expressed transgenic *MLF2*, as expected, in greater quantity as BAC copy number increased. *GNB3*-m mice did not express transgenic *MLF2* (Figure 4.2A). Mouse endogenous *Mlf2* was expressed in all 10 founder lines and expression level did not correlate with *GNB3*-m BAC copy number (Figure 4.2B).

In order to assess the effect of *GNB3* alleles on weight, we weighed all mouse lines from weaning until 25 weeks old. White adipose tissues (WAT) were dissected and

weighed at 5 and 25 weeks for all mouse lines. In this study, inguinal WAT (iWAT) and gonadal (gWAT) were collected to represent subcutaneous and visceral white adipose depots, respectively. Additionally for *GNB3*-T homozygote and *GNB3*-C heterozygote and homozygote mice, we collected blood and measured metabolic parameters at age 20 weeks to compare to the previously characterized *GNB3*-T heterozygotes.

***GNB3*-T mice**

Based on the linear mixed model analysis, the weight of the heterozygous and homozygous *GNB3*-T mice were significantly associated with BAC transgene genotype. Heterozygous *GNB3*-T mice weighed significantly more than their WT littermates ($P = 2.671x10^{-8}$) (Figure 4.3A), whereas homozygous *GNB3*-T mice weighed significantly less than WT ($P = 3.914x10^{-8}$) (Figure 4.3B). At 25 weeks, male heterozygous *GNB3*-T mice had greater total body weight than WT, while in females it was similar to WT (Figure 4.3C). Moreover, heterozygous *GNB3*-T mice had greater gWAT% and iWAT% compared to WT (Figure 4.3D,E). Body length measured from nose to anus was similar to WT in heterozygous *GNB3*-T mice (Figure 4.3F). Even though homozygous *GNB3*-T mice weighed less than WT longitudinally over the course of 25 weeks, they were not leaner than WT based on adiposity. At 20 weeks, female homozygous *GNB3*-T mice had greater total body weight compared to WT, but males were similar to WT (Figure 4.4A). Strikingly, homozygous *GNB3*-T mice had greater gWAT% than WT (Figure 4.4B). Brown adipose tissue (BAT) % was decreased in male homozygous *GNB3*-T mice compared to WT, while in females it was similar to WT (Figure 4.4C). Additionally liver % of homozygous *GNB3*-T mice was greater than WT (Figure 4.4D).

Next, we investigated fasting blood glucose and lipid parameters in homozygous *GNB3*-T mice. At 20 weeks, fasting blood glucose was elevated in homozygous *GNB3*-T mice compared to WT (Figure 4.4E). We then subjected mice to a glucose tolerance test (GTT), and as indicated by glycemia levels and calculations of area under the curve (AUC), homozygous *GNB3*-T mice exhibited glucose intolerance (Figure 4.4F,G). Lipid profiling revealed that fasting plasma triglycerides were similar for homozygous *GNB3*-T and WT mice (Figure 4.4H). Female homozygous *GNB3*-T mice had elevated fasting plasma cholesterol, phospholipids and non-esterified fatty acids (NEFA), while males had values were similar to WT (Figure 4.4I-K). This is similar to the metabolic profile of *GNB3*-T heterozygotes at 20 weeks.

***GNB3*-Δ mice**

We created BAC transgenic mice using the same BAC inserted in *GNB3*-T mice except replaced the *GNB3* gene with a neomycin cassette to show that weight gain is due to *GNB3* and not the other genes on the BAC. We generated 3 different founder lines carrying the *GNB3*-Δ BAC. Copy number analysis revealed that 2 lines (*GNB3*-Δ1a and *GNB3*-Δ1b) had a single copy, and 1 line (*GNB3*-Δ3) had 3 copies of the BAC. We then weighed heterozygous *GNB3*-Δ mice and their WT littermates from each founder line starting at weaning to 25 weeks of age (Figure 4.5A-C). The linear mixed model we used to analyze the longitudinal effects of the presence of the BAC transgene on mouse weight revealed that the weight of the mice is not significantly associated with BAC transgene genotype in any of the three *GNB3*-Δ founder lines regardless of BAC copy number (P = 0.7048, P = 0.5293, P = 0.5160, respectively for *GNB3*-Δ1a, *GNB3*-Δ1b and *GNB3*-Δ3 lines). At 5 weeks, body weight, gWAT%, iWAT% and body length of heterozygous

GNB3-Δ1a mice were similar to WT (Figure 4.6A-D). Female heterozygous *GNB3*-Δ1b mice had lower body weight, gWAT% and iWAT% than WT and length similar to WT, while in males all were similar to WT at 5 weeks (Figure 4.6E-H). In all three *GNB3*-Δ lines at 25 weeks of age, body weight, gWAT% and length were similar between heterozygous and WT mice. iWAT% was similar to WT in heterozygous *GNB3*-Δ1a and *GNB3*-Δ1b; however, it was greater in *GNB3*-Δ3 heterozygous mice compared to WT (Figure 4.5D-O).

***GNB3*-C mice**

We questioned if overexpressing the human non-risk allele C of *GNB3* in mice would also cause obesity, type 2 diabetes and metabolic syndrome as in mice overexpressing the human risk allele T of *GNB3*. We created one founder line carrying the *GNB3*-C BAC, and copy number analysis revealed that heterozygous *GNB3*-C mice carry a single copy of the BAC. Since heterozygous *GNB3*-T mice had 2 copies of the BAC inserted, in order to make comparisons to the *GNB3*-T line, we also characterized homozygous *GNB3*-C mice with two copies of the BAC. We weighed heterozygous (Figure 4.7A) and homozygous (Figure 4.7B) *GNB3*-C mice and their WT littermates from weaning to 25 years of age. Based on the linear mixed model analysis, the weight of the mice was significantly associated with BAC transgene genotype ($P = 7.448\text{x}10^{-3}$ and $P = 1.053\text{x}10^{-6}$ for heterozygote and homozygote *GNB3*-C mice, respectively). Both heterozygous and homozygous *GNB3*-C weighed significantly less than WT. At 5 weeks, heterozygous *GNB3*-C mice had body weight, gWAT%, iWAT%, lean mass and fat mass similar to WT (Figure 4.8). At 25 weeks, male heterozygous and homozygous *GNB3*-C mice weighed significantly less than WT, while female heterozygous and homozygous *GNB3*-

C mice weights were similar to WT (Figure 4.7C). gWAT% was similar to WT in heterozygous and homozygous *GNB3*-C mice (Figure 4.7D). iWAT% was greater than WT only in female homozygous *GNB3*-C mice, but it was similar to WT in heterozygous and male homozygous *GNB3*-C mice (Figure 4.7E). Both heterozygous and homozygous *GNB3*-C mice had significantly shorter body length than WT at 25 weeks (Figure 4.7F).

We then measured metabolic parameters of 20 week old *GNB3*-C mice to compare to data from *GNB3*-T mice at the same age. Body weight, gWAT%, iWAT%, BAT%, liver %, lean mass and fat mass in heterozygous *GNB3*-C mice were similar to WT at 20 weeks. Additionally, male homozygous *GNB3*-C mice had similar lean and fat mass to WT (Figure 4.9A-G). Heterozygous *GNB3*-C mice had similar fasting blood glucose to WT (Figure 4.9H), and when subjected to GTT, both heterozygous and homozygous *GNB3*-C mice did not have impaired glucose tolerance as indicated by glycemia levels and calculations of AUC (Figure 4.9I,J). However, male heterozygous *GNB3*-C mice had elevated fasting plasma triglycerides and phospholipids compared to WT, while fasting plasma cholesterol and NEFA were similar to WT (Figure 4.9K-N).

***GNB3*-m mice**

In addition to evaluating the effect of overexpressing risk and non-risk alleles of human *GNB3* on mouse weight, we asked if overexpressing mouse *Gnb3* would also cause obesity in mice. We created 5 different transgenic mouse founder lines with the mouse *Gnb3* BAC. Copy number analysis revealed that 2 mouse lines (*GNB3*-m1a and *GNB3*-m1b) carry a single copy of the BAC, 2 mouse lines (*GNB3*-m2a and *GNB3*-m2b) carry 2 copies of the BAC, and 1 mouse line (*GNB3*-m4) carries 4 copies of the BAC. We weighed heterozygous *GNB3*-m mice and their WT littermates from weaning to 25 years

of age. For mouse lines carrying a single copy of the BAC, based on the linear mixed model analysis, the weight of the mice was not significantly associated with BAC transgene genotype (P = 0.8047 and P = 0.8455 for *GNB3*-m1a and *GNB3*-m1b mice, respectively) (Figure 4.10A,B). Five week old female heterozygous *GNB3*-m1a mice had greater body weight than WT, while in males it was similar to WT (Figure 4.11A). Male heterozygous *GNB3*-m1a mice had greater gWAT% than WT, but in females it was similar to WT (Figure 4.11B). iWAT% and body length were similar to WT in heterozygous *GNB3*-m1a mice (Figure 4.11C,D). At 5 weeks, body weight, gWAT% and body length were similar between heterozygous *GNB3*-m1b mice and WT; however, iWAT% was greater in male heterozygous *GNB3*-m1b mice, while in females it was similar to WT (Figure 4.11E-H). At 25 weeks, heterozygous *GNB3*-m1a and *GNB3*-m1b mice had body weight, gWAT%, iWAT% and body length similar to WT (Figure 4.10C-J).

Next, for mouse lines with 2 copies of the BAC, based on the linear mixed model analysis, the weight of the mice was significantly associated with BAC transgene genotype (P = 0.0458 and P = 0.0021 for *GNB3*-m2a and *GNB3*-m2b mice, respectively) (Figure 4.10K,L). Heterozygous *GNB3*-m mice with 2 copies of the BAC weighed significantly more than WT. At 5 weeks, male heterozygous *GNB3*-m2b mice weighed less than WT, while in females body weight was similar to WT (Figure 4.11I). gWAT%, iWAT% and length were similar between heterozygous *GNB3*-m2b mice and WT (Figure 4.11J-L). At 25 weeks, heterozygous *GNB3*-m2a mice had body weight similar to WT; however, female heterozygous *GNB3*-m2a mice had greater gWAT% than WT, while in males gWAT% was similar to WT (Figure 4.10N,O). iWAT% was greater in

heterozygous *GNB3*-m2a mice, but body length was similar to WT (Figure 4.10P,Q). On the other hand, heterozygous *GNB3*-m2b mice had greater body weight, gWAT% and iWAT% than WT, while body length was similar to WT (Figure 4.10R-U). Lastly, for the mouse line carrying 4 copies of the BAC, based on the linear mixed model analysis, the weight of the mice was not significantly associated with BAC transgene genotype (P = 0.6293 for *GNB3*-m4) (Figure 4.10M). At 25 weeks, body weight, gWAT%, iWAT% and body length were similar between heterozygous *GNB3*-m4 mice and WT (Figure 4.10V,Y).

Discussion

Previously, our grouped showed that heterozygous mice that overexpress the human risk allele T of *GNB3* are obese with metabolic syndrome (Chapter 3). However, it is unknown how overexpressing the human non-risk allele C of *GNB3* or mouse *Gnb3* will affect mouse weight. In this study, we evaluated the contributions of *GNB3* alleles and gene expression levels on mouse weight. Overall, our results show that overexpression of the *GNB3* human non-risk allele C protects from increased adiposity and impaired glucose tolerance characterized in *GNB3*-T mice, but fails to protect from elevated levels of fasting blood lipids. Additionally, overexpression of the mouse endogenous *Gnb3* leads to an increase in body weight and adiposity in mice based on the inserted BAC copy number.

In this study, due to the nature of developing BAC transgenic mice, different founder lines had different BAC transgene copy number, which in turn affected transgene expression levels. The thoroughly characterized heterozygous *GNB3*-T mice in our

previous study had a BAC copy number of 2; whereas, heterozygous *GNB3*-C mice had a copy number of 1. Since our multiple attempts of developing a heterozygous *GNB3*-C line with BAC copy number of 2 failed, we decided to characterize homozygous *GNB3*-C mice to make phenotypic comparisons with the previously characterized heterozygous *GNB3*-T mice. Admittedly, these comparisons are not ideal since each founder line has a different insertion site into the genome; moreover, heterozygous *GNB3*-T and homozygous *GNB3*-C mice do not have same levels of transgenic *GNB3* gene expression in the brain. On the other hand, we could generate *GNB3*-m mice with BAC copy numbers 1, 2 and 4. Therefore, comparisons between heterozygous *GNB3*-T and *GNB3*-m mice with BAC copy number 2, and comparisons between heterozygous *GNB3*-C and *GNB3*-m mice with BAC copy number 1 would be more appropriate. Additionally, homozygous *GNB3*-T mice and heterozygous *GNB3*-m mice with BAC copy number 4 may be compared.

Interestingly, even though heterozygous *GNB3*-T mice weighed more than WT, homozygous *GNB3*-T mice weighed less than WT. Upon, closer investigation, we noticed homozygous *GNB3*-T mice had elevated adiposity and impaired glucose tolerance, a phenotype similar to heterozygous *GNB3*-T mice. In contrast to *GNB3*-T mice, heterozygous *GNB3*-C mice weighed less than WT, and homozygous *GNB3*-C mice weighed less than heterozygous *GNB3*-C mice. Additionally, heterozygous *GNB3*-C mice had shorter body length than WT, and homozygous *GNB3*-C mice had shorter body length than heterozygous *GNB3*-C mice. Body length may explain why there was no difference in adiposity even though difference in body weight exists. We cannot exclude the possibility that a different founder line of heterozygous *GNB3*-C mice which have a

BAC copy number of 2, may have been similar to or heavier than WT mice. However, based on the comparison between heterozygous *GNB3*-T mice and homozygous *GNB3*-C mice, we may conclude that *GNB3* human non-risk allele C is protective of increased adiposity and impaired glucose tolerance seen in *GNB3*-T mice, but is not protective of elevated levels of fasting blood lipids.

Heterozygous *GNB3*-m mice with BAC copy number of 1 had similar weight and adiposity compared to WT mice. However, heterozygous *GNB3*-m mice with BAC copy number of 2 had greater adiposity and body weight compared to WT, a phenotype similar to heterozygous *GNB3*-T mice. Further phenotypic characterization is needed to identify if heterozygous *GNB3*-m mice with BAC copy number of 2 have impaired glucose tolerance and elevated levels of fasting blood lipids similar to heterozygous *GNB3*-T mice. In summary, BAC copy number seemed to influence weight gain and adiposity in *GNB3*-m mice rather than *Gnb3* expression level in brain. However, it is possible that *Gnb3* expression level in another tissue or at another time point may have led to the weight gain phenotype in *GNB3*-m mice.

Site of integration, copy number of transgene and expression level of transgene are some of the limitations of the BAC transgenic mouse models when one comparing mouse lines with different BAC insertions. Different experimental approaches can be taken to address and bypass these limitations. Ideally, *GNB3*-T and *GNB3*-C knock-in mice can be developed. Thus, gene expression levels and tissue specificity of gene expression can be controlled and manipulated in order to have a deeper understanding of the effects of overexpressing the risk and non-risk allele of *GNB3* on weight, as well as the tissues involved in the process.

In conclusion, our study demonstrates that overexpression of *GNB3*-T leads to weight gain while overexpression of *GNB3*-C is protective of weight gain in mice. Additionally, overexpression of mouse *Gnb3* may increase adiposity depending on BAC copy number. However, further investigation is needed to uncover the role of Gβ3 and the shorter splice variant Gβ3-s on body weight and adiposity.

Materials and Methods

Animals. Mice were maintained in an Association for Assessment and Accreditation of Laboratory Animal Care (AAALAC)-accredited facility in accordance with the National Research Council's Guide for the Care and Use of Laboratory Animals. All mouse studies were performed according to protocols approved by the Institutional Animal Care and Use Committee at Emory University. Mice were housed in a 22–23 °C climate controlled room on a 12-h light/dark cycle (lights on at 0700 h), in static micro-isolator cages with free access to water and standard rodent chow (Purina LabDiet 5001). Transgenic mice were developed on a FVB background using the following BACs: Human BAC (RP11-578M14) with a 184-kb insert, including the genes *COPS7A*, *MLF2*, *PTMS*, *LAG3*, *CD4*, *GPR162*, *LEPREL2*, *GNB3*, *CDCA3*, *USP5*, *TPI1*, *SPSB2*, *RPL13P5*, *DSTNP2*. Human BAC (CTD-2640D15) with a 222-kb insert, including the genes *PIANP*, *COPS7A*, *MLF2*, *PTMS*, *LAG3*, *CD4*, *GPR162*, *LEPREL2*, *GNB3*, *CDCA3*, *USP5*, *TPI1*, *SPSB2*, *RPL13P5*, *DSTNP2*. Mouse BAC (RP23-384O24) with a 195-kb insert, including the genes *Emg1*, *Phb2*, *Ptpn6*, *AK048048*, *Grcc10*, *Atn1*, *Eno2*, *Lrrc23*, *Spsb2*, *Tpi1*, *Usp5*, *Cdca3*, *Gnb3*, *Lepre12*, *Gpr162*, *Cd4*. Detailed methods on

generating transgenic mice and recombineering the ΔGNB3 BAC is described in (Goldlust et al., 2013).

BAC copy number analysis. The number of copies of the BAC transgene that integrated into the genome of each mouse line was measured as described in (Goldlust et al., 2013).

Quantitative RT-PCR. Taqman quantitative RT-PCR was performed as described (Goldlust et al., 2013) to measure *GNB3, Gnb3, MLF2* and *Mlf2* expression.

Weight tracking. Mice were weighed once a week or once every 5 weeks from weaning to 25 weeks of age.

Tissue weights. Inguinal and gonadal WAT, BAT and liver were dissected and weighed. % tissue weight was calculated by dividing tissue weight by total body weight of the mouse. Mouse length was measured from nose to anus.

DXA. Lean mass and fat mass (body composition) were measured using DXA scanning (Lunar PIXImus2 densitometer, GE Medical Systems) after anesthesia using isoflurane.

Blood analysis. Mice were fasted for 6 hours. Blood glucose was measured by a glucometer (Accu-Check Aviva, Roche) from a drop of tail blood collected by milking the tail. For lipid profiling, blood was collected by cardiac puncture following euthanasia using isoflurane. Blood collection started between 1:00 and 2:00 pm each day. Fasting

blood plasma was separated immediately by centrifuge (1000×g) for 10 minutes at room temperature and was aliquoted and stored at −20°C. Plasma triglycerides, cholesterol, phospholipids and non-esterified fatty acids were measured at the Mouse Metabolic Phenotyping Center (Cincinnati, OH, USA).

Glucose tolerance test. Mice were fasted for 6 hours and injected intraperitoneally with 1 mg/g D-glucose (Sigma-Aldrich, St. Louis, MO, USA). Blood glucose levels were measured from the tip of the tail using a glucometer (Accu-Check Aviva, Roche) at -5, 0, 5, 10, 15, 20, 25, 30, 60, 120 min after injection.

Statistical analysis. We used the R package nlme to analyze the longitudinal effect of the BAC transgenes on mouse weight. Weight (grams) was modeled as a linear function of presence/absence of the BAC transgene, sex, age [log(days)], litter, and a mouse-specific random effect to account for the repeated observations of individual mice. The significance of the association between the BAC transgene and mouse weight in the presence of the other variables was assessed by the *p*-value corresponding to presence/absence of the BAC transgene. Other statistical analyses were performed using GraphPad Prism version 6 for Mac (GraphPad Software, Inc., La Jolla, CA, USA). Data are presented as mean ± SD (or SEM where indicated). Unpaired Student's *t*-test was used to compare two groups. Comparisons with *p*-values <0.05 were considered significant.

Figure 4.1

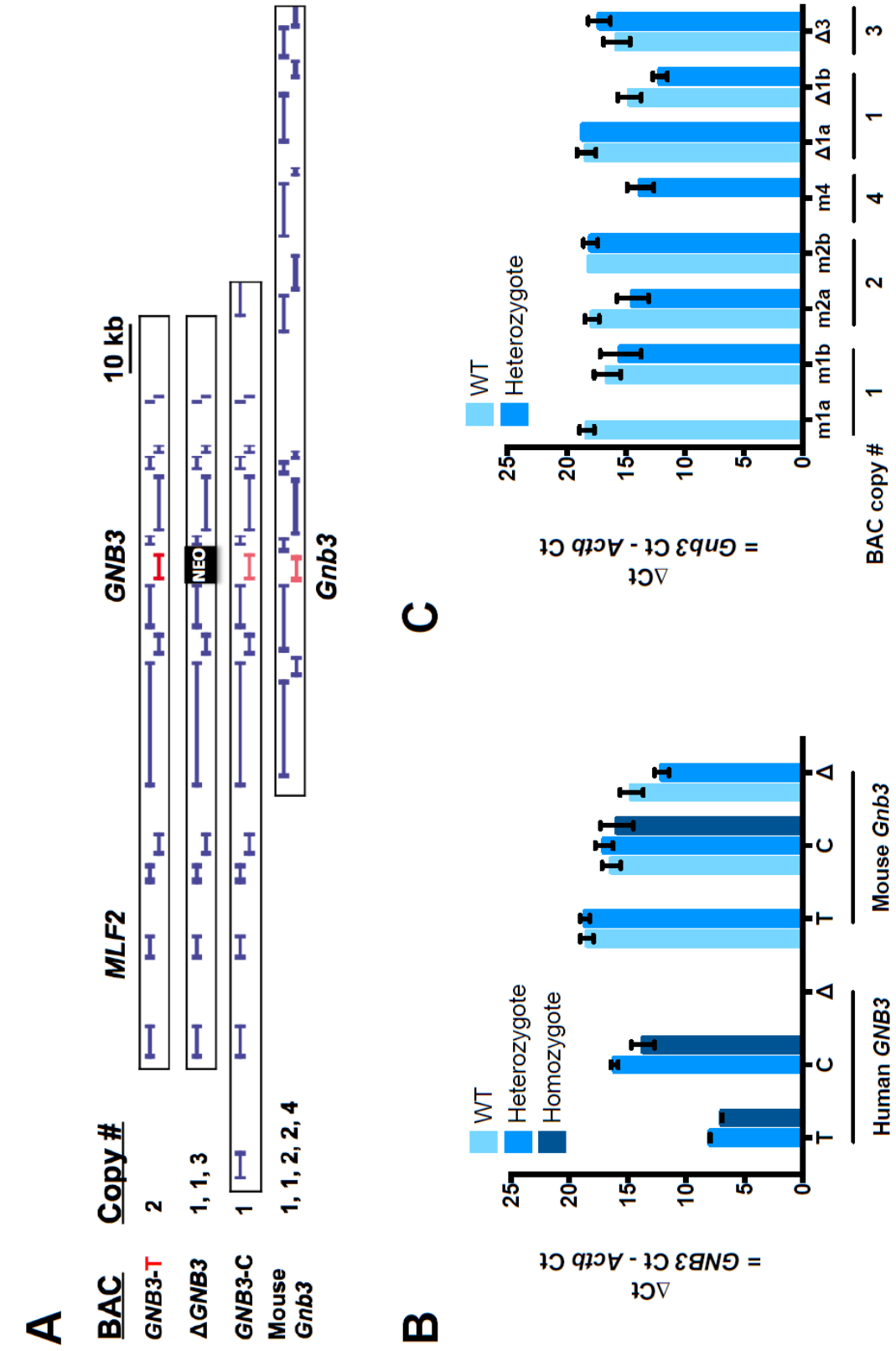
A
BAC
Copy #
MLF2
GNB3
10 kb
GNB3-T
2
ΔGNB3
1, 1, 3
Neo
GNB3-C
1
Mouse Gnb3
1, 1, 2, 2, 4
Gnb3
B
WT
Heterozygote
Homozygote
ΔCt = GNB3 Ct - Actb Ct
T
C
Δ
T
C
Δ
Human GNB3
Mouse Gnb3
C
WT
Heterozygote
ΔCt = Gnb3 Ct - Actb Ct
m1a
m1b
m2a
m2b
m4
Δ1a
Δ1b
Δ3
BAC copy #
1
2
4
1
3

Figure 4.1

Transgenic *GNB3* is highly expressed in the brain in *GNB3*-T mice, at levels greater than in *GNB3*-C mice, and homozygous mice have greater transgenic *GNB3* expression than heterozygous mice. BACs used to generate the transgenic lines used in the study (A). Transgenic human *GNB3* and mouse endogenous *Gnb3* gene expression in brain tissues of WT, heterozygous and homozygous mice from *GNB3*-T, *GNB3*-C and *GNB3*-Δ mouse lines (B). Mouse endogenous *Gnb3* gene expression in brain tissues of WT and heterozygous mice from *Gnb3*-m and *GNB3*-Δ mouse lines (C). All mice are 8 weeks old. n = 2 mice per group. 3 technical replicates for both. Ct, cycle threshold.

Figure 4.2

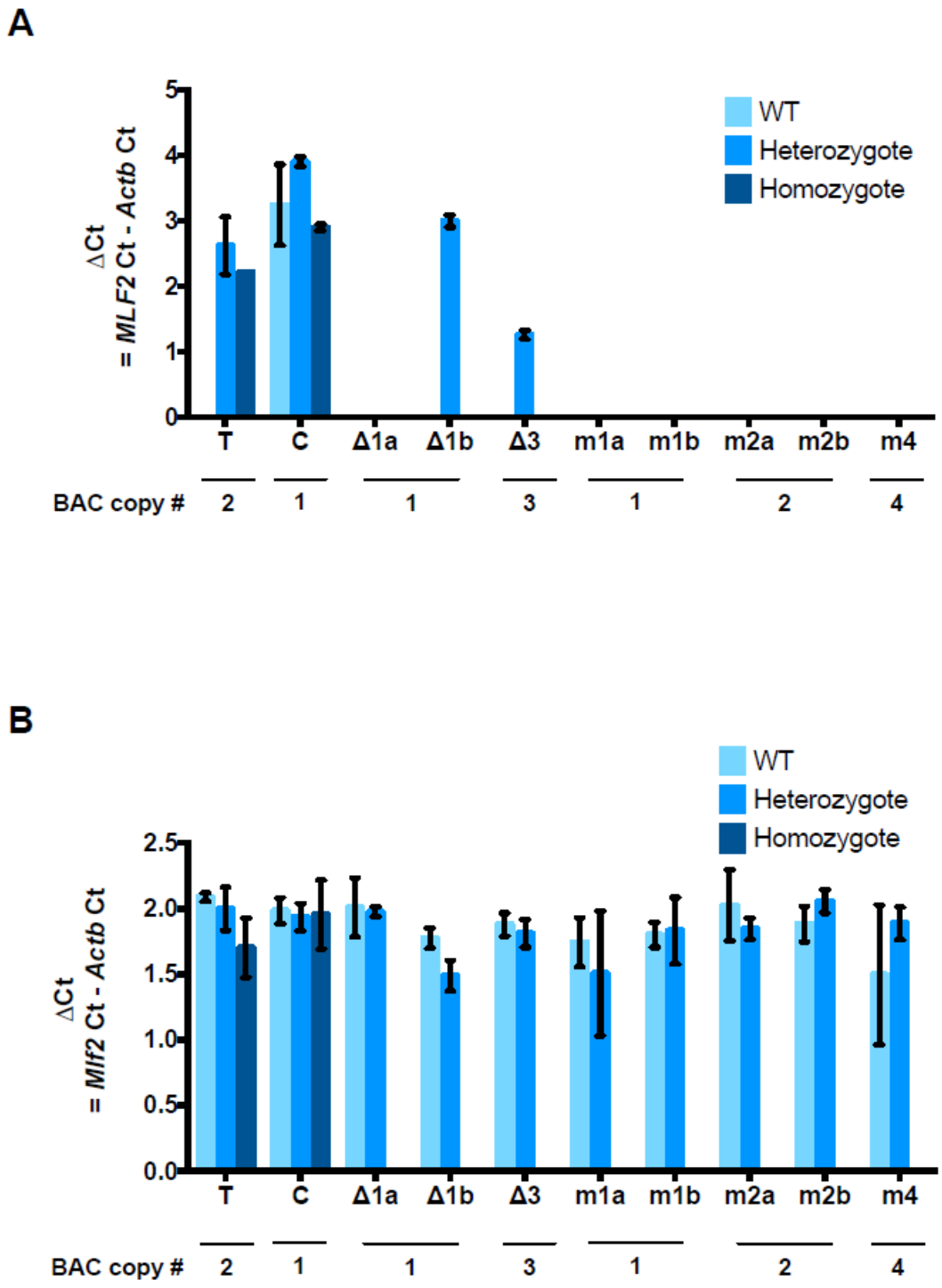
A
ΔCt
= MLF2 Ct - Actb Ct
WT
Heterozygote
Homozygote
T
C
Δ1a
Δ1b
Δ3
m1a
m1b
m2a
m2b
m4
BAC copy #
2
1
1
3
1
2
4
B
ΔCt
= Mlf2 Ct - Actb Ct
WT
Heterozygote
Homozygote
T
C
Δ1a
Δ1b
Δ3
m1a
m1b
m2a
m2b
m4
BAC copy #
2
1
1
3
1
2
4

Figure 4.2

Transgenic *MLF2* expression depends on BAC copy number in mouse lines. Transgenic human *MLF2* (A) and mouse endogenous *Mlf2* (B) gene expression in brain tissues of WT, heterozygous and homozygous mice from *GNB3*-T, *GNB3*-C, *GNB3*-Δ and *GNB3*-m lines. *MLF2* levels are undetectable in *GNB3*-Δ1a and *GNB3*-m lines. All mice are 8 weeks old. *n* = 2 mice per group. 3 technical replicates for both. Ct, cycle threshold.

Figure 4.3

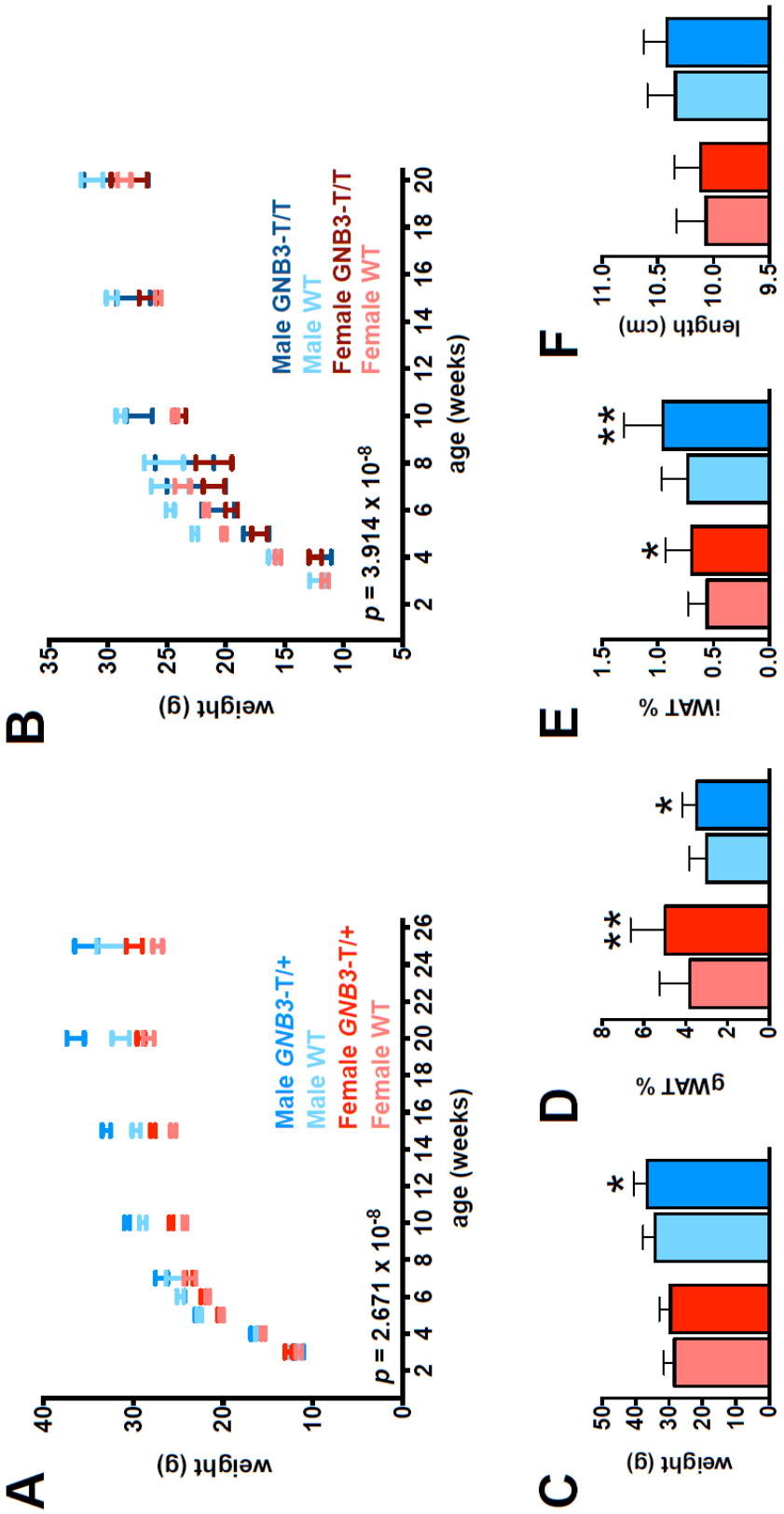
A
weight (g)
age (weeks)
p = 2.671 x 10-8
Male GNB3-T/+
Male WT
Female GNB3-T/+
Female WT
B
weight (g)
age (weeks)
p = 3.914 x 10-8
Male GNB3-T/T
Male WT
Female GNB3-T/T
Female WT
C
weight (g)
D
gWAT %
E
iWAT %
F
length (cm)

Figure 4.3

Heterozygous *GNB3*-T mice (*GNB3*-T/+) are heavier, while homozygous *GNB3*-T mice (*GNB3*-T/T) are lighter than WT littermates. Body weight curves of *GNB3*-T/+ (A) and *GNB3*-T/T (B) mice vs WT between 3 and 25 weeks of age. Body weight (C), gWAT weight/body weight (gWAT%) (D), iWAT weight/body weight (iWAT %) (E) and length (F) of 25-week-old WT and *GNB3*-T/+ mice. Data are mean ± SD, and $*P < 0.05$, $**P < 0.01$ vs. WT of same sex by unpaired Student's *t*-test in C-F.

Figure 4.4

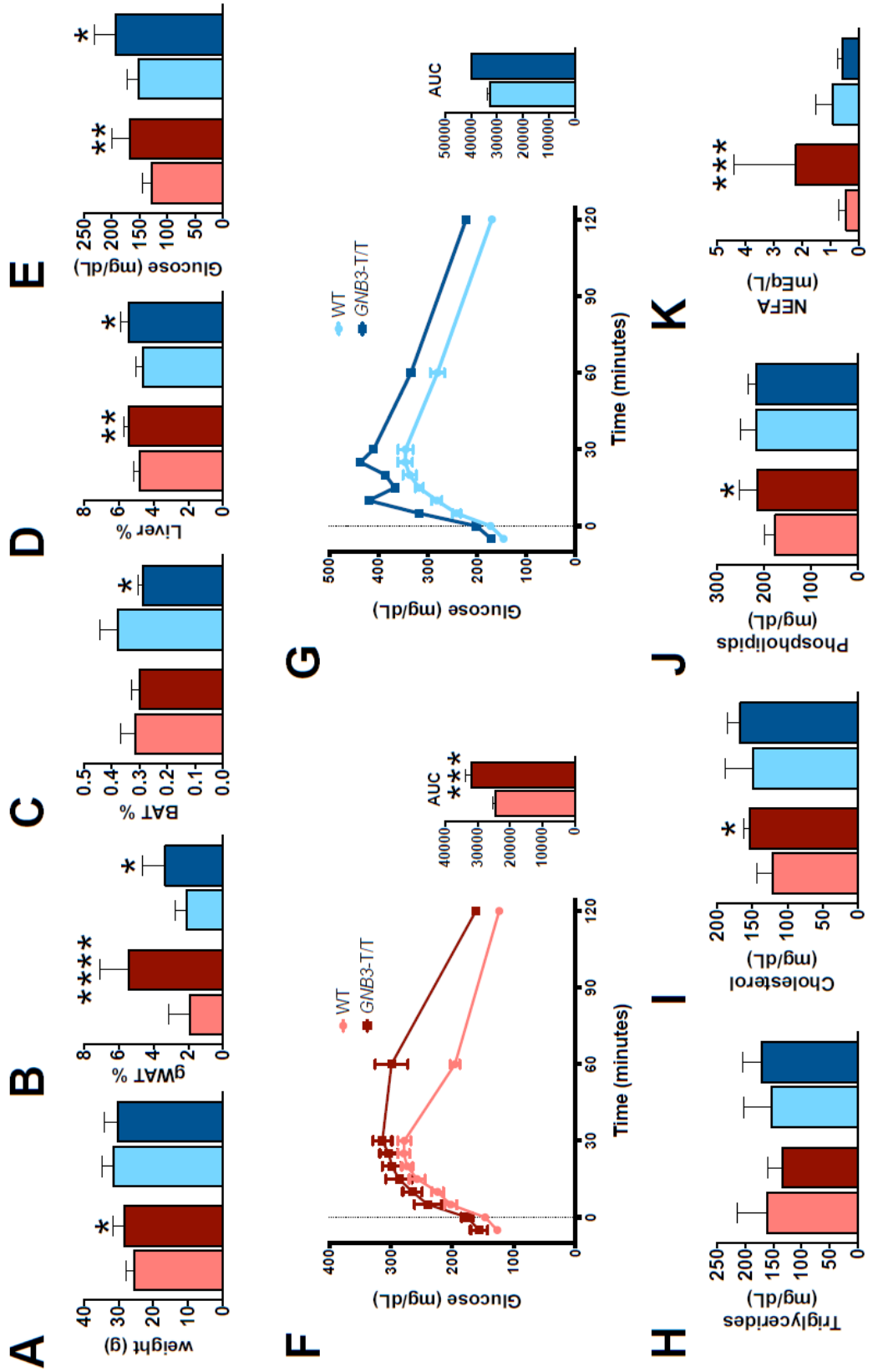
A
weight (g)
B
gWAT %
C
BAT %
D
Liver %
E
Glucose (mg/dL)
F
Glucose (mg/dL)
Time (minutes)
WT
GNB3-T/T
AUC
G
Glucose (mg/dL)
Time (minutes)
WT
GNB3-T/T
AUC
H
Triglycerides (mg/dL)
I
Cholesterol (mg/dL)
J
Phospholipids (mg/dL)
K
NEFA (mEq/L)

Figure 4.4

Homozygous *GNB3*-T mice have greater adiposity, elevated fasting blood glucose and impaired glucose tolerance. Body weight (A), gWAT% (B), BAT weight/body weight (BAT%) (C), liver weight/body weight (liver %) (D), and fasting blood glucose (E) of *GNB3*-T/T and WT mice. Glucose tolerance test (GTT) and areas under the curve (AUC) of female (F) and male (G) mice. Fasting blood triglycerides (H), cholesterol (I), phospholipids (J) and non-esterified fatty acids (K) of mice. All mice are 20 weeks old. Data are mean ± SD. **P* < 0.05, ***P* < 0.01, ****P* < 0.001, *****P* < 0.0001 vs. WT of same sex by unpaired Student's *t*-test.

Figure 4.5

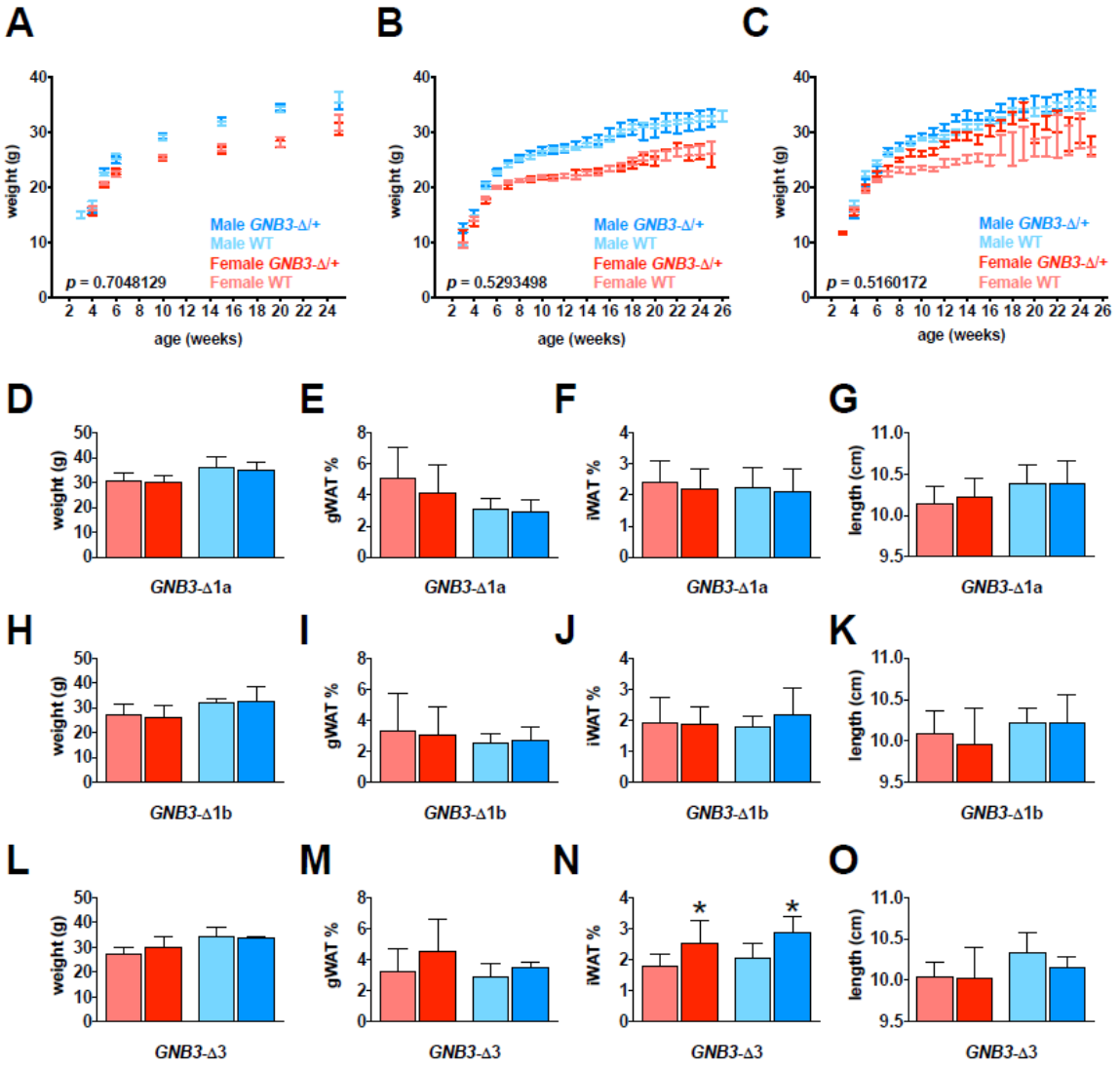
A
B
C
weight (g)
age (weeks)
Male GNB3-Δ/+
Male WT
Female GNB3-Δ/+
Female WT
p = 0.7048129
p = 0.5293498
p = 0.5160172
D
E
F
G
H
I
J
K
L
M
N
O
weight (g)
gWAT %
iWAT %
length (cm)
GNB3-Δ1a
GNB3-Δ1b
GNB3-Δ3
*
*

Figure 4.5

Heterozygous *GNB3*-Δ mice (*GNB3*-Δ/+) have similar weight to WT littermates regardless of BAC copy number. Body weight curves of *GNB3*-Δ/+ and WT mice from *GNB3*-Δ1a (A), *GNB3*-Δ1b (B) and *GNB3*-Δ3 (C) mouse lines between 3 and 25 weeks of age. Body weight (D), gWAT% (E), iWAT% (F) and length (G) of *GNB3*-Δ1a mice. Body weight (H), gWAT %(I), iWAT% (J) and length (K) of *GNB3*-Δ1b mice. Body weight (L), gWAT% (M), iWAT% (N) and length (O) of *GNB3*-Δ3 mice. Mice are 25 weeks old in D-O. Data are mean ± SD, and $*P < 0.05$ vs. WT of same sex by unpaired Student's *t*-test in D-O.

Figure 4.6

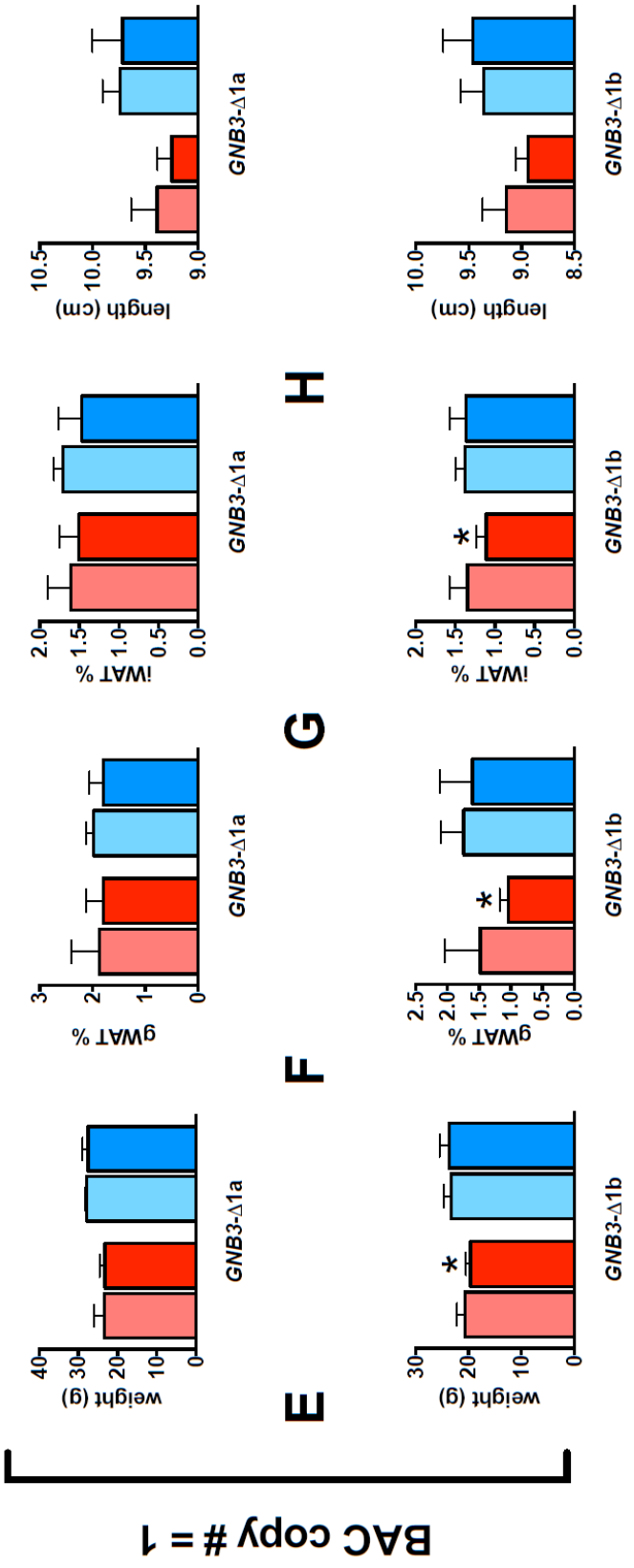
A
B
C
D
E
F
G
H
BAC copy # = 1
weight (g)
gWAT %
iWAT %
length (cm)
GNB3-Δ1a
GNB3-Δ1b
*

Figure 4.6

Heterozygous *GNB3*-Δ mice have similar weight to WT littermates at 5 weeks old. Body weight (A), gWAT% (B), iWAT% (C) and length (D) of *GNB3*-Δ1a mice. Body weight (E), gWAT% (F), iWAT% (G) and length (H) of *GNB3*-Δ1b mice. All mice are 5 weeks old. Data are mean ± SD. **P* < 0.05 vs. WT of same sex by unpaired Student's *t*-test.

Figure 4.7

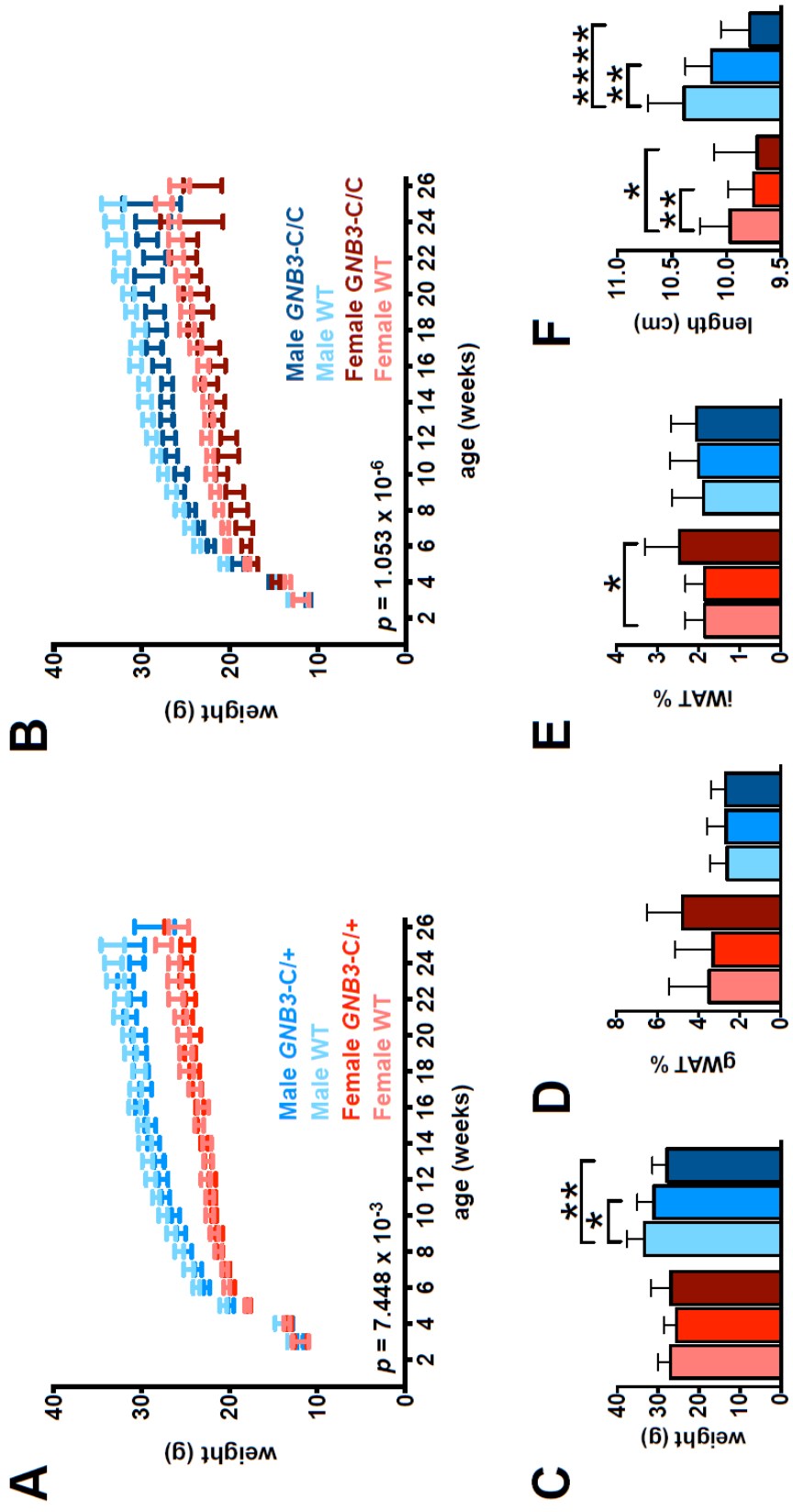
A
B
C
D
E
F
weight (g)
age (weeks)
p = 7.448 x 10-3
p = 1.053 x 10-6
Male GNB3-C/+
Male WT
Female GNB3-C/+
Female WT
Male GNB3-C/C
Female GNB3-C/C
gWAT %
iWAT %
length (cm)

Figure 4.7

Heterozygous and homozygous *GNB3*-C mice (*GNB3*-C/+ and *GNB3*-C/C) are lighter than WT littermates. Body weight curves of *GNB3*-C/+ (A) and *GNB3*-C/C (B) mice vs WT between 3 and 25 weeks of age. Body weight (C), gWAT% (D), iWAT% (E) and length (F) of 25-week-old WT, *GNB3*-C/+ and *GNB3*-C/C mice. Data are mean ± SD, and $*P < 0.05$, $**P < 0.01$, $****P < 0.0001$ vs. WT of same sex by unpaired Student's *t*-test in C-F.

Figure 4.8

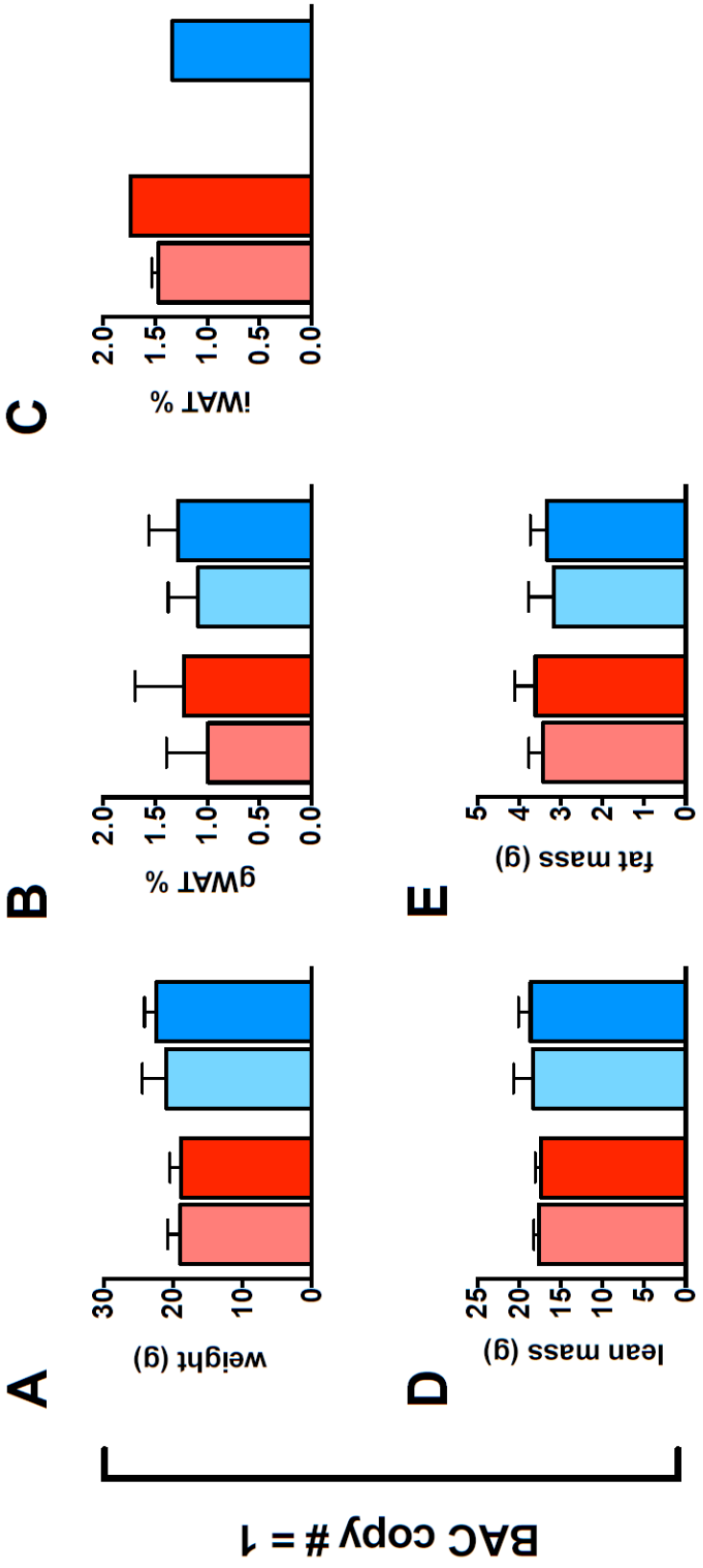
BAC copy # = 1
A
weight (g)
30
20
10
0
B
gWAT %
2.0
1.5
1.0
0.5
0.0
C
iWAT %
2.0
1.5
1.0
0.5
0.0
D
lean mass (g)
25
20
15
10
5
0
E
fat mass (g)
5
4
3
2
1
0

Figure 4.8

Heterozygous *GNB3*-C mice have similar weight to WT littermates at 5 weeks old. Body weight (A), gWAT% (B), iWAT% (C), lean mass (D) and fat mass (E) of *GNB3*-C mice. All mice are 5 weeks old. Data are mean ± SD.

Figure 4.9

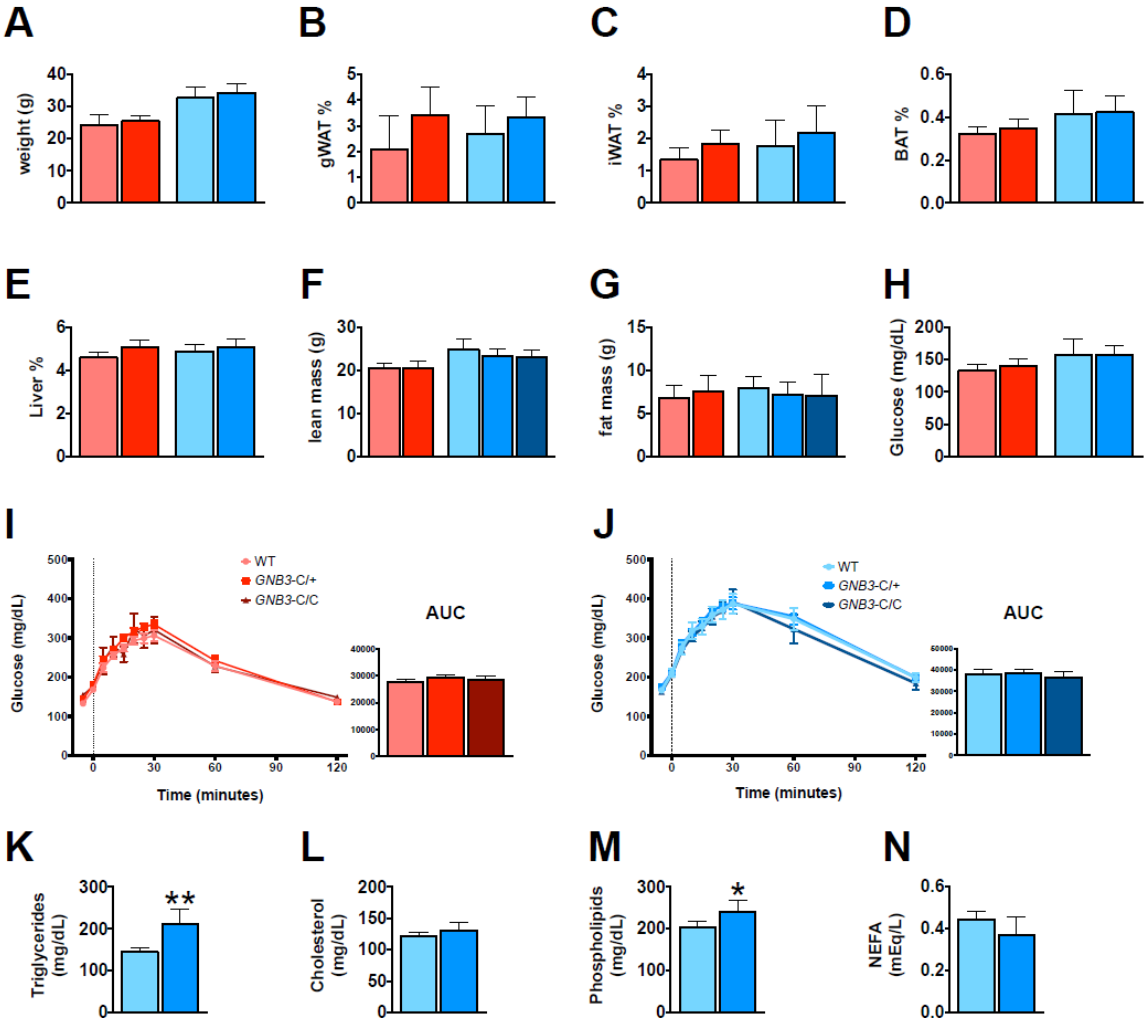
A
weight (g)
B
gWAT %
C
iWAT %
D
BAT %
E
Liver %
F
lean mass (g)
G
fat mass (g)
H
Glucose (mg/dL)
I
Glucose (mg/dL)
WT
GNB3-C/+
GNB3-C/C
Time (minutes)
AUC
J
Glucose (mg/dL)
WT
GNB3-C/+
GNB3-C/C
Time (minutes)
AUC
K
Triglycerides (mg/dL)
**
L
Cholesterol (mg/dL)
M
Phospholipids (mg/dL)
*
N
NEFA (mEq/L)

Figure 4.9

***GNB3*-C mice have elevated fasting blood lipids but do not have impaired glucose tolerance.** Body weight (A), gWAT% (B), iWAT% (C), BAT% (D), liver % (E), lean mass (F), fat mass (G), and fasting blood glucose (H) of *GNB3*-C mice. GTT and AUC of female (I) and male (J) mice. Fasting blood triglycerides (K), cholesterol (L), phospholipids (M) and non-esterified fatty acids (N) of mice. All mice are 20 weeks old. Data are mean ± SD. **P* < 0.05, ***P* < 0.01 vs. WT of same sex by unpaired Student's *t*-test.

Figure 4.10

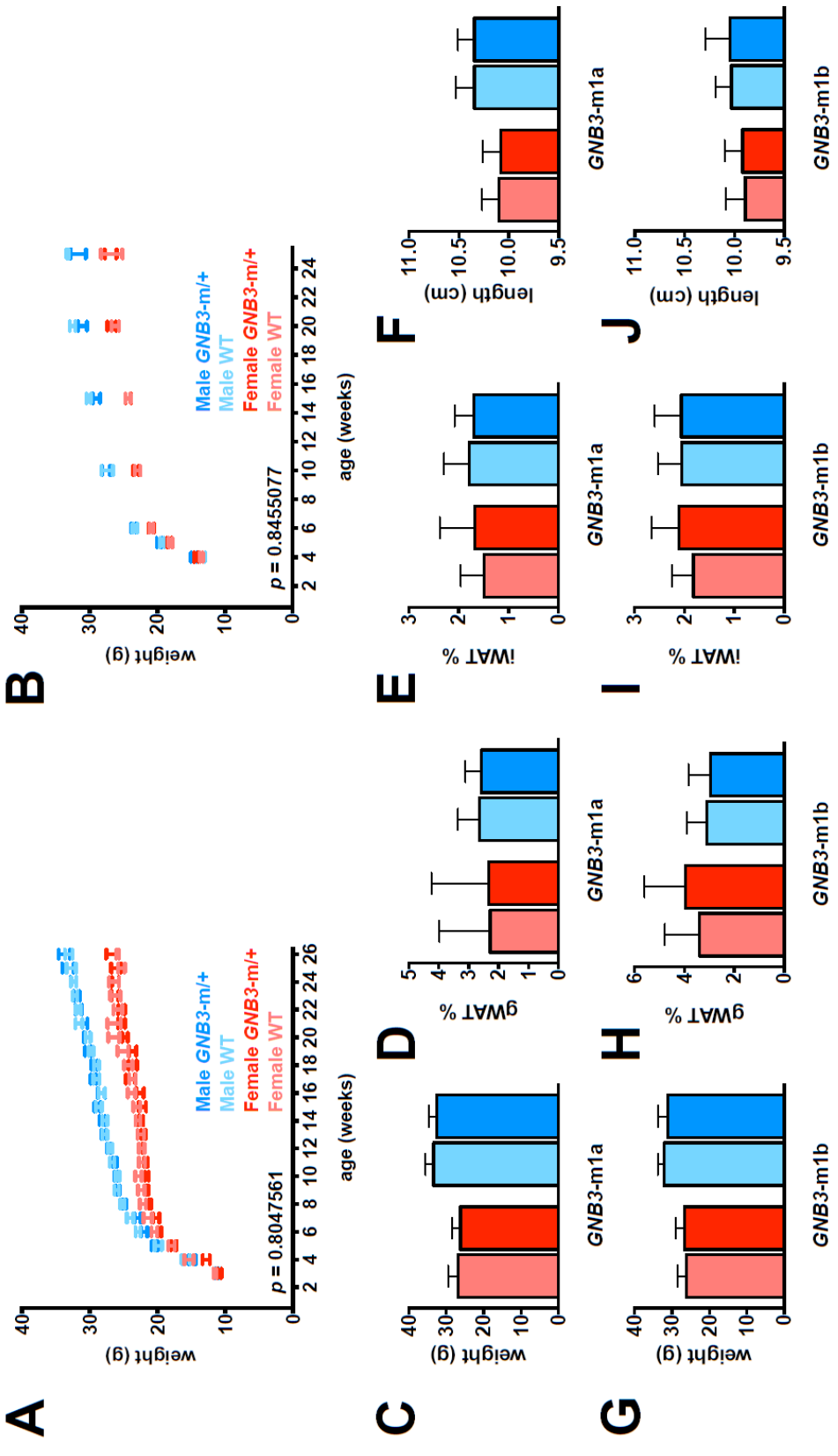
A
weight (g)
age (weeks)
p = 0.8047561
Male GNB3-m/+
Male WT
Female GNB3-m/+
Female WT
B
weight (g)
age (weeks)
p = 0.8455077
C
weight (g)
GNB3-m1a
GNB3-m1b
D
gWAT %
E
iWAT %
F
length (cm)
G
H
I
J

Figure 4.10

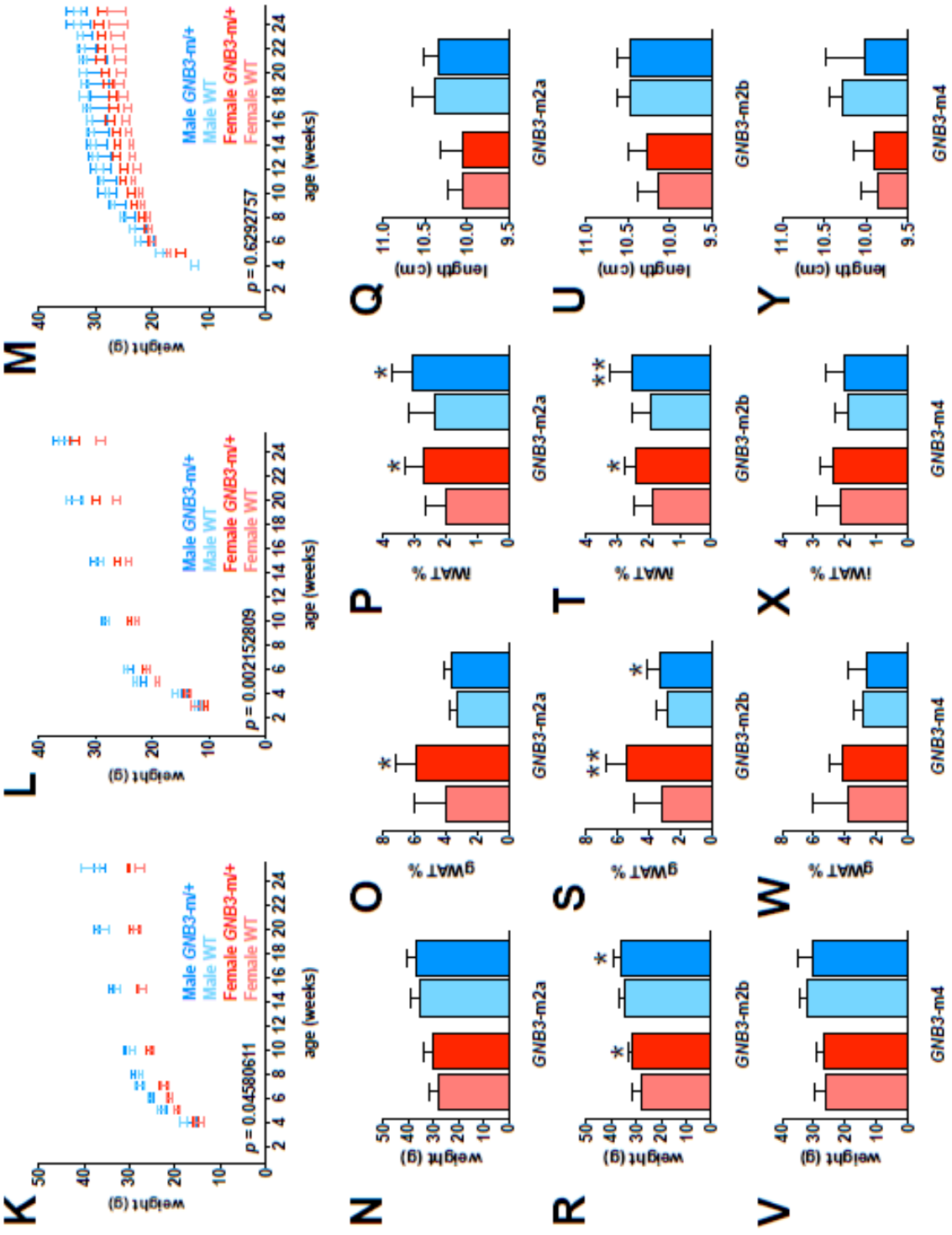
K
L
M
N
O
P
Q
R
S
T
U
V
W
X
Y
weight (g)
age (weeks)
Male GNB3-m/+
Male WT
Female GNB3-m/+
Female WT
p = 0.04580611
p = 0.0021152809
p = 0.6292757
gWAT %
iWAT %
length (cm)
GNB3-m2a
GNB3-m2b
GNB3-m4

Figure 4.10

Heterozygous *GNB3*-m mice (*GNB3*-m/+) with BAC copy number 1 have similar weight to WT, while mice with BAC copy number 2 are heavier than WT littermates. Body weight curves of *GNB3*-m/+ and WT mice from *GNB3*-m1a (A) and *GNB3*-m1b (B) mouse lines between 3 and 25 weeks of age. Body weight (C), gWAT% (D), iWAT% (E) and length (F) of *GNB3*-m1a mice. Body weight (G), gWAT% (H), iWAT% (I) and length (J) of *GNB3*-m1b mice. Body weight curves of *GNB3*-m/+ and WT mice from *GNB3*-m2a (K), *GNB3*-m2b (L) and *GNB3*-m4 (M) mouse lines between 3 and 25 weeks of age. Body weight (N), gWAT% (O), iWAT% (P) and length (Q) of *GNB3*-m2a mice. Body weight (R), gWAT% (S), iWAT% (T) and length (U) of *GNB3*-m2b mice. Body weight (V), gWAT% (W), iWAT% (X) and length (Y) of *GNB3*-m4 mice. Mice are 25 weeks old in C-J and N-Y. Data are mean ± SD, and $*P < 0.05$, $**P < 0.01$ vs. WT of same sex by unpaired Student's *t*-test in C-J and N-Y.

Figure 4.11

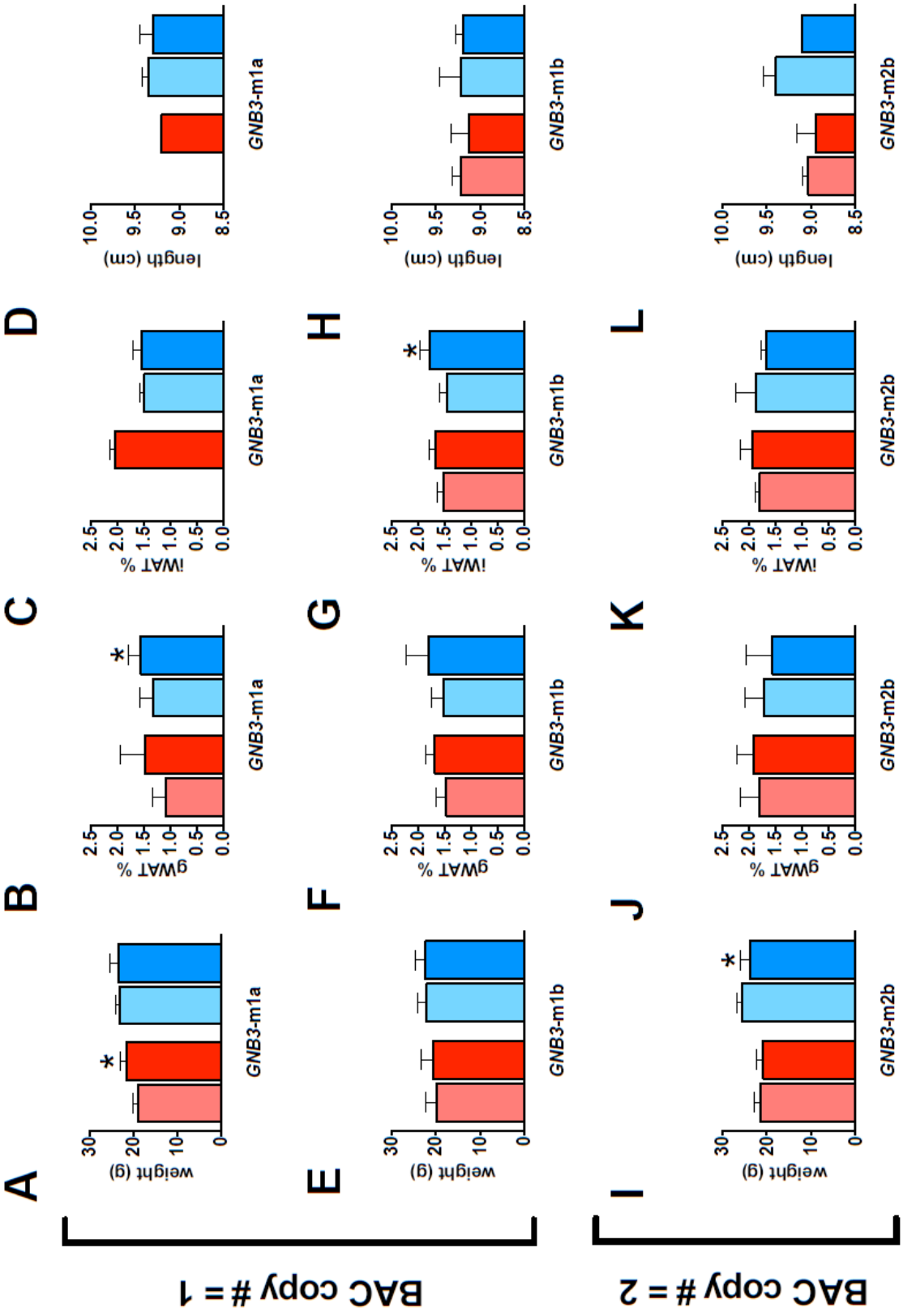
A
B
C
D
E
F
G
H
I
J
K
L
BAC copy # = 1
BAC copy # = 2
weight (g)
gWAT %
iWAT %
length (cm)
GNB3-m1a
GNB3-m1b
GNB3-m2b
*

Figure 4.11

Heterozygous *GNB3*-m mice have similar weight to WT littermates at 5 weeks old. Body weight (A), gWAT% (B), iWAT% (C) and length (D) of *GNB3*-m1a mice. Body weight (E), gWAT% (F), iWAT% (G) and length (H) of *GNB3*-m1b mice. Body weight (I), gWAT% (J), iWAT% (K) and length (L) of *GNB3*-m2b mice. All mice are 5 weeks old. Data are mean ± SD. **P* < 0.05 vs. WT of same sex by unpaired Student's *t*-test.

Table 4.1

Mouse line	**BAC type**	**BAC copy #**	**Heterozygote**	**Homozygote**
GNB3-T	Human risk allele	2	*GNB3*-T/+	*GNB3*-T/T
GNB3-C	Human non-risk allele	1	*GNB3*-C/+	*GNB3*-C/C
GNB3-m1a	Mouse allele	1	*GNB3*-m/+	n/a
GNB3-m1b	Mouse allele	1	*GNB3*-m/+	n/a
GNB3-m2a	Mouse allele	2	*GNB3*-m/+	n/a
GNB3-m2b	Mouse allele	2	*GNB3*-m/+	n/a
GNB3-m4	Mouse allele	4	*GNB3*-m/+	n/a
GNB3-Δ1a	Human risk allele w/o *GNB3*	1	*GNB3*-Δ/+	n/a
GNB3-Δ1b	Human risk allele w/o *GNB3*	1	*GNB3*-Δ/+	n/a
GNB3-Δ3	Human risk allele w/o *GNB3*	3	*GNB3*-Δ/+	n/a

Table 4.1

List of different BAC transgenic mouse lines used in this study.

Chapter 5

General conclusions and future directions

General conclusions

Recently, we described a new obesity and intellectual disability syndrome in children that is caused by an unbalanced chromosome translocation resulting in an 8.5-Mb duplication of chromosome 12p and a 7.0-Mb deletion of chromosome 8p (Goldlust et al., 2013). More than 100 genes lie within the 12p duplication, including the obesity candidate gene, *GNB3*. A cytosine to thymine (C825T) polymorphism in exon 10 of *GNB3* has been associated with hypertension and obesity in adults (Siffert et al., 1998). The C825T polymorphism does not alter the amino acid sequence (TCC to TCT Serine), but causes alternative splicing of exon 9 with a 123 bp in-frame deletion, resulting in a shorter splice variant. The shorter transcript, *GNB3*-s, encoded by the risk allele T of GNB3 is only present in those with a TT or TC genotype (Siffert et al., 1998). Little is known about the function of *GNB3*-s; however, it may explain obesity risk associated with the T allele. To date, the functional role of *GNB3* in obesity is unknown.

In this study, we attempted to narrow the 12p duplication to a critical region required for obesity by creating a BAC transgenic mouse model that carries a 184-kb insert spanning 14 human genes, including the T allele of *GNB3*. In order to uncover the role of *GNB3* in adiposity, feeding, activity and physiology, we carried out a comprehensive phenotypic characterization of heterozygous *GNB3*-T mice (*GNB3*-T/+). First, we tracked body weight of *GNB3*-T/+ mice and their WT littermates from weaning until 25 weeks of age. *GNB3*-T/+ mice weighed significantly more than their WT littermates starting from age 6-7 weeks onwards. Our mouse model of *GNB3*-T duplication recapitulated the obesity phenotype seen in children with the 12p duplication syndrome that we described. Next we were interested in uncovering whether this weight

gain was due to fat accumulation or possibly a difference in lean mass. We dissected and weighed gWAT and iWAT, representative of visceral and subcutaneous WAT depots, respectively, as well as BAT. *GNB3*-T/+ mice had greater gWAT%, iWAT%, BAT% compared to WT littermates. We then carried out H&E staining to determine if fat depots exhibited hypertrophy. gWAT adipocytes were 50% larger in *GNB3*-T/+ mice, while iWAT adipocytes were 27% larger in *GNB3*-T/+ mice compared to WT. We also performed DXA scanning to measure fat mass and lean mass. Fat mass was increased in *GNB3*-T/+ mice, but lean mass was the same between *GNB3*-T/+ mice and WT, indicating that the difference in weight is strictly due to a difference in fat mass in *GNB3*-T/+ mice.

Since obesity is a risk factor for impaired glucose metabolism and type 2 diabetes, it was crucial to investigate the metabolic profiles of *GNB3*-T/+ mice. We collected fasting blood and measured blood glucose, lipids and metabolic hormones. *GNB3*-T/+ mice had elevated fasting blood glucose, plasma insulin and C-peptide compared to WT. Fasting plasma insulin and blood lipids including triglycerides, cholesterol and phospholipids were also elevated in *GNB3*-T/+ mice compared to WT. Altogether, these results indicate that *GNB3*-T/+ mice have metabolic syndrome. We then subjected mice to GTT to assess glucose metabolism and found that *GNB3*-T/+ mice showed glucose intolerance compared to WT. Lastly, we subjected mice to ITT; however, insulin sensitivity was similar between *GNB3*-T/+ mice and WT. Thus, the glucose metabolism phenotype in *GNB3*-T/+ mice is milder than other mouse models of type 2 diabetes.

We also measured levels of inflammatory markers and pituitary hormones to evaluate the impact of *GNB3* overexpression. Of the inflammatory markers measured,

including IL-6, TNF-alpha and MCP-1, all had similar levels in WT and *GNB3*-T/+ mice. On the other hand, pituitary hormones, GH, TSH, FSH, LH and prolactin were lower in male *GNB3*-T/+ mice. GH levels are lower in obese humans, consistent with our mouse model.

The relationship between depression and obesity is an emerging topic of interest in the fields of obesity and psychology. Both human and animal studies indicate there is overlap between anxiety, depression, and obesity. Epidemiologic studies show that affective disorders such as depression, anxiety, are associated with obesity (Bodenlos et al., 2011; Luppino et al., 2010), and that severe depression and anxiety symptoms are associated with abdominal obesity and dyslipidemia (van Reedt Dortland et al., 2013). It was therefore important to determine whether *GNB3*-T/+ mice exhibited anxiety-like or depressive-like behaviors, because these affective phenotypes could potentially contribute to, or be caused by, obesity and metabolic syndrome. We thus conducted a battery of behavioral tests commonly used to investigate affective behaviors in rodents. Based on the results of the behavioral tests, *GNB3*-T/+ mice did not show anxiety-like feeding behaviors or anxiety- or depressive-like phenotypes, indicating that the mentioned phenotypes are not involved in *GNB3*-related obesity.

Energy imbalance between calories consumed and calories expended leads to increase in adiposity. We carried out a series of experiments in an attempt to understand if the increased body weight and adiposity in *GNB3*-T/+ mice are due to an increase in food intake, decrease in activity or a defect in energy expenditure. First, we measured food consumption when mice were 5, 10, 15, 20 and 25 weeks old. Food intake was similar between *GNB3*-T/+ mice and WT at all time points. We also measured fasting

levels of certain satiety hormones, including ghrelin, PYY and amylin. Satiety hormone levels were consistent with proper satiety in *GNB3*-T/+ mice. Based on these results, we conclude that the increase in weight and adiposity in *GNB3*-T/+ mice is not due to hyperphagia or a satiety defect.

Next we placed mice in a metabolic chamber to measure horizontal and vertical activity as well as oxygen consumed and carbon dioxide produced to calculate heat produced. *GNB3*-T/+ mice did not have statistically significant difference in activity levels, oxygen consumption or heat produced compared to WT. However, we cannot rule out subtle differences in activity or heat production that may have contributed to adiposity in *GNB3*-T/+ mice.

The results of the food intake and locomotor activity experiments indicate that the increased adiposity in *GNB3*-T/+ mice is not due to increased food intake or decreased locomotion. Therefore, we hypothesized that *GNB3*-T/+ mice have impaired BAT function. Failure to maintain core body temperature during a cold challenge experiment points to impaired BAT. We subjected mice to an acute cold challenge and found that *GNB3*-T/+ mice had difficulty maintaining their core body temperature compared to WT. BAT is responsible for heat production and is essential for classic nonshivering thermogenesis (Cannon and Nedergaard, 2004). Mitochondria in brown adipocytes express UCP1 and dissipate chemical energy as heat (Tam et al., 2012). White adipose tissue also contains $UCP1^{+}$ cells, called beige adipocytes (Cousin et al., 1992; Ghorbani and Himms-Hagen, 1997; Guerra et al., 1998), which have different molecular signatures than brown adipocytes (Wu et al., 2012). We measured gene expression levels of white, beige and brown adipocytes, as well as mitochondria markers in BAT, iWAT and gWAT.

Overall, we detected lower gene expression of *Ucp1* in BAT, gWAT, and most dramatically in iWAT in *GNB3*-T/+ mice. Additionally, *GNB3*-T/+ mice had lower gene expression of beige and brown adipocyte markers in BAT. Adipogenic markers in iWAT were elevated in *GNB3*-T/+ mice. Based on these results, *GNB3*-T/+ mice have worsened beige adipocyte function in subcutaneous fat since iWAT had lower levels of *Ucp1* expression. Furthermore, subcutaneous adipose tissue in *GNB3*-T/+ mice acquired properties of visceral fat as indicated by increased expression of adipogenic markers. In summary, *GNB3*-T/+ mice had a conversion of subcutaneous WAT into a less $UCP1^{+}$, less beige, and whiter tissue. *GNB3* overexpression led to a white-like remodeling of iWAT and loss of brown and beige properties in BAT.

These data describe a comprehensive characterization of heterozygous transgenic mice that overexpress *GNB3*-T. We also investigated the contributions of *GNB3* alleles and expression levels on mouse weight, to phenotypically characterize mice that overexpress *GNB3*-C and the mouse allele of *Gnb3*.

Although heterozygous *GNB3*-T mice weighed more than WT, homozygous *GNB3*-T mice weighed less than WT. However, homozygous *GNB3*-T had greater adiposity than WT as well as impaired glucose tolerance, which is similar to the phenotype of heterozygous *GNB3*-T mice.

On the contrary, *GNB3*-C overexpression seemed to have a subtle but opposite effect on weight. Heterozygous *GNB3*-C mice weighed less and had shorter body length than WT, and homozygous *GNB3*-C mice weighed less and had shorter body length than *GNB3*-C heterozygotes. The reduction in weight can be explained by shorter body length in mice due to *GNB3*-C overexpression. *GNB3*-C overexpression did not alter adiposity

or glucose tolerance. Furthermore, *GNB3*-C overexpression did not protect from elevated fasting blood lipids.

In mice that overexpress *GNB3*-m, BAC copy number influenced body weight and adiposity but not *Gnb3* expression levels in brain. Heterozygous *GNB3*-m mice with one BAC copy had body weight and adipose tissue weight similar to WT. However, heterozygous *GNB3*-m mice with two BAC copies, which is same copy number as in the *GNB3*-T heterozygotes, had greater body weight and adiposity compared to WT. Overall, these results demonstrate that *GNB3* alleles and expression levels impact body weight. Overexpression of *GNB3*-T led to weight gain in mice, but *GNB3*-C overexpression was protective of weight gain. Mouse *Gnb3* overexpression also led to an increase in adiposity and weight gain, but was dependent on BAC copy number. However, it should be noted that given the process of generating BAC transgenic mice, each founder line had a different BAC insertion site, which may be responsible for the differences between strains, and further complicates the comparisons made in this study.

In summary, the data in this dissertation implicate *GNB3* overexpression in obesity and in impaired WAT and BAT. This dissertation provides, for the first time, a functional link between *GNB3* and obesity pathogenesis.

Overall, the phenotype of mice that overexpress *GNB3*-T is not similar to that of *ob*/*ob* mice, the first identified obesity mouse strain. *ob*/*ob* mice have hyperphagia and are three times the weight of WT mice; whereas, *GNB3*-T/+ mice do not have hyperphagia and have mild weight gain starting at age 6-7 weeks onwards. *ob*/*ob* mice are deficient in leptin, and leptin is a part of the leptin-melanocortin signaling pathway which controls food intake. *GNB3* overexpression likely does not have a direct role in

food intake, and Gβ3 does not seem to have a significant role in the leptin-melanocortin signaling pathway. In contrast, *GNB3*-T/+ mice seem to have a phenotype that is more similar to mice with PRDM16 (PR domain containing 16) deletion in white and brown adipose tissues (Adipo-PRDM16 KO mice). PRDM16 ablation induced obesity, enlargement of subcutaneous adipose tissue and severe insulin resistance in mice on a high-fat diet. In addition, subcutaneous adipose tissue in Adipo-PRDM16 KO mice acquired many key properties of visceral fat (Cohen et al., 2014). This whitening of subcutaneous adipose tissue is what we see in *GNB3*-T/+ mice. PRDM16 seems to be required for the "browning" of white adipose tissue, similar to WT Gβ3 levels being required for healthy subcutaneous adipose tissue.

Unlike *GNB3*-T overexpression, Gβ3 deficiency does not seem to impact weight or metabolism since Gβ3 deficient mice have normal weight, glucose tolerance and insulin sensitivity (Ye et al., 2014). As all Gβ subunits are highly conserved, the other four Gβ subunits may be compensating for the function of Gβ3 in Gβ3 deficient mice. In humans, *GNB3*-T allele is associated with the presence of a shorter splice variant of Gβ3, called Gβ3-s, which has enhanced activation of G proteins. Carriers of the *GNB3*-T allele are also at a higher risk for hypertension, obesity and metabolic syndrome based on GWAS (Siffert et al., 1998). Mice that overexpress *GNB3*-T are obese with metabolic syndrome. Increased amount of Gβ3-s in *GNB3*-T mice is likely responsible for enhanced activation of G proteins, and enhanced activation of downstream targets of Gβ3-s in the cell. Downstream targets of Gβ3-s may have roles in weight regulation and beigeing of white adipose tissue. *GNB3*-C allele is only associated with the presence of full length Gβ3, and not Gβ3-s. Mice that overexpress *GNB3*-C had similar adiposity to WT mice. I

propose that an increase in Gβ3-s is responsible for the weight gain, and mice that overexpress *GNB3*-C are protected from weight gain due to the absence of Gβ3-s.

Future directions

In this study, we investigated the effects of *GNB3* overexpression on mouse weight and physiology by generating transgenic mice that carry BAC inserts approximately 190 kb in size. Generating BAC transgenic mouse models of *GNB3* overexpression was the essential first step to narrow down the obesity critical region from 107 to 14 duplicated genes. The first transgenic mouse line we generated had a BAC insert with 14 genes, one of which was the T-allele of *GNB3*. This mouse line weighed significantly more than WT longitudinally. In order to rule out the effect of the other 13 genes on mouse weight, we generated another BAC transgenic mouse line, called *ΔGNB3*. We recombineered the BAC insert in *GNB3*-T mice by replacing *GNB3* with a neomycin cassette, but kept the rest of the 13 genes. Δ*GNB3* mice weighed similar to WT longitudinally and had adiposity similar to WT. Therefore, we concluded that the other 13 genes on the *GNB3*-T BAC did not have an appreciable effect on mouse weight or adiposity, and overexpression of *GNB3* T allele was responsible for weight gain. Later we created additional transgenic mouse lines that overexpressed the C allele of *GNB3* and mouse *Gnb3* in order to evaluate contributions of various alleles on mouse weight. For each line, we compared the phenotypes of the BAC transgenics and WT mice; however, this approach had some inherent limitations.

GNB3-T, *GNB3*-C and mouse *Gnb3* mice have different BAC insertion sites, BAC copy numbers, and *GNB3* expression levels. Therefore, we cannot directly compare

contributions of *GNB3* alleles and gene expression levels on obesity. Although BAC transgenic mice have the advantage of retaining local regulatory elements, these mouse models are complicated by multiple genes on the BAC constructs.

In order to determine the role of GNB3 in obesity physiology and metabolism, a knock-in mouse model that includes only one inserted gene is needed. The *GNB3* T allele is associated with a shorter splice variant of *GNB3* called *GNB3*-s. We propose to insert cDNA from *GNB3* and *GNB3*-s separately into the Rosa26 locus. This knock-in system will allow us to directly compare the phenotypes of *GNB3* and *GNB3*-s mouse models to determine the role of *GNB3* duplication and splice variants in obesity. Additionally, the knock-in system will allow us to only express *GNB3* in distinct tissue types and study GNB3 in key tissues related to obesity. By crossing knock-ins to tissue-specific Cre recombinase lines, we can evaluate *GNB3* expression in subcutaneous WAT, visceral WAT, BAT, hypothalamus, and other relevant tissues.

The Rosa26 locus is a well characterized and commonly used site for targeted knock-in mouse models since constructs can be targeted with high efficiency and loss of Rosa26 is not deleterious (Hohenstein et al., 2008). Knock-in mice where the endogenous mouse Rosa26 promoter drives *GNB3* or *GNB3*-s expression can be created as follows (Figure 5.1). First, *GNB3* or *GNB3*-s cDNA will be cloned into the pRosa26-DEST vector, which contains the splice acceptor (s.a.) of Rosa26, the loxP-PGK-neo-pA-3xpA-loxP cassette, and the diphtheria toxin fragment A (DTA) gene. In this vector, phosphoglycerate kinase I (PGK) is a strong promoter driving neomycin expression. PGK-neo-pA and three copies of the SV40 polyA signal (3xpA) act as a strong transcriptional STOP sequence. pROSA26-*GNB3* targeting vectors will be electroporated

into C57BL/6 embryonic stem (ES) cells to insert the constructs at the endogenous Rosa26 locus via homologous recombination. 200 neomycin-resistant/DTA-negative ES clones will be screened and correct targeting will be confirmed by Southern blot hybridization. Six targeted clones (3 *GNB3* and 3 *GNB3*-s) will be expanded and targeted ES cells will be injected into blastocysts to generate chimeric mice. Chimeric males will be bred to C57BL/6 females to generate germline F1 pups. F1s will be bred to mice with ubiquitous or tissue-specific Cre recombinase to delete the STOP cassette between the two loxP sites. This fuses Rosa26 exon 1 to *GNB3* cDNA, leading to *GNB3* expression driven by the Rosa26 promoter. qRT-PCR assays will be used to measure *GNB3* expression in whole brain and adipose tissues. Rosa26 is ubiquitously expressed in embryonic and adult tissues and expresses other constructs at consistent levels (Casola, 2010; Soriano, 1999). Approximately equal expression of *GNB3* in both knock-ins is ideal to separate the effects of the risk allele and differences in expression level.

After generating full-length *GNB3* and *GNB3*-s knock-in mouse lines, it will be essential to characterize the physiology and metabolism of the mice. First, each mouse line should be weighed longitudinally and total body weights should be tested for a statistically significant difference from WT. In the event that knock-in mice have a statistically significant weight curve than WT, two time points should be selected, one before the onset of the weight difference and one after. Carrying out the phenotypic characterization both before the onset of obesity and after will allow us to differentiate between direct and indirect effects of *GNB3* overexpression on obesity. Relevant tissues such as subcutaneous and visceral WAT, BAT and liver should be dissected and weighed. Lean and fat mass should be measured. Histology, including H&E staining for

cell size and Oil Red O staining for lipid staining of relevant tissues should be done. Daily food intake, horizontal and vertical locomotor activity levels should be measured. Metabolic chambers can measure amount of oxygen consumed and carbon dioxide produced, and with these data, amount of heat produced by mice should be calculated. Mice should be fasted, and fasting blood glucose levels should be measured and fasting plasma should be collected. A panel of blood lipids, adipokines, obesity- and diabetes-related metabolic hormones, as well as pituitary hormones should be measured. Mice should be subjected to GTT and ITT to evaluate glucose metabolism and insulin resistance. Mice can be placed on a high fat diet to analyze weight curve changes based on high calorie intake. If mice show difficulty breeding, fertility experiments such as semen analysis will be warranted. Additionally, gene expression levels of adipogenic, beige and brown adipocyte markers, as well as mitochondria markers in subcutaneous and visceral WAT, and BAT should be measured.

The experiments to phenotypically characterize our *GNB3*-T BAC transgenic mouse line should be also done for the knock-in *GNB3* mouse lines. Additional experiments can also be done on knock-in *GNB3* mice if necessary. Circulating levels of triiodothyronine (T_3) and thyroxine (T_4), which are secreted by the thyroid after stimulation by TSH, should be analyzed given the role of these hormones in thermogenesis and lipid mobilization and storage. We also observed that male *GNB3*-T mice have difficulty impregnating females after about 3 months of age, while WT male mice or female *GNB3*-T mice have no issues in reproduction. The biological reason underlying the difficulty in mating in male *GNB3*-T mice is unclear and can be

investigated further by measuring testosterone levels or counting sperm. Whether or not *GNB3* overexpression causes hypothyroidism or infertility are open questions.

To measure BAT function in mice directly, assessment of maximal thermogenic capacity should be considered. The greatest quantity of heat a mouse can produce is defined as maximal thermogenic capacity. Mice will be given a supramaximal dose of a thermogenic drug to activate BAT, and energy expenditure will be measured in metabolic chambers. Maximal thermogenic capacity will need to be assessed at two different temperatures: thermoneutrality (30°C) and cold (4°C). Thermoneutrality minimizes, while cold increases BAT thermogenic capacity. Mice should be acclimated to either temperature for approximately 3 weeks before taking heat measurements.

Furthermore, WAT and BAT function can also be assessed via tissue culture experiments. We propose harvesting and culturing WAT and BAT from *GNB3* knock-in and WT mice to characterize the cell lines. For example, amount of lipid produced by the cell line, adipocyte size, the amount of oxygen consumed and carbon dioxide produced, and the heat output can be measured. After the initial characterization of the WAT and BAT cell lines from *GNB3* knock-in mice, experiments can be designed to test for rescue of the *GNB3* overexpression phenotype. For example, since *Ucp1* expression in iWAT of *GNB3*-T/+ mice is low, *Ucp1* expression in cultured cell lines harvested from iWAT, gWAT and BAT of *GNB3* knock-in mice should be measured. If *Ucp1* expression is low in cultured iWAT cells of *GNB3* knock-in mice, then *Ucp1* can be overexpressed in the cell line to test for rescue of the *GNB3* overexpression phenotype.

Downstream binding partners of Gβ3 and Gβ3-s are unknown. Knock-in mouse lines with tagged full-length *GNB3* and *GNB3*-s can be created. WAT and BAT tissues

from these mice can be harvested and the biotinylated Gβ3 and Gβ3-s can be purified together with their associated proteins and other molecules. The pulled down proteins and molecules can be identified by mass spectrometry. These targets can then be investigated further for involvement in metabolic pathways or for potential downstream interactions with UCP1. Generating a tissue culture model of *GNB3* overexpression will be a valuable tool to further investigate other aspects of GNB3 biology, including identifying binding partners of Gβ3 and finding drug targets to manage GNB3 related obesity.

In summary, this dissertation is a novel direction for *GNB3* research. We proposed and showed that *GNB3* gene duplication and overexpression leads to obesity. Further, we showed that genetic variation within *GNB3* can further modulate obesity risk. Though most obese children do not have a *GNB3* duplication, understanding how aberrant *GNB3* signaling relates to obesity can point to new genes and pathways that may underlie more common forms of childhood obesity.

Figure 5.1

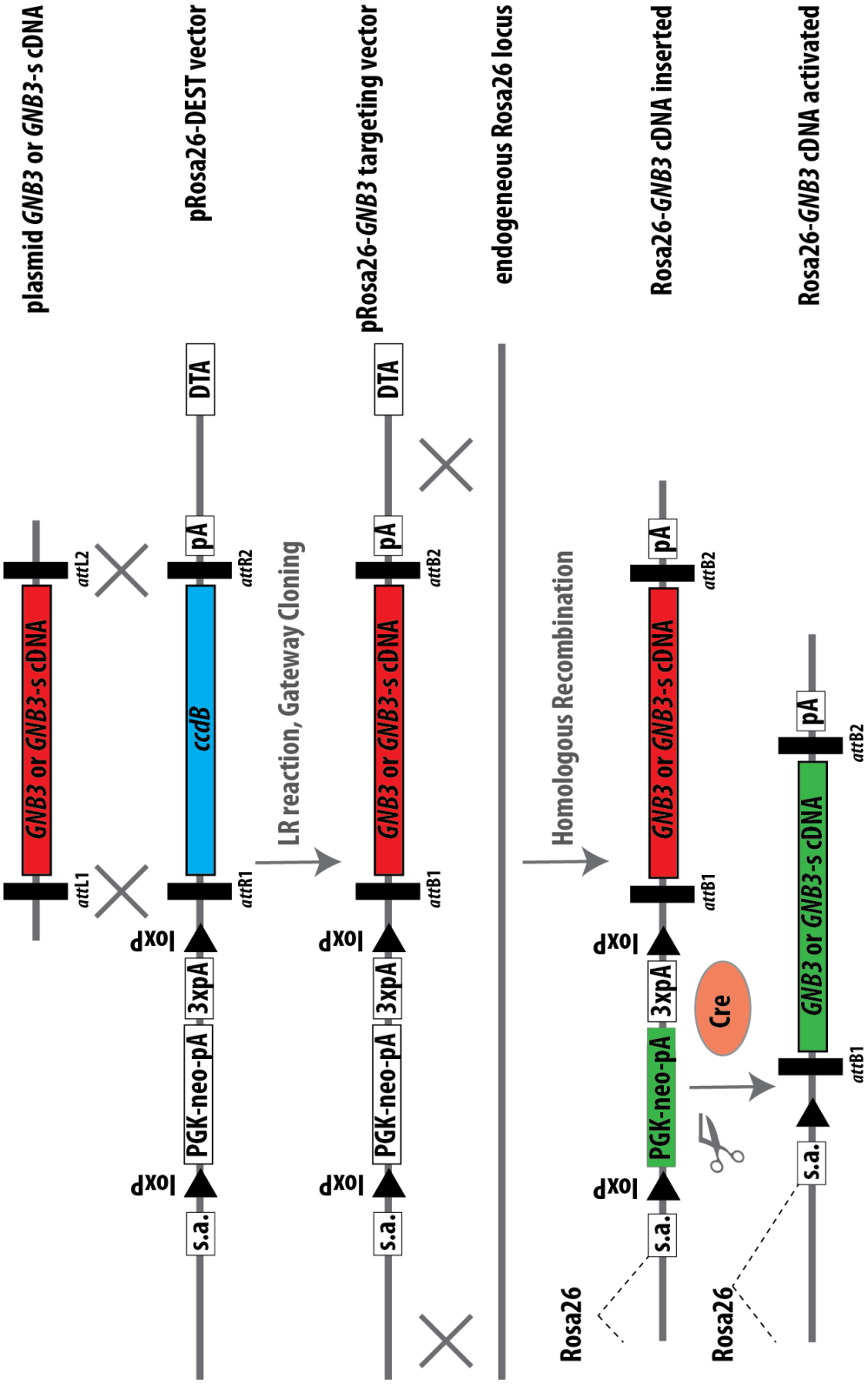
plasmid GNB3 or GNB3-s cDNA
pRosa26-DEST vector
pRosa26-GNB3 targeting vector
endogeneous Rosa26 locus
Rosa26-GNB3 cDNA inserted
Rosa26-GNB3 cDNA activated
attL2
attL1
attR2
attR1
attB2
attB1
DTA
pA
ccdB
GNB3 or GNB3-s cDNA
loxP
3xpA
PGK-neo-pA
s.a.
LR reaction, Gateway Cloning
Homologous Recombination
Cre
Rosa26

Figure 5.1

Knock-in strategy to insert GNB3 and GNB3-s cDNA at the Rosa26 locus.

References

Ansley, S.J., Badano, J.L., Blacque, O.E., Hill, J., Hoskins, B.E., Leitch, C.C., Kim, J.C., Ross, A.J., Eichers, E.R., Teslovich, T.M., et al. (2003). Basal body dysfunction is a likely cause of pleiotropic Bardet-Biedl syndrome. Nature *425*, 628–633.

Bachmann-Gagescu, R., Mefford, H.C., Cowan, C., Glew, G.M., Hing, A. V, Wallace, S., Bader, P.I., Hamati, A., Reitnauer, P.J., Smith, R., et al. (2010). Recurrent 200-kb deletions of 16p11.2 that include the SH2B1 gene are associated with developmental delay and obesity. Genet. Med. *12*, 641–647.

Baldwin, E.L., Lee, J.-Y., Blake, D.M., Bunke, B.P., Alexander, C.R., Kogan, A.L., Ledbetter, D.H., and Martin, C.L. (2008). Enhanced detection of clinically relevant genomic imbalances using a targeted plus whole genome oligonucleotide microarray. Genet. Med. *10*, 415–429.

Benussi, D.G., Costa, P., Zollino, M., Murdolo, M., Petix, V., Carrozzi, M., and Pecile, V. (2009). Trisomy 12p and monosomy 4p: phenotype-genotype correlation. Genet. Test. Mol. Biomarkers *13*, 199–204.

Berry, D.C., Stenesen, D., Zeve, D., and Graff, J.M. (2013). The developmental origins of adipose tissue. Development *140*, 3939–3949.

Blakemore, A.I.F., and Froguel, P. (2010). Investigation of Mendelian forms of obesity holds out the prospect of personalized medicine. Ann. N. Y. Acad. Sci. *1214*, 180–189.

Bochukova, E.G., Huang, N., Keogh, J., Henning, E., Purmann, C., Blaszczyk, K., Saeed, S., Hamilton-Shield, J., Clayton-Smith, J., O'Rahilly, S., et al. (2010). Large, rare chromosomal deletions associated with severe early-onset obesity. Nature *463*, 666–670.

Bodenlos, J.S., Lemon, S.C., Schneider, K.L., August, M.A., and Pagoto, S.L. (2011). Associations of mood and anxiety disorders with obesity: comparisons by ethnicity. J. Psychosom. Res. *71*, 319–324.

Bogardus, C. (2009). Missing heritability and GWAS utility. Obesity (Silver Spring). *17*, 209–210.

Bourne, H.R. (1997). How receptors talk to trimeric G proteins. Curr. Opin. Cell Biol. *9*, 134–142.

Bradfield, J.P., Taal, H.R., Timpson, N.J., Scherag, A., Lecoeur, C., Warrington, N.M., Hypponen, E., Holst, C., Valcarcel, B., Thiering, E., et al. (2012). A genome-wide association meta-analysis identifies new childhood obesity loci. Nat. Genet. *44*, 526–531.

Burgado, J., Harrell, C.S., Eacret, D., Reddy, R., Barnum, C.J., Tansey, M.G., Miller, A.H., Wang, H., and Neigh, G.N. (2014). Two weeks of predatory stress induces anxiety-like behavior with co-morbid depressive-like behavior in adult male mice. Behav. Brain Res. *275*, 120–125.

Burns, B., Schmidt, K., Williams, S.R., Kim, S., Girirajan, S., and Elsea, S.H. (2010). Rai1 haploinsufficiency causes reduced Bdnf expression resulting in hyperphagia, obesity and altered fat distribution in mice and humans with no evidence of metabolic syndrome. Hum. Mol. Genet. *19*, 4026–4042.

Campfield, L.A., Smith, F.J., Guisez, Y., Devos, R., and Burn, P. (1995). Recombinant mouse OB protein: evidence for a peripheral signal linking adiposity and central neural networks. Science *269*, 546–549.

Cannon, B., and Nedergaard, J. (2004). Brown adipose tissue: function and physiological significance. Physiol. Rev. *84*, 277–359.

Carola, V., D'Olimpio, F., Brunamonti, E., Mangia, F., and Renzi, P. (2002). Evaluation of the elevated plus-maze and open-field tests for the assessment of anxiety-related behaviour in inbred mice. Behav. Brain Res. *134*, 49–57.

Casola, S. (2010). Mouse models for miRNA expression: the ROSA26 locus. Methods Mol. Biol. *667*, 145–163.

Chan, J.M., Rimm, E.B., Colditz, G.A., Stampfer, M.J., and Willett, W.C. (1994). Obesity, fat distribution, and weight gain as risk factors for clinical diabetes in men. Diabetes Care *17*, 961–969.

Chen, H., Charlat, O., Tartaglia, L.A., Woolf, E.A., Weng, X., Ellis, S.J., Lakey, N.D., Culpepper, J., Moore, K.J., Breitbart, R.E., et al. (1996). Evidence that the diabetes gene encodes the leptin receptor: identification of a mutation in the leptin receptor gene in db/db mice. Cell *84*, 491–495.

Cheung, C.C., Clifton, D.K., and Steiner, R.A. (1997). Proopiomelanocortin neurons are direct targets for leptin in the hypothalamus. Endocrinology *138*, 4489–4492.

Choleris, E., Thomas, A.W., Kavaliers, M., and Prato, F.S. (2001). A detailed ethological analysis of the mouse open field test: effects of diazepam, chlordiazepoxide and an extremely low frequency pulsed magnetic field. Neurosci. Biobehav. Rev. *25*, 235–260.

Choquet, H., and Meyre, D. (2011a). Molecular basis of obesity: current status and future prospects. Curr. Genomics *12*, 154–168.

Choquet, H., and Meyre, D. (2011b). Genetics of Obesity: What have we Learned? Curr. Genomics *12*, 169–179.

Chua, S.C., Chung, W.K., Wu-Peng, X.S., Zhang, Y., Liu, S.M., Tartaglia, L., and Leibel, R.L. (1996). Phenotypes of mouse diabetes and rat fatty due to mutations in the OB (leptin) receptor. Science *271*, 994–996.

Cinti, S. (2005). The adipose organ. Prostaglandins. Leukot. Essent. Fatty Acids *73*, 9–15.

Clapham, D.E., and Neer, E.J. (1997). G protein beta gamma subunits. Annu. Rev. Pharmacol. Toxicol. *37*, 167–203.

Clément, K., Vaisse, C., Lahlou, N., Cabrol, S., Pelloux, V., Cassuto, D., Gourmelen, M., Dina, C., Chambaz, J., Lacorte, J.M., et al. (1998). A mutation in the human leptin receptor gene causes obesity and pituitary dysfunction. Nature *392*, 398–401.

Cohen, P., Levy, J.D., Zhang, Y., Frontini, A., Kolodin, D.P., Svensson, K.J., Lo, J.C., Zeng, X., Ye, L., Khandekar, M.J., et al. (2014). Ablation of PRDM16 and beige adipose causes metabolic dysfunction and a subcutaneous to visceral fat switch. Cell *156*, 304–316.

Coleman, D.L. (1978). Obese and diabetes: two mutant genes causing diabetes-obesity syndromes in mice. Diabetologia *14*, 141–148.

Conrad, D.F., Pinto, D., Redon, R., Feuk, L., Gokcumen, O., Zhang, Y., Aerts, J., Andrews, T.D., Barnes, C., Campbell, P., et al. (2010). Origins and functional impact of copy number variation in the human genome. Nature *464*, 704–712.

Cooper, G.M., Coe, B.P., Girirajan, S., Rosenfeld, J.A., Vu, T.H., Baker, C., Williams, C., Stalker, H., Hamid, R., Hannig, V., et al. (2011). A copy number variation morbidity map of developmental delay. Nat. Genet. *43*, 838–846.

Coppari, R., and Bjørbæk, C. (2012). Leptin revisited: its mechanism of action and potential for treating diabetes. Nat. Rev. Drug Discov. *11*, 692–708.

Cordeira, J.W., Frank, L., Sena-Esteves, M., Pothos, E.N., and Rios, M. (2010). Brain-derived neurotrophic factor regulates hedonic feeding by acting on the mesolimbic dopamine system. J. Neurosci. *30*, 2533–2541.

Cousin, B., Cinti, S., Morroni, M., Raimbault, S., Ricquier, D., Pénicaud, L., and Casteilla, L. (1992). Occurrence of brown adipocytes in rat white adipose tissue: molecular and morphological characterization. J. Cell Sci. *103 (Pt 4*, 931–942.

Creemers, J.W.M., Choquet, H., Stijnen, P., Vatin, V., Pigeyre, M., Beckers, S., Meulemans, S., Than, M.E., Yengo, L., Tauber, M., et al. (2012). Heterozygous mutations causing partial prohormone convertase 1 deficiency contribute to human obesity. Diabetes *61*, 383–390.

Crowley, V.E.F. (2008). Overview of human obesity and central mechanisms regulating energy homeostasis. Ann. Clin. Biochem. *45*, 245–255.

Dick, K.J., Nelson, C.P., Tsaprouni, L., Sandling, J.K., Aïssi, D., Wahl, S., Meduri, E., Morange, P.-E., Gagnon, F., Grallert, H., et al. (2014). DNA methylation and body-mass index: a genome-wide analysis. Lancet (London, England) *383*, 1990–1998.

Faivre, L., Cormier-Daire, V., Lapierre, J.M., Colleaux, L., Jacquemont, S., Geneviéve, D., Saunier, P., Munnich, A., Turleau, C., Romana, S., et al. (2002). Deletion of the SIM1

gene (6q16.2) in a patient with a Prader-Willi-like phenotype. J. Med. Genet. *39*, 594–596.

Farooqi, I.S., Jebb, S.A., Langmack, G., Lawrence, E., Cheetham, C.H., Prentice, A.M., Hughes, I.A., McCamish, M.A., and O'Rahilly, S. (1999). Effects of recombinant leptin therapy in a child with congenital leptin deficiency. N. Engl. J. Med. *341*, 879–884.

Farooqi, I.S., Keogh, J.M., Yeo, G.S.H., Lank, E.J., Cheetham, T., and O'Rahilly, S. (2003). Clinical spectrum of obesity and mutations in the melanocortin 4 receptor gene. N. Engl. J. Med. *348*, 1085–1095.

Farooqi, I.S., Volders, K., Stanhope, R., Heuschkel, R., White, A., Lank, E., Keogh, J., O'Rahilly, S., and Creemers, J.W.M. (2007). Hyperphagia and early-onset obesity due to a novel homozygous missense mutation in prohormone convertase 1/3. J. Clin. Endocrinol. Metab. *92*, 3369–3373.

Feinberg, A.P., Irizarry, R.A., Fradin, D., Aryee, M.J., Murakami, P., Aspelund, T., Eiriksdottir, G., Harris, T.B., Launer, L., Gudnason, V., et al. (2010). Personalized epigenomic signatures that are stable over time and covary with body mass index. Sci. Transl. Med. *2*, 49ra67.

Feinleib, M., Garrison, R.J., Fabsitz, R., Christian, J.C., Hrubec, Z., Borhani, N.O., Kannel, W.B., Rosenman, R., Schwartz, J.T., and Wagner, J.O. (1977). The NHLBI twin study of cardiovascular disease risk factors: methodology and summary of results. Am. J. Epidemiol. *106*, 284–285.

Feldmann, H.M., Golozoubova, V., Cannon, B., and Nedergaard, J. (2009). UCP1 ablation induces obesity and abolishes diet-induced thermogenesis in mice exempt from thermal stress by living at thermoneutrality. Cell Metab. *9*, 203–209.

Fiese, B.H., Bost, K.K., McBride, B. a, and Donovan, S.M. (2013). Childhood obesity prevention from cell to society. Trends Endocrinol. Metab. *24*, 375–377.

File, S.E. (1980). The use of social interaction as a method for detecting anxiolytic activity of chlordiazepoxide-like drugs. J. Neurosci. Methods *2*, 219–238.

File, S.E., and Seth, P. (2003). A review of 25 years of the social interaction test. Eur. J. Pharmacol. *463*, 35–53.

Finkelstein, E. a, Khavjou, O. a, Thompson, H., Trogdon, J.G., Pan, L., Sherry, B., and Dietz, W. (2012). Obesity and severe obesity forecasts through 2030. Am. J. Prev. Med. *42*, 563–570.

Firth, H. V, Richards, S.M., Bevan, A.P., Clayton, S., Corpas, M., Rajan, D., Van Vooren, S., Moreau, Y., Pettett, R.M., and Carter, N.P. (2009). DECIPHER: Database of Chromosomal Imbalance and Phenotype in Humans Using Ensembl Resources. Am. J. Hum. Genet. *84*, 524–533.

Flegal, K.M., Wei, R., and Ogden, C. (2002). Weight-for-stature compared with body mass index-for-age growth charts for the United States from the Centers for Disease Control and Prevention. Am. J. Clin. Nutr. *75*, 761–766.

Fontaine, K.R., Redden, D.T., Wang, C., Westfall, A.O., and Allison, D.B. (2003). Years of life lost due to obesity. JAMA *289*, 187–193.

Ford, C.E., Skiba, N.P., Bae, H., Daaka, Y., Reuveny, E., Shekter, L.R., Rosal, R., Weng, G., Yang, C.S., Iyengar, R., et al. (1998). Molecular basis for interactions of G protein betagamma subunits with effectors. Science *280*, 1271–1274.

Frayling, T.M., Timpson, N.J., Weedon, M.N., Zeggini, E., Freathy, R.M., Lindgren, C.M., Perry, J.R.B., Elliott, K.S., Lango, H., Rayner, N.W., et al. (2007). A common variant in the FTO gene is associated with body mass index and predisposes to childhood and adult obesity. Science *316*, 889–894.

Friedman, J.M., and Halaas, J.L. (1998). Leptin and the regulation of body weight in mammals. Nature *395*, 763–770.

Fukumoto, K., Iijima, M., and Chaki, S. (2014). Serotonin-1A receptor stimulation mediates effects of a metabotropic glutamate 2/3 receptor antagonist, 2S-2-amino-2-(1S,2S-2-carboxycycloprop-1-yl)-3-(xanth-9-yl)propanoic acid (LY341495), and an N-methyl-D-aspartate receptor antagonist, ketamine, in the. Psychopharmacology (Berl). *231*, 2291–2298.

Gesta, S., Tseng, Y.-H., and Kahn, C.R. (2007). Developmental origin of fat: tracking obesity to its source. Cell *131*, 242–256.

Ghorbani, M., and Himms-Hagen, J. (1997). Appearance of brown adipocytes in white adipose tissue during CL 316,243-induced reversal of obesity and diabetes in Zucker fa/fa rats. Int. J. Obes. Relat. Metab. Disord. *21*, 465–475.

Giglio, S., Calvari, V., Gregato, G., Gimelli, G., Camanini, S., Giorda, R., Ragusa, A., Guerneri, S., Selicorni, A., Stumm, M., et al. (2002). Heterozygous submicroscopic inversions involving olfactory receptor-gene clusters mediate the recurrent t(4;8)(p16;p23) translocation. Am. J. Hum. Genet. *71*, 276–285.

Giralt, M., and Villarroya, F. (2013). White, brown, beige/brite: different adipose cells for different functions? Endocrinology 1–9.

Glessner, J.T., Bradfield, J.P., Wang, K., Takahashi, N., Zhang, H., Sleiman, P.M., Mentch, F.D., Kim, C.E., Hou, C., Thomas, K.A., et al. (2010). A genome-wide study reveals copy number variants exclusive to childhood obesity cases. Am. J. Hum. Genet. *87*, 661–666.

Godfrey, K.M., Sheppard, A., Gluckman, P.D., Lillycrop, K.A., Burdge, G.C., McLean, C., Rodford, J., Slater-Jefferies, J.L., Garratt, E., Crozier, S.R., et al. (2011). Epigenetic gene promoter methylation at birth is associated with child's later adiposity. Diabetes *60*,

1528–1534.

Goldlust, I.S., Hermetz, K.E., Catalano, L.M., Barfield, R.T., Cozad, R., Wynn, G., Ozdemir, A.C., Conneely, K.N., Mulle, J.G., Dharamrup, S., et al. (2013). Mouse model implicates GNB3 duplication in a childhood obesity syndrome. Proc. Natl. Acad. Sci. U. S. A. *110*, 14990–14994.

Goldstone, A.P. Prader-Willi syndrome: advances in genetics, pathophysiology and treatment. Trends Endocrinol. Metab. *15*, 12–20.

Grauer, W.O., Moss, A.A., Cann, C.E., and Goldberg, H.I. (1984). Quantification of body fat distribution in the abdomen using computed tomography. Am. J. Clin. Nutr. *39*, 631–637.

Gray, J., Yeo, G.S.H., Cox, J.J., Morton, J., Adlam, A.-L.R., Keogh, J.M., Yanovski, J.A., El Gharbawy, A., Han, J.C., Tung, Y.C.L., et al. (2006). Hyperphagia, severe obesity, impaired cognitive function, and hyperactivity associated with functional loss of one copy of the brain-derived neurotrophic factor (BDNF) gene. Diabetes *55*, 3366–3371.

Gu, W., Tu, Z., Kleyn, P.W., Kissebah, A., Duprat, L., Lee, J., Chin, W., Maruti, S., Deng, N., Fisher, S.L., et al. (1999). Identification and functional analysis of novel human melanocortin-4 receptor variants. Diabetes *48*, 635–639.

Guerra, C., Koza, R.A., Yamashita, H., Walsh, K., and Kozak, L.P. (1998). Emergence of brown adipocytes in white fat in mice is under genetic control. Effects on body weight and adiposity. J. Clin. Invest. *102*, 412–420.

Halaas, J.L., Gajiwala, K.S., Maffei, M., Cohen, S.L., Chait, B.T., Rabinowitz, D., Lallone, R.L., Burley, S.K., and Friedman, J.M. (1995). Weight-reducing effects of the plasma protein encoded by the obese gene. Science *269*, 543–546.

Han, J.C., Liu, Q.-R., Jones, M., Levinn, R.L., Menzie, C.M., Jefferson-George, K.S., Adler-Wailes, D.C., Sanford, E.L., Lacbawan, F.L., Uhl, G.R., et al. (2008). Brain-derived neurotrophic factor and obesity in the WAGR syndrome. N. Engl. J. Med. *359*, 918–927.

Haraksingh, R.R., and Snyder, M.P. (2013). Impacts of variation in the human genome on gene regulation. J. Mol. Biol. *425*, 3970–3977.

Haslam, D.W., and James, W.P.T. (2005). Obesity. Lancet *366*, 1197–1209.

Heijmans, B.T., Tobi, E.W., Stein, A.D., Putter, H., Blauw, G.J., Susser, E.S., Slagboom, P.E., and Lumey, L.H. (2008). Persistent epigenetic differences associated with prenatal exposure to famine in humans. Proc. Natl. Acad. Sci. U. S. A. *105*, 17046–17049.

Hermetz, K.E., Surti, U., Cody, J.D., and Rudd, M.K. (2012). A recurrent translocation is mediated by homologous recombination between HERV-H elements. Mol. Cytogenet. *5*, 6.

Himms-Hagen, J., Melnyk, A., Zingaretti, M.C., Ceresi, E., Barbatelli, G., and Cinti, S. (2000). Multilocular fat cells in WAT of CL-316243-treated rats derive directly from white adipocytes. Am. J. Physiol. Cell Physiol. *279*, C670-81.

Hinney, A., Schmidt, A., Nottebom, K., Heibült, O., Becker, I., Ziegler, A., Gerber, G., Sina, M., Görg, T., Mayer, H., et al. (1999). Several mutations in the melanocortin-4 receptor gene including a nonsense and a frameshift mutation associated with dominantly inherited obesity in humans. J. Clin. Endocrinol. Metab. *84*, 1483–1486.

Hohenstein, P., Slight, J., Ozdemir, D.D., Burn, S.F., Berry, R., and Hastie, N.D. (2008). High-efficiency Rosa26 knock-in vector construction for Cre-regulated overexpression and RNAi. Pathogenetics *1*, 3.

Holder, J.L., Butte, N.F., and Zinn, A.R. (2000). Profound obesity associated with a balanced translocation that disrupts the SIM1 gene. Hum. Mol. Genet. *9*, 101–108.

Hummel, K.P., Dickie, M.M., and Coleman, D.L. (1966). Diabetes, a new mutation in the mouse. Science *153*, 1127–1128.

Huszar, D., Lynch, C.A., Fairchild-Huntress, V., Dunmore, J.H., Fang, Q., Berkemeier, L.R., Gu, W., Kesterson, R.A., Boston, B.A., Cone, R.D., et al. (1997). Targeted disruption of the melanocortin-4 receptor results in obesity in mice. Cell *88*, 131–141.

Ingalls, A.M., Dickie, M.M., and Snell, G.D. (1950). Obese, a new mutation in the house mouse. J. Hered. *41*, 317–318.

International HapMap Consortium (2005). A haplotype map of the human genome. Nature *437*, 1299–1320.

Jackson, R.S., Creemers, J.W., Ohagi, S., Raffin-Sanson, M.L., Sanders, L., Montague, C.T., Hutton, J.C., and O'Rahilly, S. (1997). Obesity and impaired prohormone processing associated with mutations in the human prohormone convertase 1 gene. Nat. Genet. *16*, 303–306.

Jackson, R.S., Creemers, J.W.M., Farooqi, I.S., Raffin-Sanson, M.-L., Varro, A., Dockray, G.J., Holst, J.J., Brubaker, P.L., Corvol, P., Polonsky, K.S., et al. (2003). Small-intestinal dysfunction accompanies the complex endocrinopathy of human proprotein convertase 1 deficiency. J. Clin. Invest. *112*, 1550–1560.

Jacquemont, S., Reymond, A., Zufferey, F., Harewood, L., Walters, R.G., Kutalik, Z., Martinet, D., Shen, Y., Valsesia, A., Beckmann, N.D., et al. (2011). Mirror extreme BMI phenotypes associated with gene dosage at the chromosome 16p11.2 locus. Nature *478*, 97–102.

Jarick, I., Vogel, C.I.G., Scherag, S., Schäfer, H., Hebebrand, J., Hinney, A., and Scherag, A. (2011). Novel common copy number variation for early onset extreme obesity on chromosome 11q11 identified by a genome-wide analysis. Hum. Mol. Genet. *20*, 840–852.

Kaminsky, E.B., Kaul, V., Paschall, J., Church, D.M., Bunke, B., Kunig, D., Moreno-De-Luca, D., Moreno-De-Luca, A., Mulle, J.G., Warren, S.T., et al. (2011). An evidence-based approach to establish the functional and clinical significance of copy number variants in intellectual and developmental disabilities. Genet. Med. *13*, 777–784.

Kelly, T., Yang, W., Chen, C.-S., Reynolds, K., and He, J. (2008). Global burden of obesity in 2005 and projections to 2030. Int. J. Obes. (Lond). *32*, 1431–1437.

Khan, S.M., Sleno, R., Gora, S., Zylbergold, P., Laverdure, J.-P., Labbé, J.-C., Miller, G.J., and Hébert, T.E. (2013). The expanding roles of Gβγ subunits in G protein-coupled receptor signaling and drug action. Pharmacol. Rev. *65*, 545–577.

Klenke, S., Kussmann, M., and Siffert, W. (2011). The GNB3 C825T polymorphism as a pharmacogenetic marker in the treatment of hypertension, obesity, and depression. Pharmacogenet. Genomics *21*, 594–606.

Knowler, W.C., Pettitt, D.J., Saad, M.F., and Bennett, P.H. (1990). Diabetes mellitus in the Pima Indians: incidence, risk factors and pathogenesis. Diabetes. Metab. Rev. *6*, 1–27.

Korbel, J.O., Urban, A.E., Affourtit, J.P., Godwin, B., Grubert, F., Simons, J.F., Kim, P.M., Palejev, D., Carriero, N.J., Du, L., et al. (2007). Paired-end mapping reveals extensive structural variation in the human genome. Science *318*, 420–426.

Krude, H., Biebermann, H., Luck, W., Horn, R., Brabant, G., and Grüters, A. (1998). Severe early-onset obesity, adrenal insufficiency and red hair pigmentation caused by POMC mutations in humans. Nat. Genet. *19*, 155–157.

Krumins, A.M., and Gilman, A.G. (2006). Targeted knockdown of G protein subunits selectively prevents receptor-mediated modulation of effectors and reveals complex changes in non-targeted signaling proteins. J. Biol. Chem. *281*, 10250–10262.

Kublaoui, B.M., Holder, J.L., Tolson, K.P., Gemelli, T., and Zinn, A.R. (2006). SIM1 overexpression partially rescues agouti yellow and diet-induced obesity by normalizing food intake. Endocrinology *147*, 4542–4549.

Lacaria, M., Saha, P., Potocki, L., Bi, W., Yan, J., Girirajan, S., Burns, B., Elsea, S., Walz, K., Chan, L., et al. (2012). A duplication CNV that conveys traits reciprocal to metabolic syndrome and protects against diet-induced obesity in mice and men. PLoS Genet. *8*, e1002713.

Lania, a, Mantovani, G., and Spada, A. (2001). G protein mutations in endocrine diseases. Eur. J. Endocrinol. *145*, 543–559.

Lee, G.H., Proenca, R., Montez, J.M., Carroll, K.M., Darvishzadeh, J.G., Lee, J.I., and Friedman, J.M. (1996). Abnormal splicing of the leptin receptor in diabetic mice. Nature *379*, 632–635.

Lein, E.S., Hawrylycz, M.J., Ao, N., Ayres, M., Bensinger, A., Bernard, A., Boe, A.F., Boguski, M.S., Brockway, K.S., Byrnes, E.J., et al. (2007). Genome-wide atlas of gene expression in the adult mouse brain. Nature *445*, 168–176.

Locke, A.E., Kahali, B., Berndt, S.I., Justice, A.E., Pers, T.H., Day, F.R., Powell, C., Vedantam, S., Buchkovich, M.L., Yang, J., et al. (2015). Genetic studies of body mass index yield new insights for obesity biology. Nature *518*, 197–206.

Loos, R.J.F., Lindgren, C.M., Li, S., Wheeler, E., Zhao, J.H., Prokopenko, I., Inouye, M., Freathy, R.M., Attwood, A.P., Beckmann, J.S., et al. (2008). Common variants near MC4R are associated with fat mass, weight and risk of obesity. Nat. Genet. *40*, 768–775.

López-León, S., Janssens, A.C.J.W., González-Zuloeta Ladd, A.M., Del-Favero, J., Claes, S.J., Oostra, B.A., and van Duijn, C.M. (2008). Meta-analyses of genetic studies on major depressive disorder. Mol. Psychiatry *13*, 772–785.

Lumey, L.H., Stein, A.D., Kahn, H.S., and Romijn, J.A. (2009). Lipid profiles in middle-aged men and women after famine exposure during gestation: the Dutch Hunger Winter Families Study. Am. J. Clin. Nutr. *89*, 1737–1743.

Luo, Y., Hermetz, K.E., Jackson, J.M., Mulle, J.G., Dodd, A., Tsuchiya, K.D., Ballif, B.C., Shaffer, L.G., Cody, J.D., Ledbetter, D.H., et al. (2011). Diverse mutational mechanisms cause pathogenic subtelomeric rearrangements. Hum. Mol. Genet. *20*, 3769–3778.

Luppino, F.S., de Wit, L.M., Bouvy, P.F., Stijnen, T., Cuijpers, P., Penninx, B.W.J.H., and Zitman, F.G. (2010). Overweight, obesity, and depression: a systematic review and meta-analysis of longitudinal studies. Arch. Gen. Psychiatry *67*, 220–229.

Lupski, J.R. (2004). Hotspots of homologous recombination in the human genome: not all homologous sequences are equal. Genome Biol. *5*, 242.

Maes, H.H., Neale, M.C., and Eaves, L.J. (1997). Genetic and environmental factors in relative body weight and human adiposity. Behav. Genet. *27*, 325–351.

Manolio, T.A., Collins, F.S., Cox, N.J., Goldstein, D.B., Hindorff, L.A., Hunter, D.J., McCarthy, M.I., Ramos, E.M., Cardon, L.R., Chakravarti, A., et al. (2009). Finding the missing heritability of complex diseases. Nature *461*, 747–753.

Margari, L., Di Cosola, M.L., Buttiglione, M., Pansini, A., Buonadonna, A.L., Craig, F., Cariola, F., Petruzzelli, M.G., and Gentile, M. (2012). Molecular cytogenetic characterization and genotype/phenotype analysis in a patient with a de novo 8p23.2p23.3 deletion/12p13.31p13.33 duplication. Am. J. Med. Genet. A *158A*, 1713–1718.

McGraw, L.A., Davis, J.K., Lowman, J.J., ten Hallers, B.F.H., Koriabine, M., Young, L.J., de Jong, P.J., Rudd, M.K., and Thomas, J.W. (2010). Development of genomic resources for the prairie vole (Microtus ochrogaster): construction of a BAC library and

vole-mouse comparative cytogenetic map. BMC Genomics *11*, 70.

McMillan, D.C., Sattar, N., and McArdle, C.S. (2006). ABC of obesity. Obesity and cancer. BMJ *333*, 1109–1111.

Mefford, H.C., and Eichler, E.E. (2009). Duplication hotspots, rare genomic disorders, and common disease. Curr. Opin. Genet. Dev. *19*, 196–204.

Michaud, J.L., Boucher, F., Melnyk, A., Gauthier, F., Goshu, E., Lévy, E., Mitchell, G.A., Himms-Hagen, J., and Fan, C.M. (2001). Sim1 haploinsufficiency causes hyperphagia, obesity and reduction of the paraventricular nucleus of the hypothalamus. Hum. Mol. Genet. *10*, 1465–1473.

Moll, P.P., Burns, T.L., and Lauer, R.M. (1991). The genetic and environmental sources of body mass index variability: the Muscatine Ponderosity Family Study. Am. J. Hum. Genet. *49*, 1243–1255.

Montague, C.T., Farooqi, I.S., Whitehead, J.P., Soos, M.A., Rau, H., Wareham, N.J., Sewter, C.P., Digby, J.E., Mohammed, S.N., Hurst, J.A., et al. (1997). Congenital leptin deficiency is associated with severe early-onset obesity in humans. Nature *387*, 903–908.

Moxham, C.M., and Malbon, C.C. (1996). Insulin action impaired by deficiency of the G-protein subunit G ialpha2. Nature *379*, 840–844.

Mufunda, J., Mebrahtu, G., Usman, A., Nyarango, P., Kosia, A., Ghebrat, Y., Ogbamariam, A., Masjuan, M., and Gebremichael, A. (2006). The prevalence of hypertension and its relationship with obesity: results from a national blood pressure survey in Eritrea. J. Hum. Hypertens. *20*, 59–65.

NCD Risk Factor Collaboration (NCD-RisC) (2016). Trends in adult body-mass index in 200 countries from 1975 to 2014: a pooled analysis of 1698 population-based measurement studies with 19·2 million participants. Lancet (London, England) *387*, 1377–1396.

Neves, S.R., Ram, P.T., and Iyengar, R. (2002). G protein pathways. Science *296*, 1636–1639.

Nikitin, A.G., Chudakova, D.A., Spitsina, E. V, Minushkina, L.O., Zateĭshchikov, D.A., Nosikov, V. V, and Debabov, V.G. (2007). [Association of GNB3 gene C825T polymorphism with coronary heart disease]. Genetika *43*, 1129–1133.

Njung'e, K., and Handley, S.L. (1991). Evaluation of marble-burying behavior as a model of anxiety. Pharmacol. Biochem. Behav. *38*, 63–67.

O'Rahilly, S. (2009). Human genetics illuminates the paths to metabolic disease. Nature *462*, 307–314.

Obregon, M.-J. (2014). Adipose tissues and thyroid hormones. Front. Physiol. *5*, 479.

Offermanns, S., and Simon, M.I. (1998). Genetic analysis of mammalian G-protein signalling. Oncogene *17*, 1375–1381.

Ogden, C.L., Carroll, M.D., Fryar, C.D., and Flegal, K.M. (2015). Prevalence of Obesity Among Adults and Youth: United States, 2011-2014. NCHS Data Brief 1–8.

Okada, Y., Kubo, M., Ohmiya, H., Takahashi, A., Kumasaka, N., Hosono, N., Maeda, S., Wen, W., Dorajoo, R., Go, M.J., et al. (2012). Common variants at CDKAL1 and KLF9 are associated with body mass index in east Asian populations. Nat. Genet. *44*, 302–306.

Okae, H., and Iwakura, Y. (2010). Neural tube defects and impaired neural progenitor cell proliferation in Gbeta1-deficient mice. Dev. Dyn. *239*, 1089–1101.

Oldham, W.M., and Hamm, H.E. (2008). Heterotrimeric G protein activation by G-protein-coupled receptors. Nat. Rev. Mol. Cell Biol. *9*, 60–71.

Ou, Z., Stankiewicz, P., Xia, Z., Breman, A.M., Dawson, B., Wiszniewska, J., Szafranski, P., Cooper, M.L., Rao, M., Shao, L., et al. (2011). Observation and prediction of recurrent human translocations mediated by NAHR between nonhomologous chromosomes. Genome Res. *21*, 33–46.

Panagiotou, O.A., Ioannidis, J.P.A., and Genome-Wide Significance Project (2012). What should the genome-wide significance threshold be? Empirical replication of borderline genetic associations. Int. J. Epidemiol. *41*, 273–286.

Paz-Filho, G., Wong, M.-L., and Licinio, J. (2011). Ten years of leptin replacement therapy. Obes. Rev. *12*, e315-23.

Pelleymounter, M.A., Cullen, M.J., Baker, M.B., Hecht, R., Winters, D., Boone, T., and Collins, F. (1995). Effects of the obese gene product on body weight regulation in ob/ob mice. Science *269*, 540–543.

Petrovic, N., Walden, T.B., Shabalina, I.G., Timmons, J.A., Cannon, B., and Nedergaard, J. (2010). Chronic peroxisome proliferator-activated receptor gamma (PPARgamma) activation of epididymally derived white adipocyte cultures reveals a population of thermogenically competent, UCP1-containing adipocytes molecularly distinct from classic brown adipocyt. J. Biol. Chem. *285*, 7153–7164.

Poon, L.S.W., Chan, A.S.L., and Wong, Y.H. (2009). Gbeta3 forms distinct dimers with specific Ggamma subunits and preferentially activates the beta3 isoform of phospholipase C. Cell. Signal. *21*, 737–744.

Prut, L., and Belzung, C. (2003). The open field as a paradigm to measure the effects of drugs on anxiety-like behaviors: a review. Eur. J. Pharmacol. *463*, 3–33.

Ravelli, A.C., van der Meulen, J.H., Michels, R.P., Osmond, C., Barker, D.J., Hales, C.N., and Bleker, O.P. (1998). Glucose tolerance in adults after prenatal exposure to famine. Lancet (London, England) *351*, 173–177.

Redon, R., Ishikawa, S., Fitch, K.R., Feuk, L., Perry, G.H., Andrews, T.D., Fiegler, H., Shapero, M.H., Carson, A.R., Chen, W., et al. (2006). Global variation in copy number in the human genome. Nature *444*, 444–454.

van Reedt Dortland, A.K.B., Giltay, E.J., van Veen, T., Zitman, F.G., and Penninx, B.W.J.H. (2013). Longitudinal relationship of depressive and anxiety symptoms with dyslipidemia and abdominal obesity. Psychosom. Med. *75*, 83–89.

Ren, D., Li, M., Duan, C., and Rui, L. (2005). Identification of SH2-B as a key regulator of leptin sensitivity, energy balance, and body weight in mice. Cell Metab. *2*, 95–104.

Robberecht, C., Voet, T., Zamani Esteki, M., Nowakowska, B.A., and Vermeesch, J.R. (2013). Nonallelic homologous recombination between retrotransposable elements is a driver of de novo unbalanced translocations. Genome Res. *23*, 411–418.

Rong, J.X., Qiu, Y., Hansen, M.K., Zhu, L., Zhang, V., Xie, M., Okamoto, Y., Mattie, M.D., Higashiyama, H., Asano, S., et al. (2007). Adipose mitochondrial biogenesis is suppressed in db/db and high-fat diet-fed mice and improved by rosiglitazone. Diabetes *56*, 1751–1760.

Rosskopf, D., Manthey, I., and Siffert, W. (2002). Identification and ethnic distribution of major haplotypes in the gene GNB3 encoding the G-protein beta3 subunit. Pharmacogenetics *12*, 209–220.

Rosskopf, D., Koch, K., Habich, C., Geerdes, J., Ludwig, A., Wilhelms, S., Jakobs, K.H., and Siffert, W. (2003). Interaction of Gbeta3s, a splice variant of the G-protein Gbeta3, with Ggamma- and Galpha-proteins. Cell. Signal. *15*, 479–488.

Ruiz-Velasco, V., and Ikeda, S.R. (2003). A splice variant of the G protein beta 3-subunit implicated in disease states does not modulate ion channels. Physiol. Genomics *13*, 85–95.

Sabin, M. a, Werther, G. a, and Kiess, W. (2011). Genetics of obesity and overgrowth syndromes. Best Pract. Res. Clin. Endocrinol. Metab. *25*, 207–220.

Sahoo, T., del Gaudio, D., German, J.R., Shinawi, M., Peters, S.U., Person, R.E., Garnica, A., Cheung, S.W., and Beaudet, A.L. (2008). Prader-Willi phenotype caused by paternal deficiency for the HBII-85 C/D box small nucleolar RNA cluster. Nat. Genet. *40*, 719–721.

Sandholt, C.H., Grarup, N., Pedersen, O., and Hansen, T. (2015). Genome-wide association studies of human adiposity: Zooming in on synapses. Mol. Cell. Endocrinol. *418 Pt 2*, 90–100.

Sargolini, F., Roullet, P., Oliverio, A., and Mele, A. (2003). Effects of intra-accumbens focal administrations of glutamate antagonists on object recognition memory in mice. Behav. Brain Res. *138*, 153–163.

Scacchi, M., Pincelli, a I., and Cavagnini, F. (1999). Growth hormone in obesity. Int. J. Obes. Relat. Metab. Disord. *23*, 260–271.

Schneider, C.A., Rasband, W.S., and Eliceiri, K.W. (2012). NIH Image to ImageJ: 25 years of image analysis. Nat. Methods *9*, 671–675.

Seale, P., Bjork, B., Yang, W., Kajimura, S., Chin, S., Kuang, S., Scimè, A., Devarakonda, S., Conroe, H.M., Erdjument-Bromage, H., et al. (2008). PRDM16 controls a brown fat/skeletal muscle switch. Nature *454*, 961–967.

Seeley, R.J., Yagaloff, K.A., Fisher, S.L., Burn, P., Thiele, T.E., van Dijk, G., Baskin, D.G., and Schwartz, M.W. (1997). Melanocortin receptors in leptin effects. Nature *390*, 349.

Segel, R., Peter, I., Demmer, L.A., Cowan, J.M., Hoffman, J.D., and Bianchi, D.W. (2006). The natural history of trisomy 12p. Am. J. Med. Genet. A *140*, 695–703.

Seo, S., Guo, D.-F., Bugge, K., Morgan, D.A., Rahmouni, K., and Sheffield, V.C. (2009). Requirement of Bardet-Biedl syndrome proteins for leptin receptor signaling. Hum. Mol. Genet. *18*, 1323–1331.

Sha, B.-Y., Yang, T.-L., Zhao, L.-J., Chen, X.-D., Guo, Y., Chen, Y., Pan, F., Zhang, Z.-X., Dong, S.-S., Xu, X.-H., et al. (2009). Genome-wide association study suggested copy number variation may be associated with body mass index in the Chinese population. J. Hum. Genet. *54*, 199–202.

Sheu, S.-Y., Handke, S., Bröcker-Preuss, M., Görges, R., Frey, U.H., Ensinger, C., Ofner, D., Farid, N.R., Siffert, W., and Schmid, K.W. (2007). The C allele of the GNB3 C825T polymorphism of the G protein beta3-subunit is associated with an increased risk for the development of oncocytic thyroid tumours. J. Pathol. *211*, 60–66.

Siffert, W. (2005). G protein polymorphisms in hypertension, atherosclerosis, and diabetes. Annu. Rev. Med. *56*, 17–28.

Siffert, W., Rosskopf, D., Siffert, G., Busch, S., Moritz, A., Erbel, R., Sharma, A.M., Ritz, E., Wichmann, H.E., Jakobs, K.H., et al. (1998). Association of a human G-protein beta3 subunit variant with hypertension. Nat. Genet. *18*, 45–48.

Siffert, W., Forster, P., Jöckel, K.H., Mvere, D.A., Brinkmann, B., Naber, C., Crookes, R., Du P Heyns, A., Epplen, J.T., Fridey, J., et al. (1999). Worldwide ethnic distribution of the G protein beta3 subunit 825T allele and its association with obesity in Caucasian, Chinese, and Black African individuals. J. Am. Soc. Nephrol. *10*, 1921–1930.

de Smith, A.J., Tsalenko, A., Sampas, N., Scheffer, A., Yamada, N.A., Tsang, P., Ben-Dor, A., Yakhini, Z., Ellis, R.J., Bruhn, L., et al. (2007). Array CGH analysis of copy number variation identifies 1284 new genes variant in healthy white males: implications for association studies of complex diseases. Hum. Mol. Genet. *16*, 2783–2794.

de Smith, A.J., Purmann, C., Walters, R.G., Ellis, R.J., Holder, S.E., Van Haelst, M.M., Brady, A.F., Fairbrother, U.L., Dattani, M., Keogh, J.M., et al. (2009). A deletion of the HBII-85 class of small nucleolar RNAs (snoRNAs) is associated with hyperphagia, obesity and hypogonadism. Hum. Mol. Genet. *18*, 3257–3265.

Snijder, M.B., Dekker, J.M., Visser, M., Bouter, L.M., Stehouwer, C.D.A., Kostense, P.J., Yudkin, J.S., Heine, R.J., Nijpels, G., and Seidell, J.C. (2003a). Associations of hip and thigh circumferences independent of waist circumference with the incidence of type 2 diabetes: the Hoorn Study. Am. J. Clin. Nutr. *77*, 1192–1197.

Snijder, M.B., Dekker, J.M., Visser, M., Yudkin, J.S., Stehouwer, C.D.A., Bouter, L.M., Heine, R.J., Nijpels, G., and Seidell, J.C. (2003b). Larger thigh and hip circumferences are associated with better glucose tolerance: the Hoorn study. Obes. Res. *11*, 104–111.

Soriano, P. (1999). Generalized lacZ expression with the ROSA26 Cre reporter strain. Nat. Genet. *21*, 70–71.

South, S.T., Whitby, H., Maxwell, T., Aston, E., Brothman, A.R., and Carey, J.C. (2008). Co-occurrence of 4p16.3 deletions with both paternal and maternal duplications of 11p15: modification of the Wolf-Hirschhorn syndrome phenotype by genetic alterations predicted to result in either a Beckwith-Wiedemann or Russell-Silver phenotype. Am. J. Med. Genet. A *146A*, 2691–2697.

Speliotes, E.K., Willer, C.J., Berndt, S.I., Monda, K.L., Thorleifsson, G., Jackson, A.U., Lango Allen, H., Lindgren, C.M., Luan, J., Mägi, R., et al. (2010). Association analyses of 249,796 individuals reveal 18 new loci associated with body mass index. Nat. Genet. *42*, 937–948.

Stein, A.D., Kahn, H.S., Rundle, A., Zybert, P.A., van der Pal-de Bruin, K., and Lumey, L.H. (2007). Anthropometric measures in middle age after exposure to famine during gestation: evidence from the Dutch famine. Am. J. Clin. Nutr. *85*, 869–876.

Stunkard, A.J., Foch, T.T., and Hrubec, Z. (1986a). A twin study of human obesity. JAMA *256*, 51–54.

Stunkard, A.J., Sørensen, T.I., Hanis, C., Teasdale, T.W., Chakraborty, R., Schull, W.J., and Schulsinger, F. (1986b). An adoption study of human obesity. N. Engl. J. Med. *314*, 193–198.

Stunkard, A.J., Harris, J.R., Pedersen, N.L., and McClearn, G.E. (1990). The body-mass index of twins who have been reared apart. N. Engl. J. Med. *322*, 1483–1487.

Sun, A., Ge, J., Siffert, W., and Frey, U.H. (2005). Quantification of allele-specific G-protein beta3 subunit mRNA transcripts in different human cells and tissues by Pyrosequencing. Eur. J. Hum. Genet. *13*, 361–369.

Sun, Z., Runne, C., Tang, X., Lin, F., and Chen, S. (2012). The Gβ3 splice variant associated with the C825T gene polymorphism is an unstable and functionally inactive

protein. Cell. Signal. *24*, 2349–2359.

Tam, C.S., Lecoultre, V., and Ravussin, E. (2012). Brown adipose tissue: mechanisms and potential therapeutic targets. Circulation *125*, 2782–2791.

Tang, Y.P., Shimizu, E., Dube, G.R., Rampon, C., Kerchner, G.A., Zhuo, M., Liu, G., and Tsien, J.Z. (1999). Genetic enhancement of learning and memory in mice. Nature *401*, 63–69.

Tartaglia, L.A., Dembski, M., Weng, X., Deng, N., Culpepper, J., Devos, R., Richards, G.J., Campfield, L.A., Clark, F.T., Deeds, J., et al. (1995). Identification and expression cloning of a leptin receptor, OB-R. Cell *83*, 1263–1271.

Teerds, K.J., de Rooij, D.G., and Keijer, J. (2011). Functional relationship between obesity and male reproduction: from humans to animal models. Hum. Reprod. Update *17*, 667–683.

Thorleifsson, G., Walters, G.B., Gudbjartsson, D.F., Steinthorsdottir, V., Sulem, P., Helgadottir, A., Styrkarsdottir, U., Gretarsdottir, S., Thorlacius, S., Jonsdottir, I., et al. (2009). Genome-wide association yields new sequence variants at seven loci that associate with measures of obesity. Nat. Genet. *41*, 18–24.

Tobi, E.W., Slagboom, P.E., van Dongen, J., Kremer, D., Stein, A.D., Putter, H., Heijmans, B.T., and Lumey, L.H. (2012). Prenatal famine and genetic variation are independently and additively associated with DNA methylation at regulatory loci within IGF2/H19. PLoS One *7*, e37933.

Tranebjaerg, L., Petersen, A., Hove, K., Rehder, H., and Mikkelsen, M. (1984). Clinical and cytogenetic studies in a large (4;8) translocation family with pre- and postnatal Wolf syndrome. Ann. Genet. *27*, 224–229.

Turner, D.J., Miretti, M., Rajan, D., Fiegler, H., Carter, N.P., Blayney, M.L., Beck, S., and Hurles, M.E. (2008). Germline rates of de novo meiotic deletions and duplications causing several genomic disorders. Nat. Genet. *40*, 90–95.

Usman, A., Mebrahtu, G., Mufunda, J., Nyarang'o, P., Hagos, G., Kosia, A., Ghebrat, Y., Mosazghi, A., Atanga, S.J., and Equbamichael, M.M. (2006). Prevalence of non-communicable disease risk factors in Eritrea. Ethn. Dis. *16*, 542–546.

Vaisse, C., Clement, K., Guy-Grand, B., and Froguel, P. (1998). A frameshift mutation in human MC4R is associated with a dominant form of obesity. Nat. Genet. *20*, 113–114.

Verge, C.F., and Mowat, D. (2010). Overgrowth. Arch. Dis. Child. *95*, 458–463.

Visscher, P.M., Hill, W.G., and Wray, N.R. (2008). Heritability in the genomics era--concepts and misconceptions. Nat. Rev. Genet. *9*, 255–266.

Visser, R., Kant, S.G., Wit, J.M., and Breuning, M.H. (2009). Overgrowth

syndromes:from classical to new. Pediatr. Endocrinol. Rev. *6*, 375–394.

Walley, A.J., Asher, J.E., and Froguel, P. (2009). The genetic contribution to non-syndromic human obesity. Nat. Rev. Genet. *10*, 431–442.

Walters, R.G., Jacquemont, S., Valsesia, A., de Smith, A.J., Martinet, D., Andersson, J., Falchi, M., Chen, F., Andrieux, J., Lobbens, S., et al. (2010). A new highly penetrant form of obesity due to deletions on chromosome 16p11.2. Nature *463*, 671–675.

Wang, K., Li, W.-D., Glessner, J.T., Grant, S.F.A., Hakonarson, H., and Price, R.A. (2010). Large copy-number variations are enriched in cases with moderate to extreme obesity. Diabetes *59*, 2690–2694.

Wang, Q., Levay, K., Chanturiya, T., Dvoriantchikova, G., Anderson, K.L., Bianco, S.D.C., Ueta, C.B., Molano, R.D., Pileggi, A., Gurevich, E. V, et al. (2011). Targeted deletion of one or two copies of the G protein β subunit Gβ5 gene has distinct effects on body weight and behavior in mice. FASEB J. *25*, 3949–3957.

Wardle, J., Carnell, S., Haworth, C.M., and Plomin, R. (2008). Evidence for a strong genetic influence on childhood adiposity despite the force of the obesogenic environment. Am. J. Clin. Nutr. *87*, 398–404.

Weinstein, L.S., Chen, M., and Liu, J. (2002). Gs(alpha) mutations and imprinting defects in human disease. Ann. N. Y. Acad. Sci. *968*, 173–197.

Wen, W., Cho, Y.-S., Zheng, W., Dorajoo, R., Kato, N., Qi, L., Chen, C.-H., Delahanty, R.J., Okada, Y., Tabara, Y., et al. (2012). Meta-analysis identifies common variants associated with body mass index in east Asians. Nat. Genet. *44*, 307–311.

Wettschureck, N., and Offermanns, S. (2005). Mammalian G proteins and their cell type specific functions. Physiol. Rev. *85*, 1159–1204.

Wheeler, E., Huang, N., Bochukova, E.G., Keogh, J.M., Lindsay, S., Garg, S., Henning, E., Blackburn, H., Loos, R.J.F., Wareham, N.J., et al. (2013). Genome-wide SNP and CNV analysis identifies common and low-frequency variants associated with severe early-onset obesity. Nat. Genet.

Wheeler, P.G., Weaver, D.D., and Palmer, C.G. (1995). Familial translocation resulting in Wolf-Hirschhorn syndrome in two related unbalanced individuals: clinical evaluation of a 39-year-old man with Wolf-Hirschhorn syndrome. Am. J. Med. Genet. *55*, 462–465.

WHO Multicentre Growth Reference Study Group (2006). WHO Child Growth Standards based on length/height, weight and age. Acta Paediatr. Suppl. *450*, 76–85.

Willer, C.J., Speliotes, E.K., Loos, R.J.F., Li, S., Lindgren, C.M., Heid, I.M., Berndt, S.I., Elliott, A.L., Jackson, A.U., Lamina, C., et al. (2009). Six new loci associated with body mass index highlight a neuronal influence on body weight regulation. Nat. Genet. *41*, 25–34.

World Health Organization (2016a). Obesity and overweight fact sheet.

World Health Organization (2016b). Nauru - Diabetes country profiles.

World Health Organization (2016c). Eritrea - Diabetes country profiles.

Wu, J., Boström, P., Sparks, L.M., Ye, L., Choi, J.H., Giang, A.-H., Khandekar, M., Virtanen, K. a, Nuutila, P., Schaart, G., et al. (2012). Beige adipocytes are a distinct type of thermogenic fat cell in mouse and human. Cell *150*, 366–376.

Wu, J., Cohen, P., and Spiegelman, B.M. (2013). Adaptive thermogenesis in adipocytes: is beige the new brown? Genes Dev. *27*, 234–250.

Xia, Q., and Grant, S.F. a (2013). The genetics of human obesity. Ann. N. Y. Acad. Sci. *1281*, 178–190.

Xue, B., Coulter, A., Rim, J.S., Koza, R.A., and Kozak, L.P. (2005). Transcriptional synergy and the regulation of Ucp1 during brown adipocyte induction in white fat depots. Mol. Cell. Biol. *25*, 8311–8322.

Ye, Y., Sun, Z., Guo, A., Song, L.-S., Grobe, J.L., and Chen, S. (2014). Ablation of the GNB3 gene in mice does not affect body weight, metabolism or blood pressure, but causes bradycardia. Cell. Signal. *26*, 2514–2520.

Yeo, G.S., Farooqi, I.S., Aminian, S., Halsall, D.J., Stanhope, R.G., and O'Rahilly, S. (1998). A frameshift mutation in MC4R associated with dominantly inherited human obesity. Nat. Genet. *20*, 111–112.

Yeo, G.S.H., Connie Hung, C.-C., Rochford, J., Keogh, J., Gray, J., Sivaramakrishnan, S., O'Rahilly, S., and Farooqi, I.S. (2004). A de novo mutation affecting human TrkB associated with severe obesity and developmental delay. Nat. Neurosci. *7*, 1187–1189.

Yeung, F., Ramírez, C.M., Mateos-Gomez, P.A., Pinzaru, A., Ceccarini, G., Kabir, S., Fernández-Hernando, C., and Sfeir, A. (2013). Nontelomeric role for Rap1 in regulating metabolism and protecting against obesity. Cell Rep. *3*, 1847–1856.

Zarrei, M., MacDonald, J.R., Merico, D., and Scherer, S.W. (2015). A copy number variation map of the human genome. Nat. Rev. Genet. *16*, 172–183.

Zhang, J.-H., Pandey, M., Seigneur, E.M., Panicker, L.M., Koo, L., Schwartz, O.M., Chen, W., Chen, C.-K., and Simonds, W.F. (2011). Knockout of G protein β5 impairs brain development and causes multiple neurologic abnormalities in mice. J. Neurochem. *119*, 544–554.

Zhang, Y., Proenca, R., Maffei, M., Barone, M., Leopold, L., and Friedman, J.M. (1994). Positional cloning of the mouse obese gene and its human homologue. Nature *372*, 425–432.

Zuk, O., Hechter, E., Sunyaev, S.R., and Lander, E.S. (2012). The mystery of missing heritability: Genetic interactions create phantom heritability. Proc. Natl. Acad. Sci. U. S. A. *109*, 1193–1198.